The Dissertation Committee for Jun Lu Certifies that this is the approved version of the following dissertation:

Development of Novel Surfactants and Surfactant Methods for Chemical Enhanced Oil Recovery

Committee:

Gary A. Pope, Supervisor

Upali P. Weerasooriya

Kishore K. Mohanty

David DiCarlo

Keith P. Johnston

Development of Novel Surfactants and Surfactant Methods for Chemical Enhanced Oil Recovery

by

Jun Lu, B.E.; M.E.; M.S.

Dissertation

Presented to the Faculty of the Graduate School of

The University of Texas at Austin

in Partial Fulfillment

of the Requirements

for the Degree of

Doctor of Philosophy

The University of Texas at Austin

August 2014

Dedication

To all my family.

Acknowledgements

My deepest thanks go to my advisor, Dr. Gary A. Pope, who has inspired and motivated me to keep exploring the unknown scientific problems, as well as Dr. Upali P. Weerasooriya, without whom I would not have been able to finish my research and dissertation. I cannot thank them enough for the opportunity, knowledge, supervision, support, and guidance that they have provided to me. I would like to extend my gratitude to my committee members: Kishore Mohanty, David DiCarlo, and Keith Johnston, for insightful suggestions and comments on the dissertation and the final defense.

Thanks as well to Do Hoon Kim, Chris Britton and Stephanie Adkins for their help and support. I could not have learned everything in the lab without their help and experience. I also want to thank all the former and current staff members in our group including Gayani W. Pinnawala Arachchilage, Pathma Jith Liyanage, Thilini Kuruwita-Mudiyanselage, Erandimala Udamini Kularwardina, Nadeeka Upamali, Gayani Kennedy, Christophe Cottin, Suneth Rajapaksha, Jiajia Cai, Sung Hyun Jang, Erin Shook, Dharmika Lansakara, Sophie Dufour, Pradeep Upamali, and Austin Lim. Special thanks go to Esther Barrientes, Joanna Castillo, Frankie Hart, Glen Baum, and Gary Miscoe for their technical and administrative support.

I would like to express my gratitude former and current colleagues at the University of Texas at Austin: Vinay Sahni, Hyuntae Yang, Will Slaughter, Kyle Tipley, Robert M. Dean, Sriram Solairaj, Dustin Walker, Matthew Winters, Mike Unomah, Robert P. Fortenberry, Heesong Koh, Nabijan Nizamidin, Leonard Chang, Vincent Lee, Yuxiang Li, Ali Goudarzi, Peila Chen, Prateek Kathel.

Many undergraduate students helped with the lab experiments and deserve thanks, in particular I would like to thank Mengyuan Chen, Scott Hyde II, Ankit Suri, Alex Youssefinia, Dinara Dussenova, Siamak Chabokrow, and Tony Tran.

I would also like to thank ConocoPhillips for providing me an opportunity to intern in Bartlesville Technology Center. I am very grateful to Terry Christian, Riley B. Needham, Ahmad Moradi, David E. Torres, and Min Cheng for their great support.

Lastly, I would like to thank the 40 industrial affiliates of the Chemical EOR research program in the Center for Petroleum and Geosystems Engineering at the University of Texas at Austin for their financial support of this research and for their valuable advice.

Development of Novel Surfactants and Surfactant Methods for Chemical Enhanced Oil Recovery

Jun Lu, Ph.D.

The University of Texas at Austin, 2014

Supervisor: Gary A. Pope

The first goal of this research was to develop and experimentally test new and improved chemical formulations for enhanced oil recovery using a new class of branched large-hydrophobe alkoxy carboxylate surfactants mixed with novel co-surfactants and co-solvents to both lower IFT and alter wettability at high temperatures and high salinities.

These novel alkoxy carboxylate surfactants with large branched hydrophobes were tested and found to show excellent performance in corefloods over a wide range of reservoir conditions up to at least 120°C. The number of PO and EO groups in these new surfactants were optimized for a wide variety of oils over a broad range of salinity, hardness and temperature and mixed with various co-surfactants and co-solvents to develop high-performance formulations based on the microemulsion phase behavior. Both ultra-low IFT and clear aqueous solutions at optimum salinity were obtained for both active and inactive oils and both light and medium gravity oils over a wide range of temperatures. Both sandstone and carbonate corefloods using these carboxylate surfactants showed excellent performance at high temperature, high hardness and high salinity as indicated by high oil recovery, low pressure gradients and low surfactant retention. The advent of such a new class of cost-effective surfactants significantly

broadens the potential application of chemical enhanced oil recovery processes using surfactants under harsh reservoir conditions.

The second goal of this research was to evaluate the effect of buoyancy on oil recovery from cores using ultra-low IFT surfactant formulations under conditions where the use of polymer for mobility control is either difficult or unnecessary, determine the conditions that are favorable for a gravity-stable surfactant flood, and further improve the performance of gravity-stable surfactant floods by optimizing the microemulsion properties, especially its viscosity. The microemulsion viscosity can be varied by adjusting the structure of the surfactants and co-solvents and their concentrations.

Predictions made using classical stability theory applied to surfactant flooding experiments were determined to be inaccurate because such theory does not take into account the microemulsion phase that forms in-situ when surfactant mixes with the oil. The modification of the classical theory to account for the effect of the microemulsion on the critical velocity for a stable displacement is one of the major contributions of this research. New experiments were done to test the modified theory and it was found to be in good agreement with these experiments. Furthermore, a new method to increase the stable velocity by optimizing the microemulsion viscosity was proposed and validated by a series of coreflood experiments designed and conducted for that specific purpose.

Table of Contents

List of Tables

List of Figures

Chapter I: Introduction

BACKGROUND

New surfactant developments

Surfactants reduce the interfacial tension between oil and brine and alter the wettability of the reservoir rock. The IFT must be reduced to ultra-low levels (<0.001 mN/m) to completely displace residual oil trapped in the rock by capillary pressure (Lake, 1989; Green and Willhite, 1998; Sheng, 2011). Even lower IFT may be required to displace oil from oil-wet rocks since the residual oil is in the smaller pores of an oil-wet rock compared to a water-wet rock. The development and testing of new surfactants for EOR has been very active the past few years (Levitt, 2006; Jackson et al., 2006; Flaaten, 2007; Zhao et al., 2008; Flaaten et al., 2008; Barnes et al., 2008, 2010, 2012; Wang et al., 2010; Sahni, 2009; Yang et al., 2010; Adkins et al., 2010, Zhao et al., 2010, Dean, 2011; Solairaj, 2011; Walker, 2011; Adkins et al., 2012; Liyanage et al., 2012; Bataweel and Nasr-El-Din, 2012; Tabary et al., 2013; Shiau et al., 2013; Gao and Sharma, 2013; Luo et al., 2013; Yin and Zhang, 2013; Ahmadi and Shadizadeh, 2013; Chen et al., 2014; Puerto et al., 2014; Li et al., 2014; Lu et al., 2014a). Only a few of the most recent developments are briefly reviewed here.

Adkins et al. (2010) demonstrated that Guerbet alkoxy sulfates made with large hydrophobes exhibited good performance under a wide range of reservoir conditions. Furthermore, Guerbet alkoxy sulfates can be made in various hydrophobicities by changing the number of propylene oxide (PO) and ethylene oxide (EO) groups to tailor them to different reservoir conditions including high salinity and high hardness. However, Guerbet alkoxy sulfates are not chemically stable above about 60 °C unless the pH is increased to about 10 to 11. Such high pH requires the use of alkali and there are

circumstances when that is not practical, for example when gypsum or anhydrite is present in the reservoir rock or when soft water is unavailable for injection. Ether sulfonates are stable at high temperature and have good tolerance to hardness (Puerto et al., 2012), but they are expensive and only a limited quantity of a few structures are commercially available because of the difficulty of manufacturing them. Moreover, the commercial products have short hydrophobes that are not effective for crude oils with high equivalent alkane carbon numbers (EACN).

Adkins et al. (2012) showed that Guerbet alkoxy carboxylates can also be made with large branched hydrophobes and with a wide range of PO and EO groups added. The cost of these new carboxylate surfactants is competitive with commonly used commercial surfactants such as alkoxy sulfates. Lu et al. (2014b) showed good oil recovery results for these new large hydrophobe alkoxy carboxylate surfactants over a broad range of conditions from light to viscous oils, for both active and inactive oils and from low to high temperatures in both sandstones and carbonates. Liyanage et al. (2012) developed and tested another large-hydrophobe surfactant prepared from commercially available tristyrylphenol (TSP) and showed that it was effective for a waxy crude oil with a high EACN.

Many researchers have worked on surfactant developments for hostile reservoir conditions such as high temperature, high salinity and high hardness. Wang et al. (2010) developed 5 series of surfactants with different chemical structures and evaluated their capabilities of attaining ultra-low IFT and stability at high temperature, high salinity and high hardness conditions. The Betaine surfactants were found to be tolerant to harsh environments without the need for alkali.

Bataweel and Nasr-El-Din (2012) tested two anionic, two amphoteric surfactants, two alkalis and two types of polymers to compare ASP and SP flooding recovering

residual oil in high salinity/hardness and temperature in sandstone cores. Results showed ASP with anionic surfactant gave highest oil recovery than other formulations, and amphoteric surfactant showed lowest IFT but did not achieve higher oil recovery.

Tabary et al. (2013) reported good surfactant formulations for hard brine, high salinity and high temperature with dodecane or tetradecane as model oils by testing olefin sulfonates, alkyl aryl sulfonates, alkyl ether sulfates, and alkyl glyceryl ether sulfonates. However, no details of the chemical formulations were provided.

Luo et al. (2013) tested a series of amphoteric surfactants to obtain low IFT and compatibility with polyacrylamide polymer in high salinity and hardness brine, and showed residual heavy oil could be effectively recovered. Shiau et al. (2013) developed binary and ternary surfactant formulations for high salinity formations, and applied one surfactant-only formulation in a single-well test.

Puerto et al. (2014) tested the blends of alcohol propoxy sulfate (APS)/IOS, and APS/alcohol ethoxy sulfate in hard brine at 25 and 50 °C with n-octane and one crude oil. A salinity map was constructed based on these results to facilitate selection of injection compositions where injection and reservoir salinities differ.

Gao and Sharma (2013) synthesized a series of alkyl sulfate Gemini surfactants, and studied their interfacial properties and adsorption behavior and concluded that these surfactants have potential application for chemical EOR.

Chen et al. (2014) synthesized alcohol polyoxypropylene polyoxyethylene ether carboxylates (APPEC) by carboxymethylation reaction of alcohol polyoxypropylene polyoxyethylene ether (APPE) for ASP flooding. Ultra-low IFT was obtained with one crude oil at low temperature, and about 20% additional oil was recovered by ASP injection from two coreflood experiments.

Li et al. (2014) systematically studied the properties of mixtures of anionic-cationic surfactants and showed promising results on IFT, adsorption, phase behavior and coreflood tests. Ahmadi and Shadizadeh (2013) applied a sugar-based surfactant, saponin, extracted from the leaves of Z. spina Christi for EOR in carbonates. Yin and Zhang (2013) evaluated a green nonionic surfactant, alkyl polyglycoside (APG) for chemical EOR in carbonate reservoir. The blend of APG and NaHCO3 was selected and tested for IFT reduction, wettability alteration, static adsorption measurements and coreflood experiments.

Wettability alteration using surfactants

A lot of research has been done on wettability alteration using surfactants that do not reduce the IFT to ultra-low values (Austad et al., 1998; Zhang et al., 2004; Xie et al., 2004; Sharma and Mohanty, 2011; Chen and Mohanty, 2012). Imbibition experiments using surfactants that produce ultra-low IFT have been done by several investigators (Hirasaki and Zhang, 2004; Seethepalli et al., 2004; Abidhatla and Mohanty, 2006). Hirasaki and Zhang (2004) suggested the dominant oil recovery mechanism in ultra-low IFT imbibition to be buoyancy and wettability alteration.

With some anionic surfactants, the IFT can be reduced to ultra-low values where the capillary pressure is reduced to nearly zero. When the capillary pressure is nearly zero, then other forces must be present to account for the rapid imbibition observed in many experiments. The simulation results by Abbasi-Asl et al. (2010) showed that transverse pressure gradients between the fractures and matrix can push the surfactant further into the matrix in the dynamic imbibition process. Lu et al. (2012) showed promising results when applied low-tension surfactant flood on naturally fractured core,

and proposed a combination of IFT reduction and wettability alteration as the main oil recovery mechanism.

A large number of carbonate reservoirs are naturally fractured and are mixed-wet to oil-wet (Roehl and Choquette, 1985; Chilingar and Yen, 1983). Most carbonate reservoirs are very heterogeneous and the formations have a complex pore structure. Naturally fractured carbonate reservoirs typically have high permeability fractures and a low permeability matrix. This high permeability contrast between the matrix and fractures as well as the mixed-wet or oil-wet nature of the rock leads to poor water flood efficiency. The oil recovery from naturally fractured carbonate reservoirs is often less than one-third of the original oil in place. Thus, many of these carbonate reservoirs are candidates for EOR and for the use of surfactants in particular.

Austad and Milter (1997) proposed the ion-pair formation mechanism for cationic surfactant-induced wettability alteration. The ion pairs are formed by the interaction between positively charged surfactant head groups and the negatively charged carboxylic groups resulting in lifting some organic materials off the mineral surface, thereby altering the wettability from oil wet to water wet.

Standnes and Austad (2000) proposed that the anionic surfactant molecules could form a monolayer on the rock surface through hydrophobic interactions with the adsorbed crude oil components. The layer of adsorbed surfactants with the hydrophilic head groups covering the originally oil-wet rock surface could then change the wetting state of the rock surface to more water wet. They suggested cationic surfactants are more effective than the anionic surfactants in altering the wettability of the carbonate rock to more water wet, because the hydrophobic interactions are much weaker than the ion-pair interactions. Micellar solubilization of adsorbed organic components by ultra-low IFT anionic surfactants was also proposed by Hirasaki and Zhang (2004) and Kumar et al. (2005).

Sharma and Mohanty (2011) and Chen and Mohanty (2012) identified some surfactants showing good results for high temperature and salinity carbonates. Chen and Mohanty (2012) suggested adding EDTA to anionic surfactant formulations promotes spontaneous imbibition and higher oil recovery from dolomite cores. Possible mechanisms include increased pH causing saponification, chelation of divalent ions, and dissolution of dolomite.

Lu et al. (2012) showed promising results for a surfactant flood in a naturally fractured carbonate core at a low frontal velocity of 0.2 ft/D. This is the only published result of a dynamic displacement whereas there are numerous static imbibition experiments.

Field results

Falls et al. (1994) reported results for an alkaline/surfactant pilot in the White Castle field, Louisiana. The reservoir is a high permeability sand with a dip angle of 45^{o}. The flood was done to take advantage of gravity due of the high dip angle and for this reason polymer was not used for mobility control. The condition for a surfactant flood to be stabilized by gravity is analyzed in Chapter IV. The induction logs indicated virtually 100% displacement efficiency and ~50% vertical sweep efficiency. Falls et al. report that about 38% of the waterflood residual oil in the reservoirs was recovered as tertiary oil.

Buijse et al. (2010) reported results of a single well test of alkaline/surfactant/polymer (ASP) injection in the West Salym field in West Siberia. The results showed that 90% of the remaining oil saturation after water flood was mobilized by the ASP flood.

Stoll et al. (2011) reported results of single well tests in three fields in Oman including both sandstone and carbonate reservoirs. One test showed almost complete

desaturation from 25% to 1% remaining oil after ASP injection. Their paper also described how these SWCT pilots results are used to design a multiwell pilot.

Sharma et al. (2012) reported results of an ASP pilot with six five-spot well patterns in the Bridgeport sandstone reservoir located in the Illinois Basin. Polymer injectivity tests, single well chemical tracer (SWCT) tests and an interwell tracer test were all done for the pilot test. The SWCT showed the residual oil saturations to water and ASP were 28% and 8%, respectively. The pilot has shown the ASP was successful in displacing residual oil saturation. An observation well clearly showed formation of the oil bank. Rex Energy considers the pilot a success. However, out-of-zone and off-pattern loses of injected chemical were significant resulting in the delayed production of the oil bank, and decreases in oil cut and oil production rate. The pattern confinement problem could have been taken into account if the ASP flood would not have been started until after the complete interwell tracer results were available and analyzed.

Gao and Gao (2010) reviewed and summarized 12 ASP pilot tests in China including two foam pilot tests. Four ASP pilot tests successfully recovered about 20 % oil over water flood. Another three ASP pilot tests with large well spacing of 200 to 250 m also showed 20% oil recovery after water flood. Two foam tests did not achieve the expected goal and were considered unsuccessful.

RESEARCH OBJECTIVES

The first objective of this research was to develop and experimentally test new formulations for oil reservoirs using a new class of large-hydrophobe alkoxy carboxylate surfactants mixed with novel co-surfactants and co-solvents to both lower IFT and alter wettability at high temperatures and high salinities.

The second objective of this research was to evaluate the effect of buoyancy on oil recovery from cores using ultra-low IFT surfactant formulations under conditions where the use of polymer for mobility control is either difficult or unnecessary, determine the conditions that may be favorable for a gravity-stable surfactant flood, and further improve the performance of gravity-stable surfactant floods by optimizing the microemulsion properties, especially its viscosity.

CHAPTER OUTLINE

This dissertation is outlined by the following chapters:

Chapter II: The synthesis reaction and molecular structure of large hydrophobe Guerbet alkoxy carboxylate surfactants with a wide range of PO and EO groups are given. The long-term stability results of these surfactants in hard brine at high temperature are shown. Good phase behavior and oil recovery results for these Guerbet alkoxy carboxylate surfactants over a broad range of conditions from light to viscous oils, for both active and inactive oils at both low and high temperatures in both sandstones and carbonates are stated.

Chapter III: Ultra-low IFT surfactant formulations were developed for a naturally fractured carbonate reservoir with a high salinity/hardness formation brine at a high temperature. Both static and dynamic imbibition experiments were conducted in the fractured reservoir cores to compare the oil recovery performances.

Chapter IV: A modified stability theory is first time proposed to calculate the critical velocity for ultra-low IFT gravity-stable surfactant floods taking into account the properties of the microemulsion. A series of surfactant displacement experiments were carried out to determine the critical velocity for a gravity-stable surfactant flood and these results were then compared with the proposed stability theory. The stability theory and

experimental results are in good agreements. A new method is also proposed for increasing the critical velocity at which a stable flood can be achieved by optimizing the microemulsion viscosity. Several surfactant formulations were developed to obtain different microemulsion viscosities by varying components and concentrations in the formulations. Stable velocities of surfactant floods were improved with formulations of various microemulsion viscosities, and proposed method is validated by experimental results.

Chapter V: Several anionic-NI surfactant formulations with ultra-low IFT and good aqueous stability were identified for different oils. One formulation was tested on one coreflood and showed effective oil recovery performance. Two formulations were tested with both oil-aged calcite and cristobalite plates, and preliminary results showed capabilities to alter wettability from oil-wet toward water-wet.

Chapter VI: A summary and major conclusions of this research are presented.. The recommendations for future work are also presented.

Chapter II: Development of Novel Carboxylate Surfactants for Chemical EOR

INTRODUCTION

The recent development of new surfactants has greatly broadened the applications of chemical enhanced oil recovery (CEOR) to a much wider range of reservoir conditions with a relatively low chemical cost. A better understanding of the relationship between the surfactant structure and performance has improved the process of screening and identifying suitable high-performance surfactants for EOR (Solairaj, 2011; Solairaj *et al*., 2012). Microemulsion phase behavior observations used in this study are a very efficient way to screen surfactants (Jackson, 2006; Levitt *et al*., 2009; Zhao *et al*., 2008; Flaaten *et al*., 2010; Solairaj *et al*., 2012).

In order to obtain ultra-low IFT and low microemulsion viscosities when the equivalent alkane carbon number (EACN) of a crude oil is high, surfactants with very large hydrophobes and branched structures are required (Liu et al., 2007; Adkins et al., 2010). Conditions such as high temperature and/or high salinity and hardness can make it extremely challenging to achieve these properties. Previously, it was shown that cost-effective, high-performance surfactants can be produced in the form of Guerbet alkoxy sulfate surfactants (GAES) (Adkins et al., 2010). Very large hydrophobes can be produced from smaller linear alcohols using the Guerbet reaction which dimerizes the linear alcohol using base (plus transition metal) catalysis at high temperatures (O'Lenick, 2001). Anionic surfactants are then produced by alkoxylation of the Guerbet alcohol with the addition of propylene oxide (PO) and ethylene oxide (EO) units, followed by sulfation, which is a lower cost alternative to the more complex sulfonation process. Adkins *et al*. (2010) demonstrated that Guerbet alkoxy sulfates made with large

hydrophobes exhibited good performance under a wide range of conditions. Furthermore, Guerbet alkoxy sulfates can be made in various hydrophobicities by changing the number of propylene oxide (PO) and ethylene oxide (EO) groups to tailor them to different reservoir conditions including high salinity and high hardness.

Traditionally, alkoxy sulfate surfactants were found to have poor hydrolytic stability at elevated temperatures (>60 °C) (Talley, 1988). However, recent investigations have shown that enhanced stability can be achieved under specific alkalinity conditions at temperatures up to 120 °C (Adkins et al., 2010). Hydrolysis of the alkoxy sulfate surfactants can occur by either a very rapid acid-catalyzed mechanism (Rosen, 2004) or a less pronounced base-catalyzed reaction mechanism. The alkalinity (pH) of the surfactant solution must be controlled in order to reduce the rates of these decomposition reactions at elevated temperatures. Optimal stability of the alkoxy sulfate surfactants occurs when the pH of the solution is maintained in the range of 10-11. If the pH of the surfactant solution is outside this range, hydrolysis of the surfactant occurs more rapidly (more so in the lower pH range) and the surfactant decomposes. Therefore, in order to stabilize the alkoxy sulfate surfactants during chemical flooding at elevated temperatures (> 60 °C), alkali (usually sodium carbonate) must be used. However, there are circumstances when the use of conventional alkali is not practical, for example when gypsum or anhydrite is present in the reservoir rock or when soft water is unavailable for injection, and only thermally and chemically stable anionic surfactants can be used. Ether sulfonates are stable at high temperature and have good tolerance to hardness (Puerto *et al*., 2012), but they are expensive and quite difficult to manufacture. Moreover, only limited quantities of ether sulfonates with short hydrophobes (no PO incorporated) have been available in the past and even these products are unlikely to be available commercially in the future, so the need for a different surfactant structure to use at high temperature was compelling.

Alkyl alkoxy carboxylates offer an alternative anionic surfactant class for EOR (Shaw, 1984; Li et al., 2000; Li et al., 2005). By including PO and EO in the molecule, highly versatile alkyl polyoxy propylene/ethylene (alkoxy) carboxylates (AEC) can be formed (Abe et al., 1987). As opposed to alkyl carboxylates, which are commonly referred to as soap, AEC surfactants exhibit a high degree of tolerance to hardness combined with good water solubility and decreased sensitivity to changes in pH or electrolyte levels (DanChem Technologies Inc., 2011; Behler et al., 2001; Rosen, 2004), making the AEC a superior alternative to alkoxy sulfates.

AEC surfactants are products of the reaction of the terminal hydroxide (OH) group of an alkoxylate with sodium chloroacetate in the presence of sodium hydroxide and can be commercially made at > 90 wt% purity. The AEC surfactants are to be contrasted with ether carboxylates (EC) (DanChem Technologies Inc., 2011; Sasol, 2011; Behler et al., 2001). EC are high performance surfactants that exhibit good foaming ability, rapid surface wetting, and good detergency, and so they can be used as emulsifying, solubilizing, or dispersing agents (DanChem Technologies Inc., 2011; Behler et al., 2001; Rosen, 2004). With the inclusion of PO in the EC, the resulting AEC surfactants are highly versatile and can be utilized effectively in many different fields due to their advantageous physicochemical properties. Most importantly for EOR, the AEC have a high thermal and chemical stability and can be used at both acidic and alkaline pHs without any decomposition of the carboxylate functional group (Behler et al., 2001; Rosen, 2004).

In order to use AEC surfactants as an alternative to large hydrophobe Guerbet alkoxy sulfate (AES) surfactants for chemical EOR, cost-effective, large-hydrophobe AEC surfactants were developed. These can be produced by dimerizing linear alcohols to form a Guerbet alcohol, which can then be extended by addition of alkoxy groups such as

PO and EO followed by carboxylation (carboxymethylation).). Adkins *et al.* (2012) show that Guerbet alkoxy carboxylates can be made with large branched hydrophobes and with a wide range of PO and EO groups added. The synthesis reactions and molecular structure of these Guerbet alkoxy carboxylate surfactants are given in Figure 2-1. The conversion for each step is near quantitative. Thus the carboxylate surfactants are produced with more than 90 wt% overall yield as verified by NMR spectral analysis. The cost of these new carboxylate surfactants is competitive with commonly used commercial surfactants such as alkyl alkoxy sulfates. The Guerbet alkoxy carboxylate surfactant structures can be tailored to fit specific EOR needs by alteration of the number of carbons in the Guerbet alcohol and the number of PO and EO groups. These high-performance Guerbet alkoxy carboxylate surfactants are thus superior alternatives to Guerbet alkoxy sulfates due to their greater high-temperature stability, which greatly broadens the scope of chemical EOR.

Lu *et al.* (2014) shows good oil recovery results for these new Guerbet alkoxy carboxylate surfactants over a broad range of conditions from light to viscous oils, for both active and inactive oils at both low and high temperatures and in both sandstones and carbonates.

EXPERIMENTAL MATERIALS AND PROCEDURE

Synthesis of carboxylate surfactants

The synthesis reactions and molecular structure of these Guerbet alkoxy carboxylate surfactants are given in Figure 2-1. The conversion for each step is near quantitative. Thus the carboxylate surfactants are produced with more than 90 wt% overall yield as verified by NMR spectral analysis. The cost of these new carboxylate

surfactants is competitive with commonly used commercial surfactants such as alkyl alkoxy sulfates.

Surfactants and Materials

Anionic Surfactants

Guerbet alkoxy carboxylates were synthesized from Guerbet alkoxylates in the chemical EOR laboratory at the University of Texas at Austin. The Guerbet alkoxylates, internal olefin sulfonates (IOS), alcohol propoxy sulfates (APS) and alkyl benzene sulfonates (ABS) used in this study were obtained from Harcros Chemicals, Stepan Company, Huntsman Chemicals and Shell Chemical Company.

Co-solvents

Isobutyl alchohol (IBA), and triethylene glycol mono butyl ether (TEGBE) were received from Aldrich Chemicals.

Polymers

The polymers Flopaam 3630s and 3330s were received from SNF Floerger (Cedex, France).

Electrolytes and Brines

Sodium chloride, sodium carbonate, calcium chloride, magnesium chloride hexahydrate, and sodium sulfate were obtained from Fisher Chemical. Specific synthetic brines were made and used based on each specific reservoir application. Table 2-1 lists the brine compositions used in experiments for each oil.

Oils

Several dead crude oils and surrogate oils (a mixture of dead crude and a pure hydrocarbon) were used in this study (Table 2-2). Formulations are developed using

surrogate oils rather than live oil to save time and cost, but the final test should be done with live oil at high pressure. The surrogate oil is made based in part on the equivalent alkane carbon number (EACN) of the dead oil (Cayias et al., 1976; Salager et al., 1979; Glinsmann, 1979; Puerto and Reed, 1983; Roshanfekr, 2010; Roshanfekr et al., 2012; Jang et al., 2014).

Microemulsion Phase behavior tests

The phase behavior of various mixtures was carefully observed over an extended period of time. The mixtures that formed low-viscosity microemulsions and displayed ultra-low IFT with both oil and water were selected for the further evaluation. Their aqueous stability was tested at both room temperature and reservoir temperature. The aqueous solutions were observed to ensure that no cloudiness and/or phase separation occurred up to the desired injection salinity, which is usually the optimum salinity. These phase behavior observations are the key to our approach to the development of high-performance chemical formulations. A large number of mixtures can be made and observed over a period of time with relatively little cost or effort to explore the effect of surfactant type and concentration, co-surfactant type and concentration, co-solvent type and concentration, salinity, hardness, oil concentration, polymer type and concentration, temperature, etc. Both the interfacial tension and the viscosity can be observed by performing a quick emulsion test by briefly shaking the pipettes and then observing the coalescence of the emulsion to form separate oil, water and microemulsion phases. After reaching equilibrium, the phase volumes can be read and used to calculate interfacial tension using the Huh equation (Huh, 1979).

In this particular study, the variation of the number of POs and EOs in the carboxylate surfactants was the key method used to select the best primary surfactant

structure. For example, the number of POs and EOs in the surfactant was varied to achieve the desired optimum salinity (Bourrel and Schechter, 1988; Green and Willhite, 1988). Co-solvent was used to reduce the microemulsion viscosity and increase the aqueous solubility of the surfactants at optimum salinity using the procedures in Sahni et al. (2010).

Aqueous stability tests

The aqueous solubility of each chemical formulation is tested by adding the aqueous solution from the phase behavior experiments to 20 mL glass ampules. Typically a scan (either salinity or sodium carbonate) that mirrors the phase behavior scan is produced. When polymer is part of the chemical EOR process, then about 1000-3000 ppm of polymer is added to the aqueous solubility ampules. The ampules are blanketed with Argon and sealed using the propane-oxygen torch. The ampules are mixed using the Vortex Genie 2 until a homogenous solution is created. Observations of the aqueous solutions are recorded first at room temperature and next the ampules are equilibrated at reservoir temperature using the ovens. The aqueous solutions continue to be monitored after reaching reservoir temperature. The thermal and chemical stability of the GAEC surfactants were studied by comparing the aqueous solubility and phase behavior results over time at elevated temperatures.

Coreflood experiments

The coreflood experiments were designed with favorable salinity gradients to maximize robustness of the corefloods (Glover et al. 1979; Pope et al., 1979; Hirasaki et al., 1983; Levitt et al., 2009). The cores were evacuated and then saturated with the synthetic formation brine followed by injection of brine to measure the brine permeability. The following flooding sequence was then used: 1. oil was injected at about

100 psi to establish residual water saturation and measure oil permeability at residual water saturation; 2. water was injected to establish residual oil saturation to water; 3. aqueous chemical solutions were injected to measure residual oil saturation to chemical. Effluent samples were collected in graduated test tubes for fluid analysis. Differential pressure transducers were used to measure the pressure drop across several sections of the core and the entire core. All of the corefloods were done vertically in a convection oven at reservoir temperature. More details of the coreflood procedure can be found in Levitt et al., (2009); Flaaten et al., (2010); Zhao et al., (2008); Solairaj et al., (2012); and Unomah (2013). The coreflood experiments are summarized in Table 2-3.

RESULTS AND DISCUSSION

Experimental results for low-temperature and low-salinity active oils in sandstones

Phase behavior experiments are completed to study the behavior of the mixtures of the oil, brine, and chemicals (including the surfactant formulation plus additional salt or alkali) at reservoir temperature. Ideally after a few days a middle-phase microemulsion will form which shows a low viscosity and an ultra-low interfacial tension with both the excess aqueous and oil phases. The GAEC surfactants have been used under a wide variety of conditions of temperature, salinity, divalent ion concentration, pH, and crude oil to develop effective surfactant formulations.

Yang et al. (2010) recently reported many ASP core flooding results for viscous oils. Viscous oils with low API gravity are usually active (contain organic acids that react with alkali to form soap). The use of alkali reduces the surfactant cost and makes ASP flooding economically attractive under many circumstances. However, in some situations the use of alkali is not feasible, so SP formulations have to be developed to meet requirements.

Oil #1 with 75 cp viscosity is such an example. This oil is an active oil in a sandstone reservoir at 46 °C. The oil properties are summarized in Table 2-1. The SP formulation developed for this oil consists of 0.5 wt% C_{28}-35PO-10EO-carboxylate, 0.5 wt% C_{20-24}-IOS, 1.0 wt% IBA. Figure 2-2 shows the solubilization ratio at optimum salinity of ~32,000 ppm is about 50, which is an extremely high value indicating ultra-low interfacial tension. The surfactant aqueous stability is up to 39,000 ppm TDS. SP coreflood #1 was then designed using the phase behavior and viscosity data. The coreflood was conducted in a Berea sandstone core at reservoir temperature of 46 °C to verify the surfactant formulation performance. A 0.6 PV surfactant slug containing 0.5 wt% surfactant (PV×C=30) was injected at the optimum salinity of ~32,000 ppm followed by a polymer drive of 22,400 ppm salinity. Figure 2-3 shows the oil recovery results for coreflood #1. The final oil recovery was 90.1 % of water flood residual oil saturation and the final oil saturation was 0.041. No surfactant was detected in the effluent samples. Thus all of the injected surfactant (0.28 mg surfactant per gram of rock) was retained. More details of all the corefloods are summarized in Table 2-3.

Oil #2 is an active oil with viscosity of 10.5 cp in a sandstone reservoir with temperature of 44 °C. The surfactant formulation used for this oil was 0.25 wt% C_{28}-35PO-10EO-carboxylate, 0.25 wt% C_{12}-ABS, 0.25 wt% C_{13}-13PO-sulfate, and 0.25 wt% TEGBE. The phase behavior results after 57 days are shown in Figure 2-4. The optimum solubilization ratio is about 12 at the optimum salinity of ~30,000 ppm TDS. The aqueous stability is 40,600 ppm TDS. Coreflood #2 was performed in a Bentheimer sandstone core. A 0.4 PV (PV×C=30) surfactant slug was injected at the optimum salinity of 30,200 ppm followed by a polymer drive of 15,200 ppm salinity. The results were 98.2% recovery of the waterflood residual oil and a final oil saturation of 0.006 shown in Figure 2-5. The surfactant retention was 0.26 mg/g.

Experimental results for high-temperature and high-salinity inactive oils in carbonate

Levitt et al. (2012) reported an ASP coreflood in a high-temperature, high-salinity carbonate core. However, conventional alkali cannot be used when anhydrite is present or soft injection water is not an option, so it is useful to develop SP formulations for such cases.

When softening the injection water is not an option, chelating agents such as tetrasodium ethylene-diaminetetraacetate (EDTA-Na_4) can be used to chelate divalent cations, as reported by Yang et al. (2010). However, EDTA-Na4 is relatively expensive, and the required amount to complex divalent cations at high temperature is higher than the theoretical value of 9 to 1 weight ratio of EDTA to Ca. GAC surfactants with a large number of EOs are very tolerant of both high salinity and high divalent cation concentrations. The number of POs and EOs can be optimized for a specific brine composition, oil and temperature as part of the formulation development.

Oil #3 is an inactive oil with an API gravity of 22 degrees (oil properties can be found in Table 2-1 in an oil-wet fractured carbonate reservoir with a temperature range of 100-120 °C). Both the formation brine and injection brine are hard brine with high salinity and high hardness (Table 2-2). The EACN of oil was estimated to be about 16, which means this oil behaves more like “heavy” oil from surfactant perspective. All these conditions make this oil extremely difficult to find the suitable surfactant formulations to achieve both ultra-low IFT and aqueous stability.

During the initial screening phase with this oil, the selection process was mainly focused on all the conventional surfactants available at that time. IOS, AOS and ABS surfactants with different sizes of hydrophobes showed good results with other many different oils in our lab, so they were the first candidates to test with this oil at reservoir

conditions. Initial screening tests indicated that none of these surfactants or their combinations worked for this oil. The alkyl benzene sulfonates tested were C_{15-18}, C_{12-18}, C_{19-28}, C_{20-24} and C_{14-30}-ABS. The alpha olefin sulfonate tested was C_{20-24}-AOS. The internal olefin sulfonates tested were C_{15-18}, C_{19-23}, C_{20-24}, C_{19-28} and C_{24-28}-IOS.

For example, the formulation of 0.75 wt% C_{20-24}-AOS and 0.25 wt% C_{15-18}-IOS and 1.0 wt% Butanol-2.15EO as co-solvent showed a very low solubilization ratio of ~2 with 65,000 ppm aqueous stability in softened brine. Another example was the formulation 0.75 wt% C_{20-24}-IOS and 0.25 wt% C_{15-18}-IOS, which showed all type II over the entire salinity range. The solubilization ratio was not readable, and the aqueous stability was 40,000 ppm soft brine. These two formulations do not have aqueous stability in hard brine and the solubilization ratios are even lower. These surfactants formulations did not perform well, because AOS is a linear hydrophobe surfactant, and ABS are very sensitive to hardness leading to bad aqueous stabilities. Ether sulfonates have good tolerance to hardness and high temperature stability, so a mixture of ether sulfonate and IOS surfactants was tried and showed the best results at that time. The results are shown in Figure 2-6. This formulation has 0.5 wt% C_{12-15}-15EO glyceryl sulfonate and 0.5 wt% C_{20-24}-IOS. The results showed only type I behavior with a maximum solubilization ratio of ~6, and all aqueous solutions were cloudy. The results indicated that more co-solvent was needed to improve the aqueous stability, however, this would worsen solubilization ratios and increase the IFT. All these surfactants tested are short hydrophobe surfactants and they do not perform well for “heavier” oil that requires large hydrophobe surfactants with stronger molecular interactions with the oil.

Some alcohol ether sulfate surfactants were also tested including short-hydrophobe surfactants such as C_{16}-17-7PO-sulfate, C_{13}-30EO-sulfate, C_{12}-15-12EO-sulfate and large-hydrophobe surfactants such as C_{28}-7PO-6EO-sulfate, C_{32}-7PO-6EO-

sulfate, C_{32}-7PO-10EO-sulfate and so on. The ether sulfates require high pH or alkali uses to be stabilized at high temperature, where injection brine has to be softened for use. Even in high pH conditions, the decompositions of ether sulfates are still ongoing slowly. These restrictions ruled out ether sulfates as candidate surfactants.

After the initial development of the large-hydrophobe GAC surfactants, investigations focused on selecting GAC and sulfonates combinations. Both surfactants structures are branched, which is favorable in terms of good performance. Neither the GAC surfactant nor the IOS surfactant generated ultra-low IFT and the passed aqueous stability by itself. However, when the two surfactants are mixed together, the mixtures performed very well with this oil under such harsh conditions, thus showing a synergistic behavior. The GAC and IOS as co-surfactant formulations are tolerant to high salinity, high hardness and high temperature. They achieved ultra-low IFT and adequate long-term aqueous stability. The formulations developed for this oil did not need co-solvent to form low viscosity microemulsions due to their branched structure.

Figure 2-7 shows the microemulsion phase behavior results of a formulation consisting of 0.5 wt% C_{24}-25PO-56EO-carboxylate and 0.5 wt% C_{19-23}-IOS at 100 °C after more than 97 days. The elevated temperature of this experiment made co-solvent unnecessary. The phase behavior scan consists of brine #3 (composition in Table 2-2) with additional sodium chloride added to produce a salinity gradient. The corresponding oil (red) and water (blue) solubilization ratios are plotted as a function of salinity. The optimal salinity occurs at 38,000 ppm with an optimal solubilization ratio of 22 corresponding to an ultralow IFT of about 6.2×10^{-4} dynes/cm using the Huh equation (Huh, 1979). The aqueous solutions were clear and stable up to 57,000 ppm TDS at the reservoir temperature of 100 °C. Additionally, this phase behavior experiment also showed a low microemulsion viscosity.

To increase the optimum salinity, another surfactant formulation for the same oil was developed consisting of 0.5 wt% C_{28}-25PO-25EO-carboxylate and 0.5 wt% C_{15-18}-IOS at 100 °C with varying concentrations of brine #3 to produce the salinity scan. Figure 2-8 presents the solubilization ratios for this formulation after 170 days. The optimal salinity is 60,000 ppm with a solubilization ratio of 12. The aqueous solution is clear until a salinity of 61,000 ppm is reached. For reference, the solubilization ratios of the same formulation are also plotted after 70 days in Figure 2-9. The chemical and thermal stability of the surfactants are indicated as there is no appreciable change in the phase behavior even after 170 days.

For an even higher temperature of 120 °C for the same oil #3, the following formulation was developed: 0.5 wt% C_{28}-45PO-60EO-carboxylate and 0.5% C_{15-18}-IOS. The phase behavior salinity scan was created by varying the ratio of brine #3 to brine #4. The solubilization ratio remained greater than 10 at optimum salinity for more than 100 days at this high temperature (Fig. 2-10), which indicates the surfactants are stable at 120 °C. Alkoxy sulfate surfactants are not stable at this temperature and neutral pH. More evidence of the stability of the carboxylate surfactants is also demonstrated by the long term aqueous stability in hard brines (Adkins et al., 2012).

Oil #4a is an inactive oil in a carbonate reservoir at 105 °C. Two surfactant formulations with carboxylate and IOS surfactants were identified for this oil in hard brine: 1) 0.5 wt% C_{28}-25PO-25EO-carboxylate, 0.5 wt% C_{15-18}-IOS, 0.5 wt% TEGBE; 2) 0.5 wt% C_{28}-25PO-25EO-carboxylate, 0.4wt % C_{15-18}-IOS, 0.1 wt% C_{19-23}-IOS, 0.5 wt% TEGBE. Figure 2-11 shows both results for oil #4a at 105 °C with mixing brine #5 and #6. This is also a good example of synergism with surfactant mixtures. Keeping the total surfactant concentration the same, the formulation with three surfactant components (0.5wt% C_{28}-25PO-25EO-carboxylate, 0.4wt% C_{15-18}-IOS, 0.1wt% C_{19-23}-IOS, 0.5wt%

TEGBE) gives a higher optimum solubilization ratio than a mixture of two surfactants (0.5 wt% C_{28}-25PO-25EO-carboxylate, 0.5 wt% C_{15-18}-IOS, 0.5 wt% TEGBE). The additional component with a different carbon chain may enhance the phase behavior performance by matching more components in the crude oil.

In an attempt to seek an alternative and less expensive co-surfactant, a C_{15-17} linear alkyl benzene sulfonate (ABS) was evaluated with oil #4b replacing the IOS. ABS has long been considered to be incompatible with hard brine, however, this case shows a synergistic effect between the GAC and ABS surfactants that improved the performance of both surfactants. A novel co-solvent phenol ethoxylate was also added to improve the surfactant performance. 15,000 ppm $EDTANa_4$ was introduced to alter the wettability toward water-wet in this mixed wet carbonate rock (Chen and Mohanty, 2013), to chelate iron to avoid polymer degradation, and to raise the pH. The formulation consisted of 0.5 wt% C_{28}-45PO-60EO-carboxylate, 0.5 wt% C_{15-17}-ABS, 0.5 wt% Phenol-2EO with 15,000 ppm $EDTANa_4$ in hard brine. This formulation gave favorable phase behavior results as shown in Figure 2-12. The solubilization ratio is about 12 at the optimum salinity of about 27,000 ppm TDS. The aqueous solution is clear up to a salinity of 35,700 ppm.

Coreflood #3 was then designed based on the phase behavior results in Figure 2-12. The coreflood was conducted in an Estaillade limestone core at reservoir temperature of 105 °C to test the performance of the surfactant formulation. A 0.4 PV surfactant slug (PV×C=40) was injected at the optimum salinity of ~29,000 ppm (including 15,000 ppm $EDTANa_4$ and 14,000 ppm brine) followed by a polymer drive of 25,000 ppm salinity (15,000 ppm $EDTANa_4$ and 10,000 ppm brine). Figure 2-13 shows the oil recovery results for coreflood #3. The final oil recovery was 86.8 % of water flood residual oil saturation and the final oil saturation was 0.022. No surfactant was detected in the

effluent samples. Thus all of the injected surfactant (0.62 mg surfactant per gram of rock) was retained.

An example with high salinity and hardness is the SP formulation developed for oil #5. Coreflood #4 was done with this formulation. The SP formulation for this oil was 0.66 wt% C_{28}-25PO-45EO-carboxylate, 0.4 wt% C_{15-18}-IOS, 0.3 wt% C_{19-28}-IOS, 1.0 wt% TEGBE at 78 °C shown in Figure 2-14. This formulation exhibits high solubilization ratios and good aqueous stability. The solubilization ratio is about 42 at optimum salinity of about 63,000 ppm TDS. The aqueous solution is clear up to a salinity of 102,600 ppm TDS. This formulation was tested in a vuggy and heterogeneous Silurian dolomite core. The formation brine contained 235,400 ppm TDS with a divalent cation concentration of 31,750 ppm. The surfactant slug had a salinity of 62,700 ppm TDS with a divalent cation concentration of 1,800 ppm. A 0.3 PV (PV×C=41) slug was injected followed by a polymer drive with salinity of 32,700 ppm. The surfactant recovered 91.6% of the water flood residual oil, with a final oil saturation of 0.032. The oil recovery results are shown in Figure 2-15. The surfactant retention was 0.16 mg/g.

SUMMARY

Novel Guerbet alkoxy carboxylate surfactants with large branched hydrophobes have shown excellent performance in corefloods over a wide range of reservoir conditions up to at least 120°C. The number of PO and EO groups in these new surfactants were optimized for a wide variety of oils over a broad range of salinity, hardness and temperature and mixed with various co-surfactants and co-solvents to develop high-performance formulations based on the microemulsion phase behavior. Both ultra-low IFT and clear aqueous solutions at optimum salinity were obtained for both active and inactive oils and both light and medium gravity oils over a wide range of

temperatures. Both sandstone and carbonate corefloods using these carboxylate surfactants showed excellent performance at high temperature, high hardness and high salinity as indicated by high oil recovery, low pressure gradients and low surfactant retention. The advent of such a new class of cost-effective surfactants significantly broadens the potential application of chemical EOR processes to target oil reservoirs.

Table 2-1: Oil Properties

Oil #	Temperature (°C)	API	Total Acid Number (mg KOH/g oil)	Surrogate Oil	Surrogate Oil Viscosity (cp)
1	46	21	2.00	14 wt% cyclohexane and 86 wt% dead oil	75
2	44	22	1.30	20 wt% decalin and 80 wt% dead oil	10.5
3	100	22	0.15	30 wt% cyclohexane and 70 wt% dead oil	2.1
3	120	22	0.15	30 wt% cyclohexane and 70 wt% dead oil	1.1
4a	105	34	0.10	33.4 wt% decalin and 66.6 wt% dead oil	1.4
4b	105	34	0.10	13 wt% toluene and 87 wt% dead oil	2.0
5	78	27	0.50	35.6 wt% cyclohexane and 64.4 wt% dead oil	1.7

Table 2-2: Brine Compositions

Brine #	Na^+ (ppm)	Ca^{2+} (ppm)	Mg^{2+} (ppm)	K^+ (ppm)	SO_4^{2-} (ppm)	HCO_3^- (ppm)	Cl^- (ppm)	TDS (ppm)
1	1660	30	10	30	0	0	2670	4400
2	900	400	200	300	1900	0	1500	5200
3	12,188	480	1342	0	3250	0	21,133	38,393
4	41,473	3,880	145	0	500	0	70,971	116,969
5	8267	965	144	0	1175	329	13,844	24,758
6	885	235	35	0	1273	305	774	3516
7	57,600	30,300	1450	550	0	0	145,467	235,400

Table 2-3: Coreflood Summary

Coreflood #	1	2	3	4
Oil #	1	2	4b	5
Temperature, °C	46	44	105	78
Core type	Berea sandstone	Bentheimer sandstone	Estaillade limestone	Silurian dolomite
Brine permeability, md	283	1714	128	242
Initial oil saturation, S_{oi}	0.802	0.750	0.51	0.627
Waterflood residual oil saturation, S_{orw}	0.411	0.351	0.17	0.387
Initial salinity (ppm)	4,400	5,200	24758	235,400
Surfactant Slug				
Surfactant concentration(wt%)	0.5	0.75	1.0	1.36
PV injected	0.6	0.4	0.4	0.3
PV×C (%)	30	30	40	41
Polymer	FP 3630s	FP 3330s	FP 3330s	FP 3330s
Polymer concentration (ppm)	4,200	3,000	3,000	4,250
Viscosity (cp)	90	19.9	12	15.3
Salinity (ppm)	31,900	30,200	29,000	62,700
Velocity (ft/day)	1.2	1.0	1.0	1.0
Polymer Drive				
Polymer concentration (ppm)	4,000	2,800	3,000	4,250
Viscosity (cp)	85	19.4	15	14.4
Salinity (ppm)	22,400	15,200	25,000	32,700
Velocity (ft/day)	1.2	1.0	1.0	1.0
Coreflood Results				
Oil Recovery (%)	90.1	98.2	86.8	91.6
Final residual oil saturation, S_{orc}	0.041	0.006	0.022	0.031
Surfactant retention (mg/g)	0.28	0.26	0.62	0.16

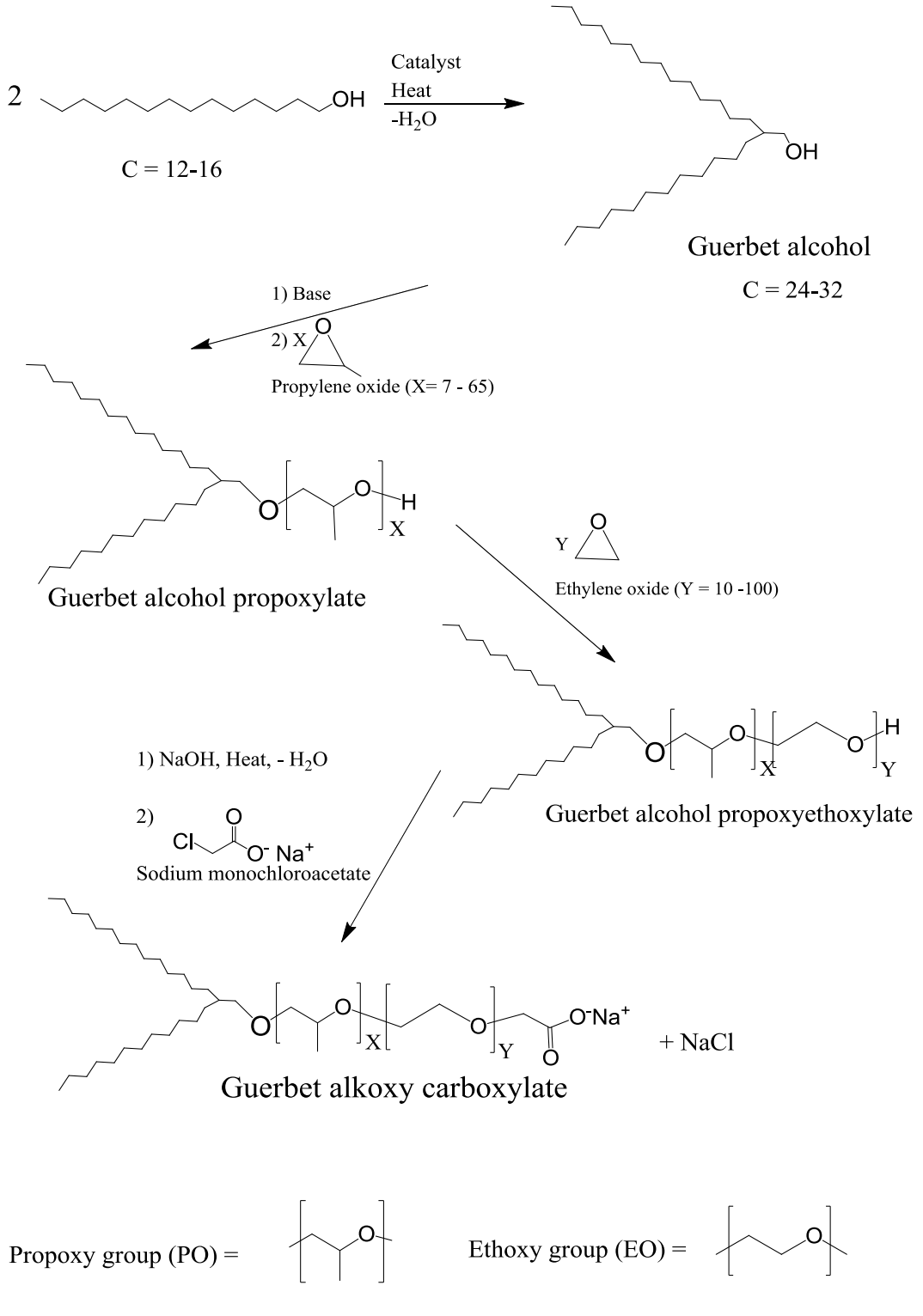

Figure 2-1: Reactions used to synthesize Guerbet alkoxy carboxylate surfactants.

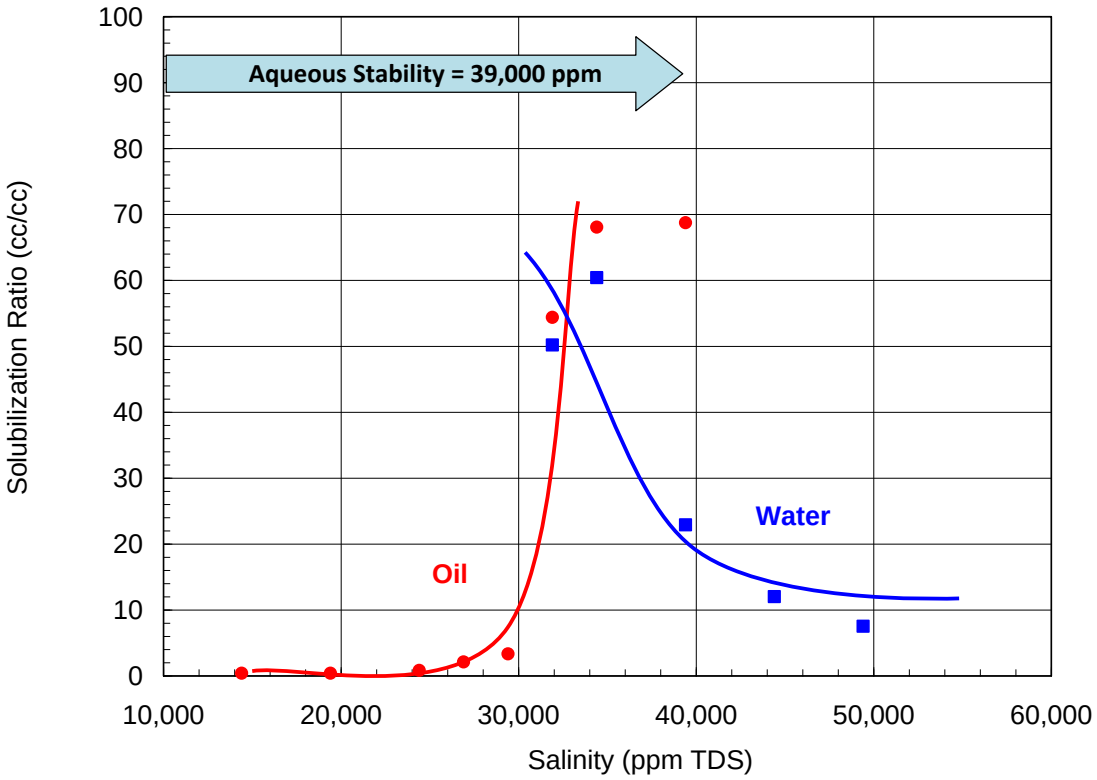

Figure 2-2: Phase behavior of 0.5wt% C_{28}-35PO-10EO-carboxylate, 0.5wt% C_{20-24}-IOS, 1.0 wt% IBA for oil #1 at 46 °C with 40 vol% oil after 70 days.

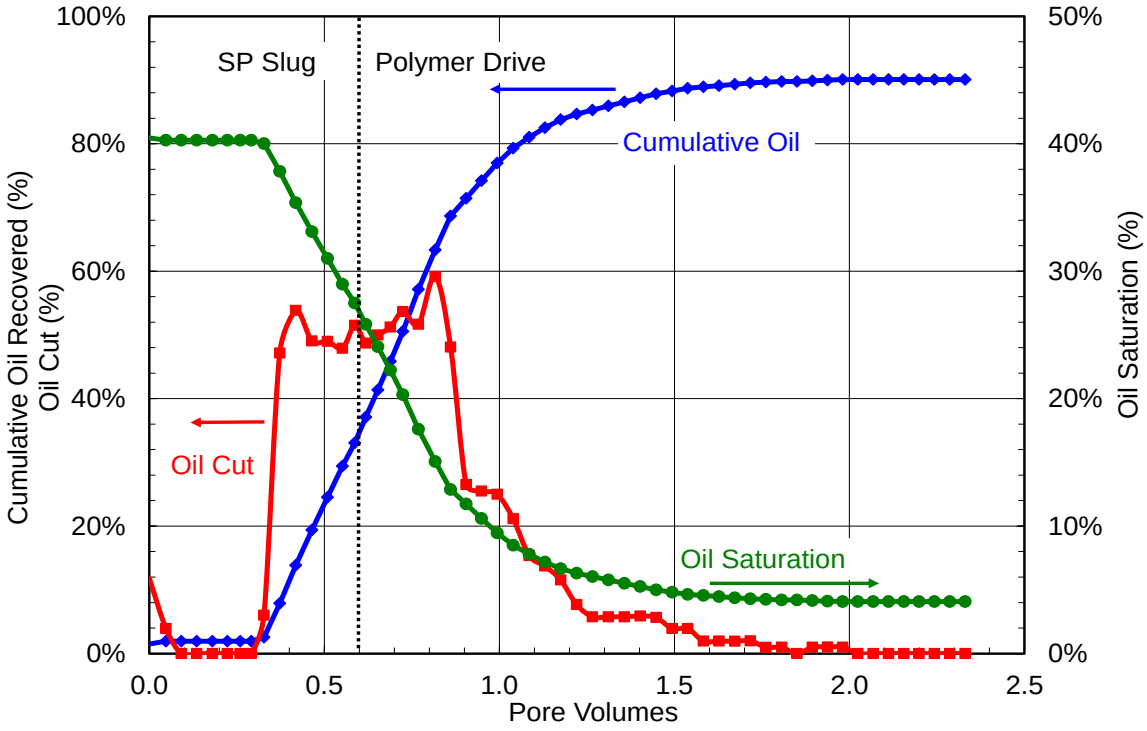

Figure 2-3: Oil recovery from coreflood #1 for oil #1 in Berea sandstone at 46 °C.

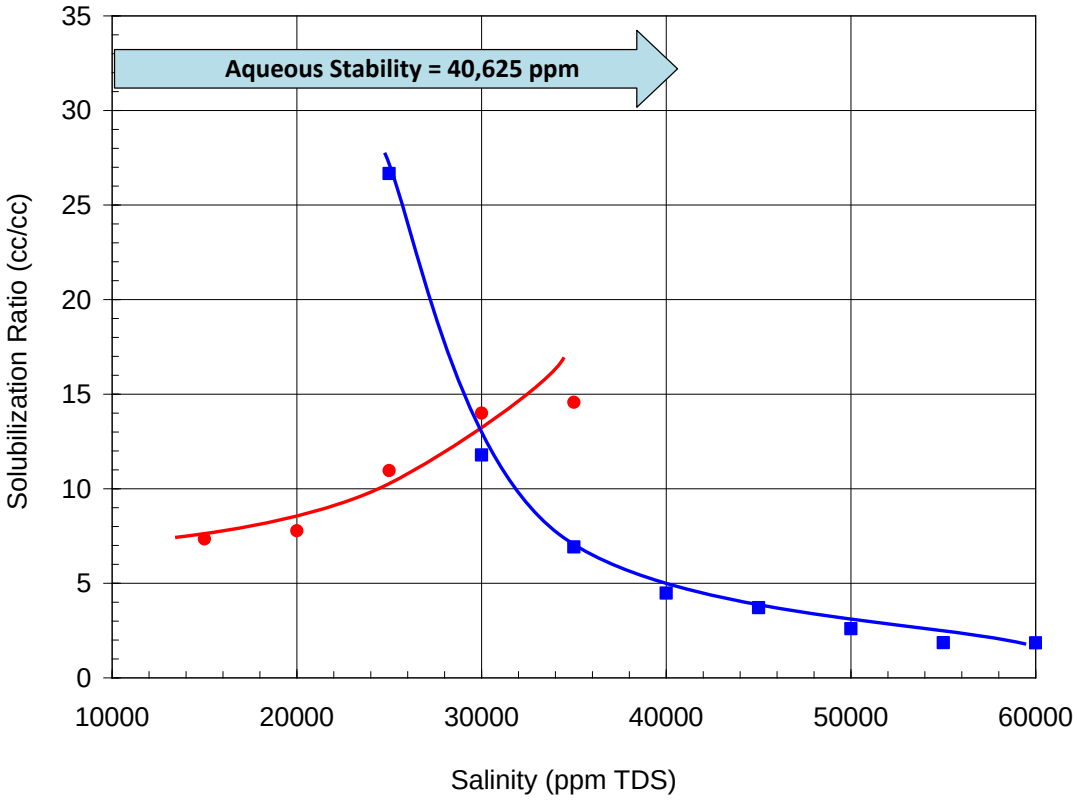

Figure 2-4: Phase behavior of 0.25wt% C_{28}-35PO-10EO-carboxylate, 0.25wt% C_{12}-ABS, 0.25 wt% C_{13}-13PO-sulfate, 0.25 wt% TEGBE for oil #2 at 44 °C with 40 vol% oil after 57 days.

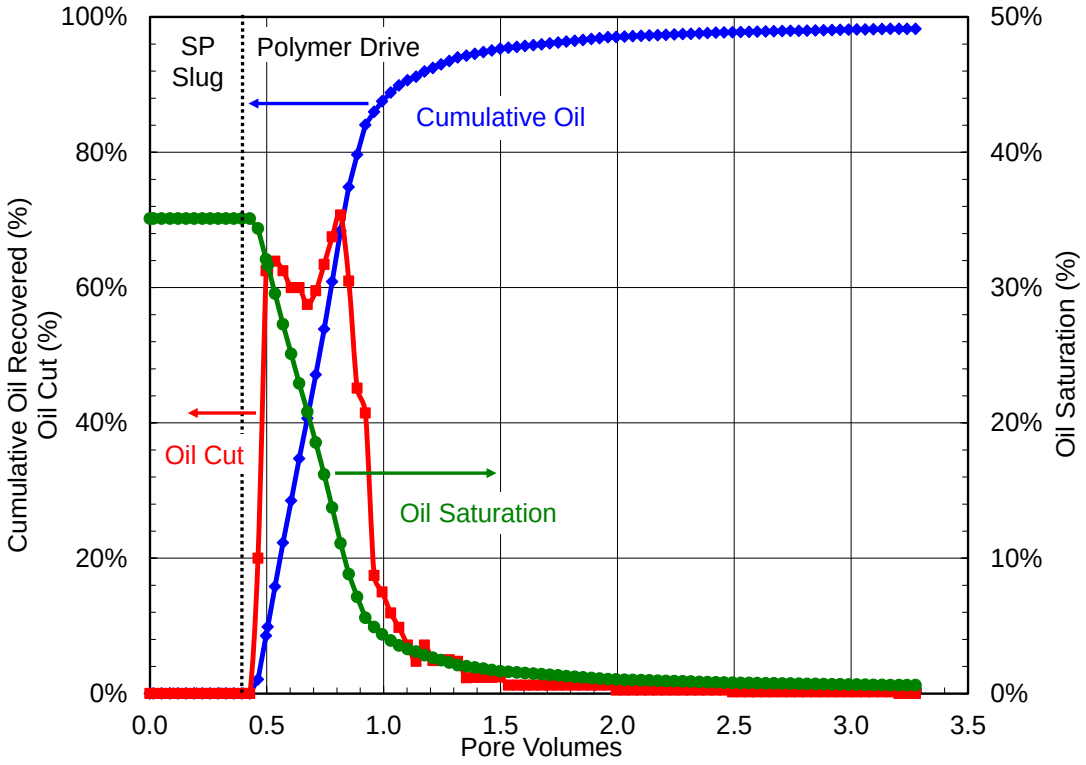

Figure 2-5: Oil recovery from coreflood #2 for oil #2 in Bentheimer sandstone at 44 °C.

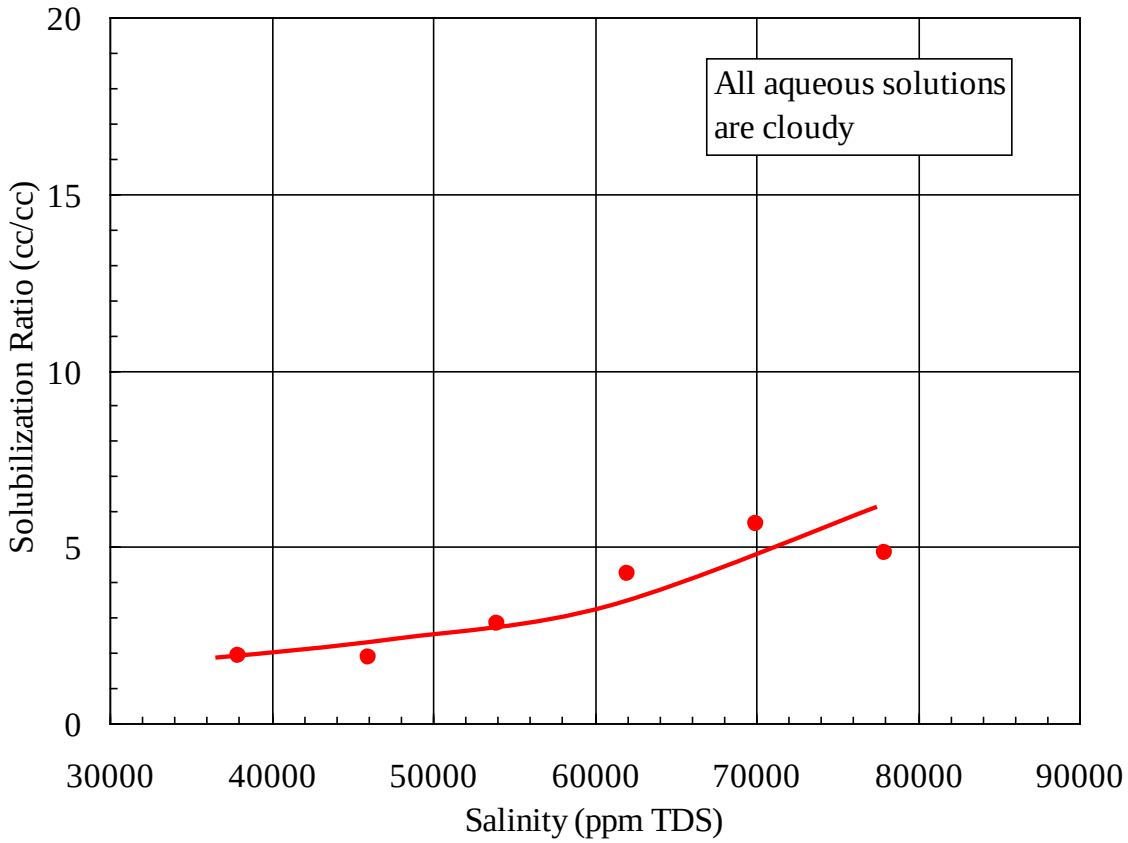

Figure 2-6: Phase behavior of 0.5 wt% C_{12-15}-15EO glyceryl sulfonate and 0.5 wt% C_{20-24}-IOS for oil #3 at 100 °C with 50 vol% oil after 18 days.

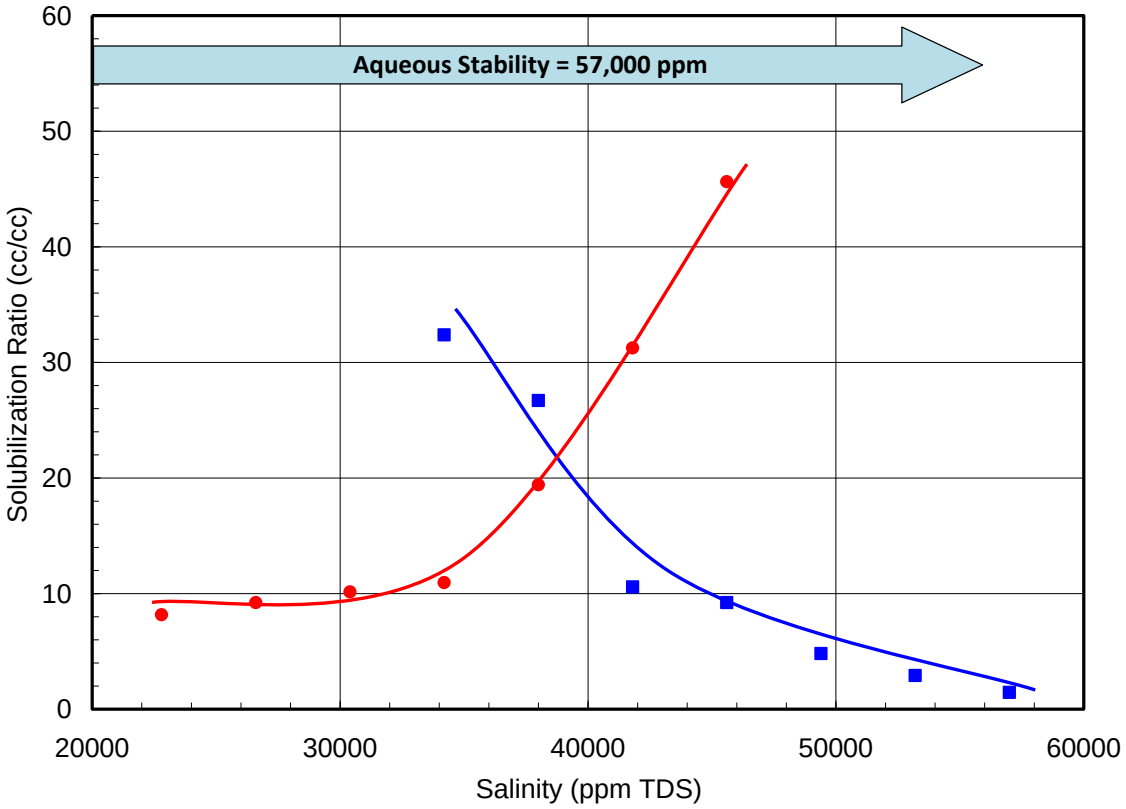

Figure 2-7: Phase behavior of 0.5 wt% C_{24}-25PO-56EO-carboxylate and 0.5 wt% C_{19-23}-IOS for oil #3 at 100°C with 50 vol% oil after 97 days.

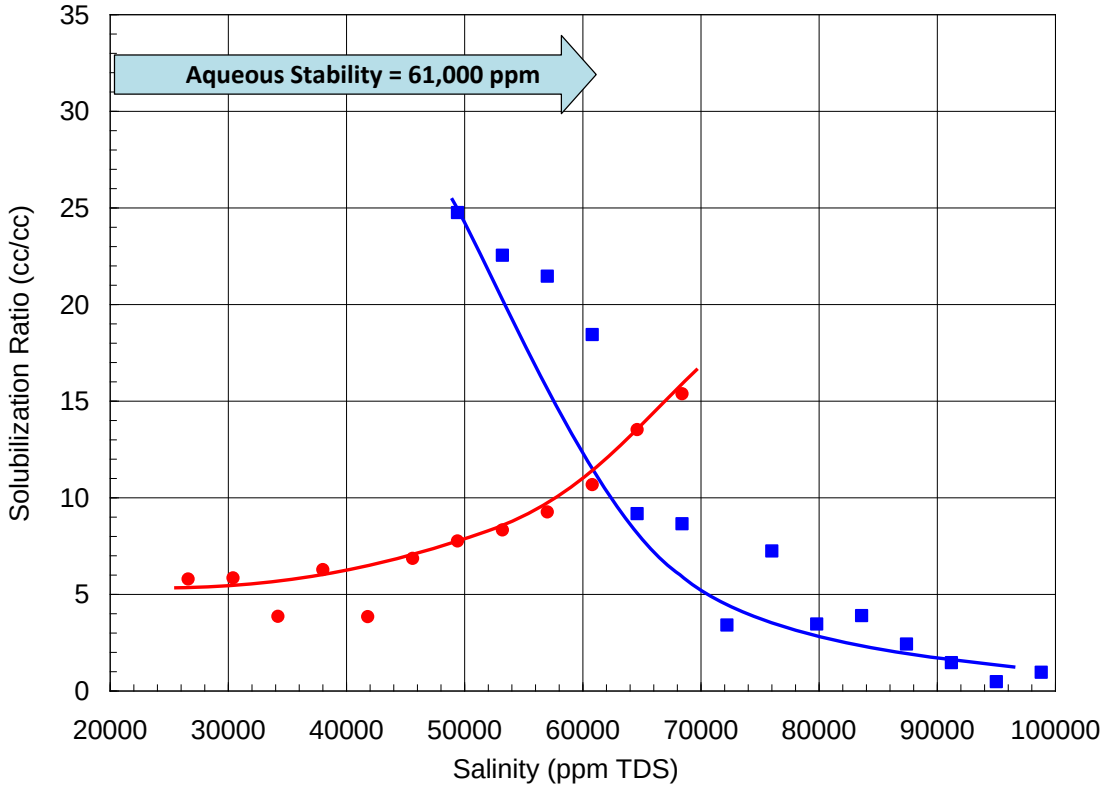

Figure 2-8: Phase behavior of 0.5 wt% C_{28}-25PO-25EO-carboxylate and 0.5 wt% C_{15-18}-IOS for oil #3 at 100°C with 50 vol% oil after 170 days.

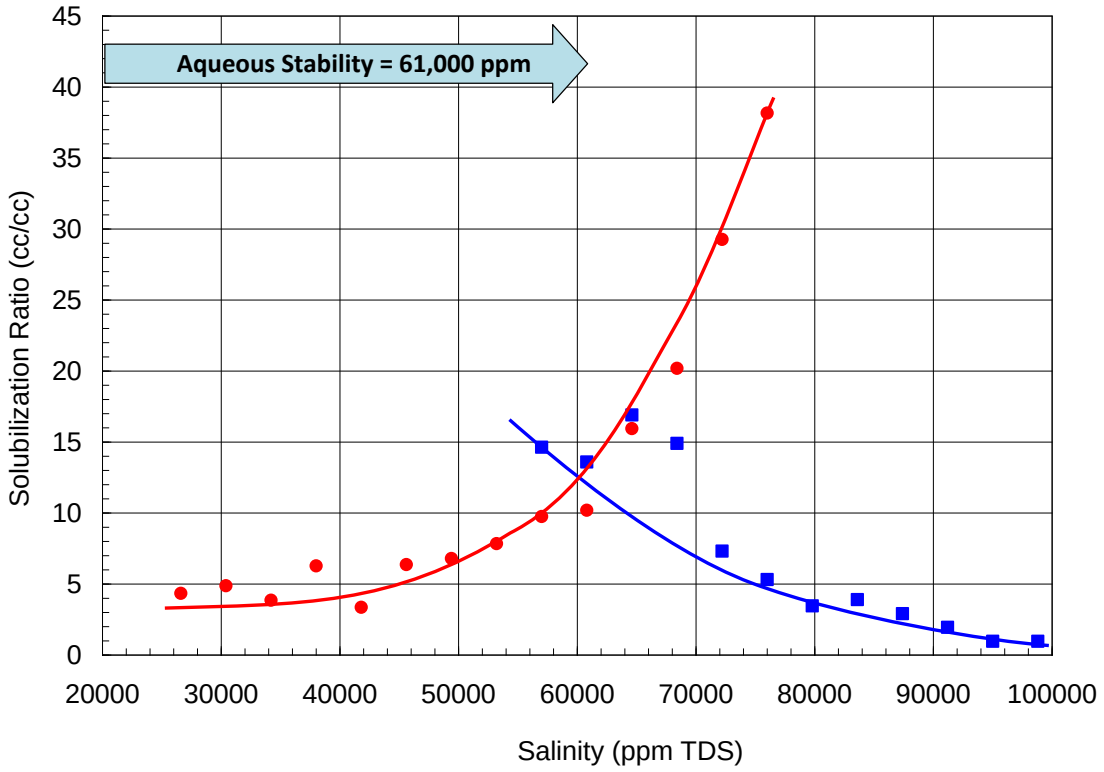

Figure 2-9: Phase behavior of 0.5 wt% C_{28}-25PO-25EO-carboxylate and 0.5 wt% C_{15-18}-IOS for oil #3 at 100°C with 50 vol% oil after 70 days.

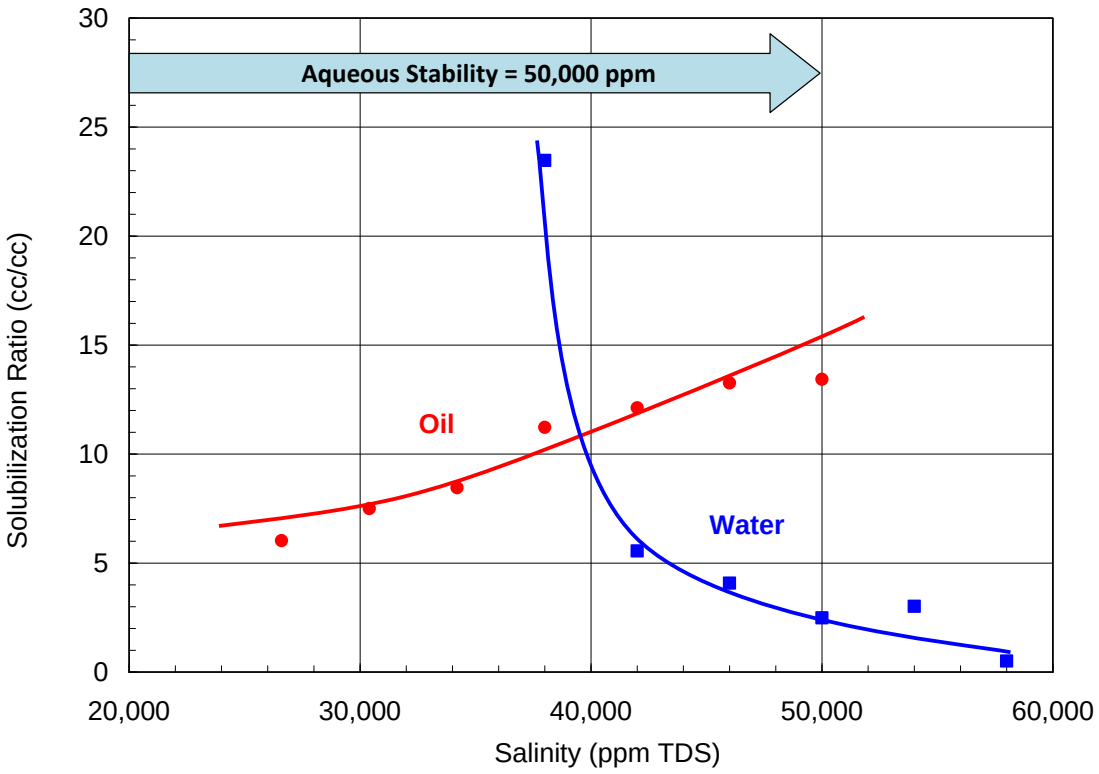

Figure 2-10: Phase behavior of 0.5 wt% C_{28}-45PO-60EO-carboxylate and 0.5 wt% $C_{15\text{-}18}$-IOS for oil #3 at 120°C with 50 vol% oil after 100 days.

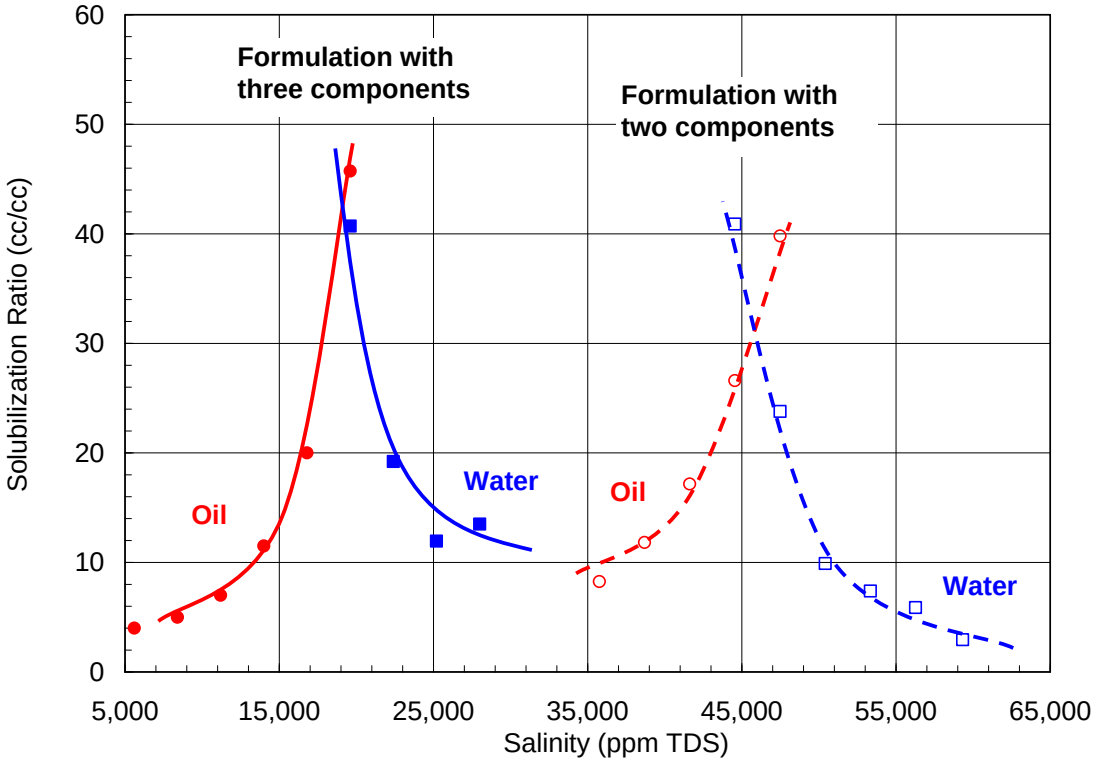

Figure 2-11: Phase behavior of two surfactant mixtures for oil #4a at 105°C with 50 vol% oil after 13 days.

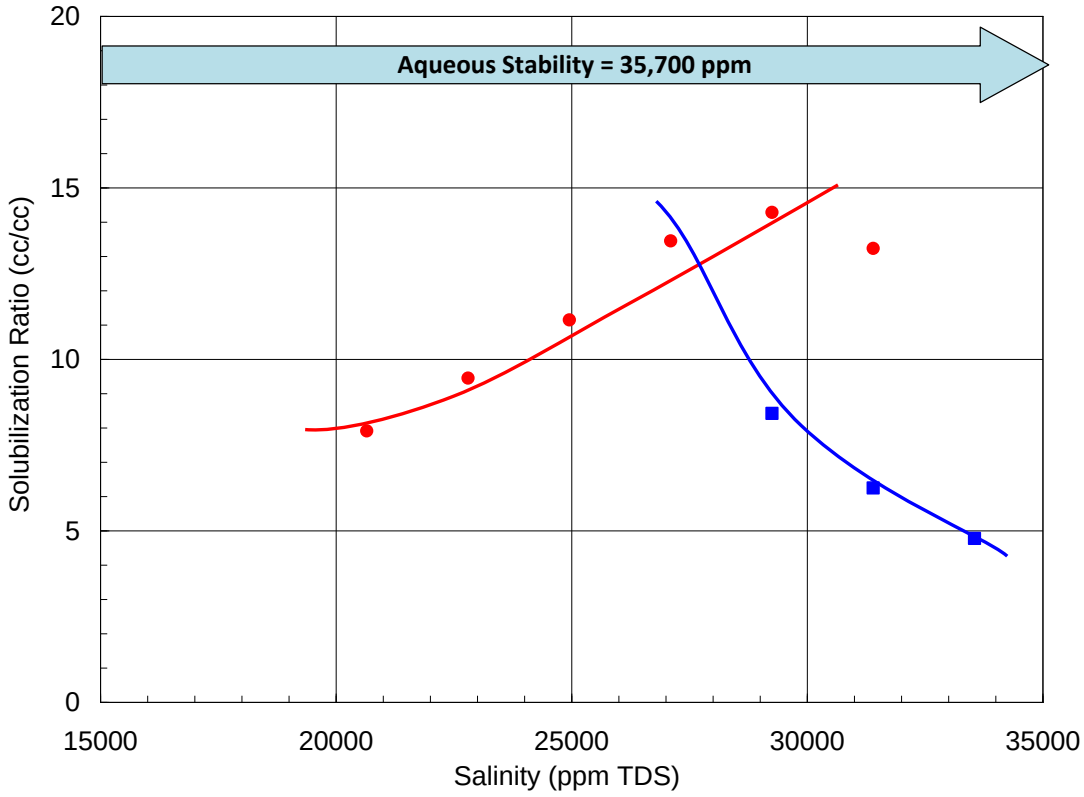

Figure 2-12: Phase behavior of 0.5 wt% C_{28}-45PO-60EO-carboxylate, 0.5 wt% $C_{15\text{-}17}$-ABS, 0.5 wt% Phenol-2EO for oil #4b at 105°C with 30 vol% oil after 41 days.

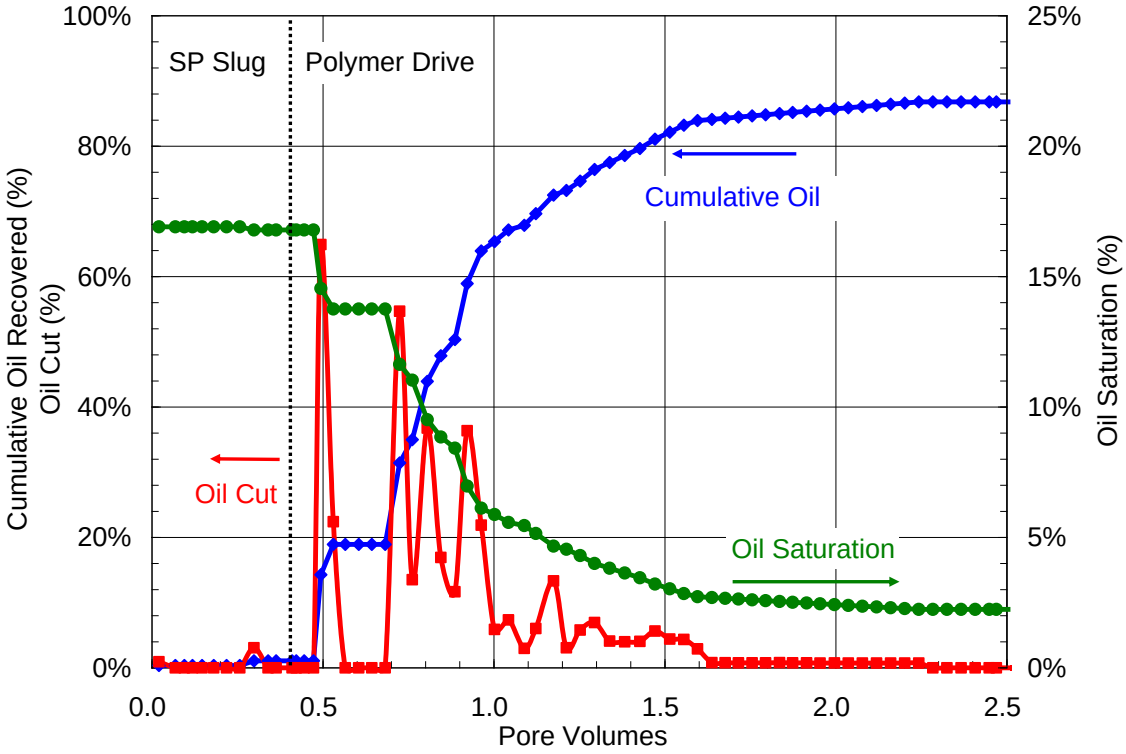

Figure 2-13: Oil recovery from coreflood #3 for oil #4b in an Estaillade limestone at 105 °C.

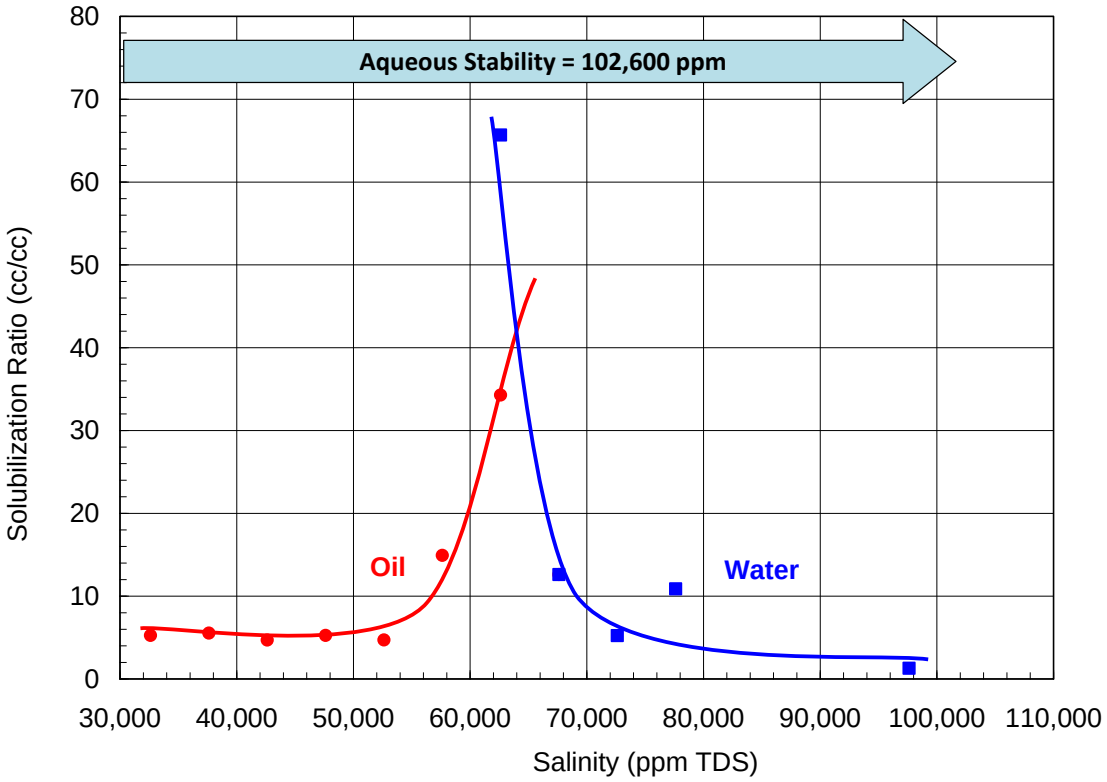

Figure 2-14: Phase behavior of 0.66 wt% C_{28}-25PO-45EO-carboxylate, 0.4 wt% $C_{15\text{-}18}$-IOS, 0.3 wt% $C_{19\text{-}28}$-IOS, 1.0 wt% TEGBE for oil #5 at 78°C with 50 vol% oil after 12 days.

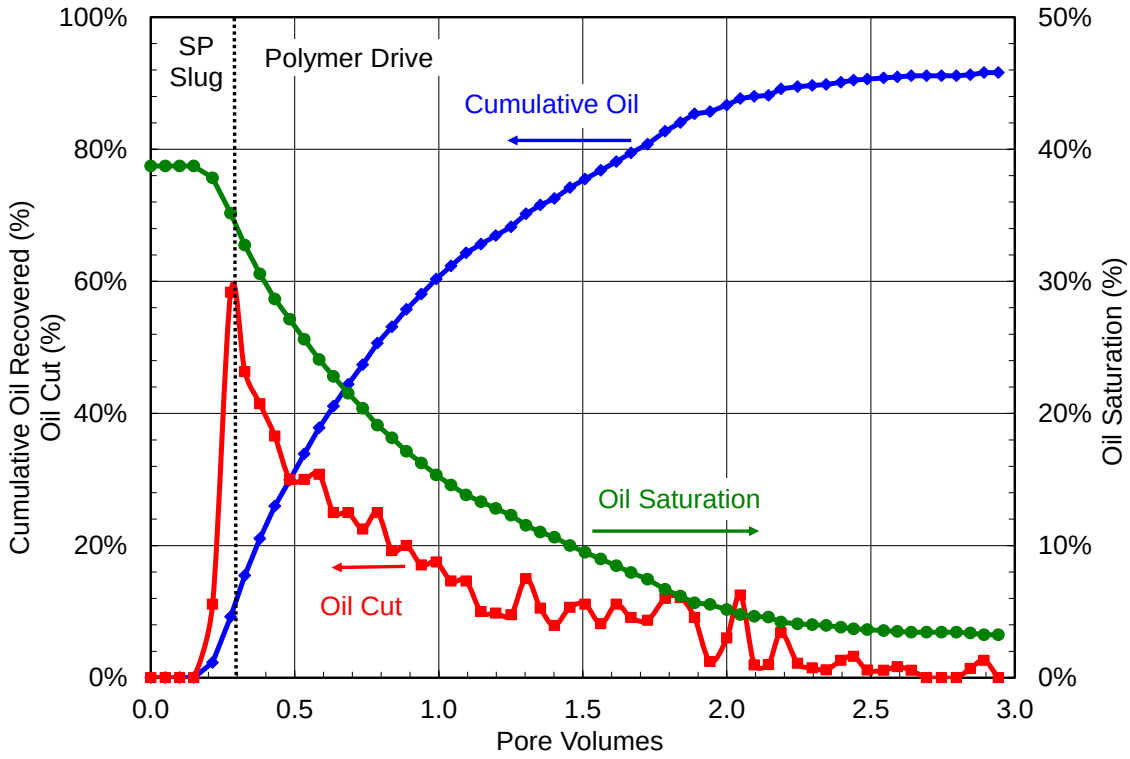

Figure 2-15: Oil recovery from coreflood #4 for oil #5 in a Silurian dolomite at 78 °C.

Chapter III: Surfactant Experiments in Fractured Carbonate Cores

INTRODUCTION

Carbonate reservoirs hold approximately 60% of the world's oil reserves (Akbar et al., 2000). A large number of carbonate reservoirs are naturally fractured and are mixed-wet to oil-wet (Roehl and Choquette, 1985; Chillenger and Yen, 1983). Most of carbonate reservoirs have a high degree of heterogeneity and complex pore structure. Naturally fractured carbonate reservoirs typically have high permeability fractures and low permeability matrix. This high contrast of permeability between matrix and fractures and mixed-wet or oil-wet reservoir leads to poor water flood efficiency. The oil recovery from naturally fractured carbonate reservoirs is typically much less than one-third.

Wettability has been long recognized as an important factor strongly affecting oil recovery using EOR methods (Austad *et al*., 1998; Zhou *et al*., 2000; Morrow and Mason, 2001; Tong *et al*., 2002; Hirasaki and Zhang, 2004). Water floods are often inefficient because many of these reservoirs are mixed-wet or oil-wet as well as extremely heterogeneous. Changing the wettability of the fractured reservoirs from oil or mixed-wet toward water-wet improves oil recovery efficiency. A lot of research has been conducted on wettability alteration by surfactants (Austad *et al*., 1998; Zhang *et al*., 2004; Seethepalli *et al*., 2004; Xie *et al*., 2004; Sharma and Mohanty, 2011; Chen and Mohanty, 2012).

Static imbibition experiments have been widely used to evaluate different EOR surfactants. The recovery from fractured carbonate reservoirs is frequently considered to be dominated by gravity and capillary forces. However, the role of viscous forces may also be important and should be investigated (Delshad *et al*., 2009). The Marangoni effect (Austad and Milter, 1997) and spontaneous emulsification (Zhang *et al*., 2008) might also

promote imbibition in some static imbibition experiments. Goudarzi *et al*. (2012) have suggested that changing the matrix block size affects the oil recovery from static imbibition experiments.

Imbibition experiments using surfactants that produce low IFT have been conducted by several investigators (Hirasaki and Zhang, 2004; Seethepalli *et al*., 2004; Abidhatla and Mohanty, 2006). Hirasaki and Zhang (2004) suggested the dominant oil recovery mechanisms in low IFT imbibition are buoyancy and wettability alteration. With some anionic surfactants, the IFT can be reduced to ultra-low values where the capillary pressure is reduced to nearly zero. When the capillary pressure is nearly zero, then other forces (gravity and viscous) can cause imbibition observed in many experiments. The simulation results by Abbasi-Asl *et al*. (2010) showed that surfactant imbibition is driven in part by transverse pressure gradients between the fractures and matrix..

The improved understanding of the relationship between the surfactant structure and performance (Solairaj *et al*., 2012; Adkins *et al*., 2012; Lu *et al*., 2014) enabled the development of a surfactant formulation that shows promising results in a high-temperature, high-salinity, heterogeneous fractured carbonate rock. The surfactant formulation was tested by doing a coreflood using the fractured carbonate rock.

EXPERIMENTAL MATERIALS AND PROCEDURE

Surfactants and Materials

Anionic Surfactants

Guerbet alkoxy carboxylates were synthesized from Guerbet alkoxylates. Internal olefin sulfonates (IOS) were obtained from Stepan Company.

Electrolytes and Brines

Sodium chloride, calcium chloride dihydrate, magnesium chloride hexahydrate, and sodium sulfate were obtained from Fisher Chemical and used as received. The synthetic sea water (SSW) and the synthetic formation brine (SFB) were prepared and their compositions are shown in Table 3-1. SSW, SFB and DI were used for phase behavior and coreflood experiments.

Oil

A dead oil was provided by an oil company. The surrogate oil (a mixture of dead crude and a low-EACN hydrocarbon to match the live oil EACN) was used for the experiments at ambient pressure to account for the effect of solution gas on phase behavior. The surrogate oil contained 30 wt% cyclohexane and 70 wt% dead oil. The API of the oil was 22, and the viscosity of surrogate oil was 2.1 cp at the reservoir temperature, 100 °C.

Microemulsion Phase behavior tests

Surfactant phase behavior tests were conducted to identify good surfactant formulations for this specific oil at the reservoir temperature. The surfactant mixtures with oil and brine were carefully observed for several months. The surfactants that form a low viscosity microemulsion in a few days and show ultra-low IFT were selected for further evaluation. The aqueous surfactant solution was observed for stability and clarity at both room temperature and reservoir temperature to determine if it was stable up to at least optimum salinity.

CT scan

A modified medical CT scanner was used to scan the core before and after being fractured. The core was scanned at the energy level of 80 kV from the top to the bottom.

The thickness of each slice (and the distance between consecutive images) was 10 mm. The reservoir core was highly vuggy and heterogeneous by visual observations and CT scan analysis.

Imbibition test

The surfactant formulations with good phase behavior were tested for their ability to imbibe into reservoir core plugs. One reservoir core plug was prepared by cleaning and saturating with the formation brine. The properties of the core plug are listed in Table 3-2. After injecting oil, the core was aged at the reservoir temperature for about a month. Because of its high heterogeneity, a high initial oil saturation could not be achieved. Imbibition cells were constructed in the Custom Lab Glass Services at The University of Texas at Austin. The oil-aged core was placed inside the imbibition cell. Then the imbibition cell was filled with the formation brine or the surfactant solution to its neck. If the surfactant solution imbibed into the core plug then the oil was pushed out of the core and accumulated in the neck of glass cell. The volume of the produced oil was monitored on a daily basis (or as often as needed).

Fractured core preparation and corefloods

A reservoir core of about 10.5 inches in length and 2.0 inches in diameter was used for the first coreflood. The core was cut into 7 pieces, and each piece of core plug was about 1-2 inches long. Axial fractures were created in the plugs to mimic the natural fractures in the reservoir. The core plugs were then stacked together to make a 10.5 inch-length composite core, and wrapped with a Teflon heat shrink tube. The core was put into the core holder for the experiment. The core was not cleaned by solvents before the coreflood, so the porosity, initial oil saturation and brine permeability were estimated for the calculations. The core was then oil flooded and soaked for 3 days at 100 °C. A second

oil flood was conducted after the core was aged to displace more brine, and then followed by a water flood with synthetic formation brine (SFB). Then the first surfactant slug was injected followed by the first brine drive. A second surfactant slug and a second brine drive were injected after the first brine drive.

The second fractured coreflood was also conducted to validate the surfactant performance on oil recovery from fractured reservoir core. A second reservoir core of about 10.8 inches in length and 4.0 inches in diameter was obtained, then dried and weighed. The core was wrapped with a Teflon heat shrink tube and then inserted into a 4-inch diameter core holder with a confined pressure of 1000 psi applied. The core was cleaned by injecting many pore volumes of toluene, methanol, and synthetic formation brine (SFB). Pressure data were recorded and the brine permeability was measured to be about 6 md, which is close to the matrix permeability.

The core was then taken out of the core holder and cut into 3 pieces. Each piece of core plug was about 3-4 inches long. Axial fractures were created in the plugs to mimic the natural fractures in the reservoir. The three core plugs were then stacked together to make a 10.8 inch-length composite core. The core was dried and put back into core holder again. The core was evacuated by a vacuum pump and then saturated with SFB to measure the pore volume of about 216 ml by material balance. The core holder was placed in the 100 °C oven with a back pressure of 100 psi, and flooded with SFB. The brine permeability of the composite fractured core was measured to be about 1970 md. Oil was then flooded from the top of the vertical standup core at a frontal velocity of 6 ft/day until no brine was produced. A second oil flood was conducted after the core was aged to displace out more brine and estimate the oil permeability and residual water saturation, and then followed by a water flood with SFB. The residual oil saturation and relative water permeability were determined.

The surfactant flood experiment was designed with a favorable salinity gradient to maximize the robustness of the flood (Pope et al., 1979). The salinities of the surfactant slug and brine drive are determined from phase behavior data. A differential pressure transducer was used to measure the pressure drop across the entire core. Effluent from the core was collected by fraction collector and sampled in glass test tubes to analyze the oil content, surfactant concentration, and salinity. The coreflood setups were similar as shown in Figure 3-1. The comparisons of the static imbibition experiment and the fractured coreflood are listed in Table 3-2. The fractured coreflood experiment is summarized in Table 3-3.

RESULTS AND DISCUSSION

The First fractured reservoir coreflood

The formulation used in this coreflood is discussed in Chapter II. The formulation is a surfactant mixture consisting of 0.5 wt% C_{24}-25PO-56EO-carboxylate and 0.5 wt% C_{19-23}-IOS. No co-solvent was needed in this formulation. Fig. 3-2 shows the oil and water solubilization ratios as a function of salinity. The salinities were achieved by mixing seawater and DI in different proportions. Winsor type I, III and II phase behavior was observed as the salinity increased. This formulation equilibrates fast and shows a high optimum solubilization ratio of about 21 at the optimum salinity of about 38,000 ppm, which is the same as seawater salinity. The solubilization ratio of 22 corresponds to an ultralow IFT of about 6.2×10^{-4} dynes/cm using the Huh equation (Huh, 1979). The aqueous solutions were clear and stable up to 57,000 ppm TDS at the reservoir temperature of 100 °C. This surfactant formulation was used in the first fractured coreflood experiment.

The 2-inch reservoir core plugs were fractured to make a composite core for the coreflood. Images of the fractured core plugs are shown in Figure 3-3. The core plugs are extremely heterogeneous and vuggy by visional observations. A CT scan of the core was conducted after the core was fractured. The images in Figure 3-4 show the core after it was fractured. The images show that some vugs are connected with fractures and some are isolated. Some parts of the core have higher vug density than other parts. The size of the vugs also varies a lot. These images show that the core is extremely heterogeneous and vuggy.

The first fractured coreflood was then performed using the surfactant formulation described above. The purpose of this coreflood experiment was to get a preliminary indication of the behavior of this surfactant formulation using a fractured reservoir core as well as to gain experience with how to prepare and use a fractured reservoir core. The frontal velocity was 0.25 ft/day to take advantage of gravity and allow more time for surfactant imbibition into the matrix. The details of this coreflood are summarized in Table 3-3.

The brine permeability was estimated to be about 1000 md after the core was fractured. The porosity of the core was estimated as 0.10 corresponding to apore volume of about 48.8 ml. After the second oil flood, the initial oil saturation (S_{oi}) was estimated to be about 0.50 and the oil relative permeability was measured to be 0.79. The waterflood was stopped when produced oil was negligible. The waterflood recovered 32.8% oil as shown in Figure 3-5. The residual oil saturation after waterflood was 0.336 and water relative permeability was 0.089. After waterflood, the first 0.4 PV surfactant slug of 0.5 wt% C_{24}-25PO-56EO-carboxylate, and 0.5 wt% C_{19-23}-IOS was injected at 0.25 ft/D and 100 °C, and then followed by the first brine drive. After 0.6 PV brine drive, a second 0.14 PV surfactant slug was injected followed by a second brine drive. The

formation brine had a salinity of about 117,000 ppm TDS with a divalent cation concentration of about 4,000 ppm. The salinity of the surfactant slug was 38,000 ppm TDS with a divalent cation concentration of about 1,800 ppm.

The novel Guerbet alkoxy carboxylate and IOS surfactant mixture can tolerate high temperature, salinity and hardness, and still produce ultra-low IFT. The oil recovery and oil saturation data of this fractured coreflood are shown in Figure 3-6. The chemical flood was stopped at about 1.7 PV with still a small amount of oil produced. The cumulative oil recovery was 76.8 % after the water flood, and the oil saturation decreased from 0.336 to 0.078. The results obtained from this first fractured coreflood were encouraging since the surfactant formulation was shown to efficiently recover oil from extremely heterogeneous fractured core at a low frontal velocity. The surfactants both lowered the IFT and altered the wettability of the rock toward water-wet.. There are some uncertainties about the final oil recovery results since the porosity and initial oil saturation were not measured. To validate the surfactant performance in fractured rock, a second coreflood was carried out in a 4-inch diameter fractured reservoir core in a similar fashion. A spontaneous imbibition experiment was also conduced to compare with the dynamic fractured coreflood. The details of these experiments are discussed in the next section.

The Second fractured reservoir coreflood

Phase Behavior Results

The surfactant formulation developed in this study was a mixture of 0.5 wt% C_{28}-25PO-25EO-Carboxylate and 0.5 wt% $C_{15\text{-}18}$-IOS. No co-solvent and alkali were needed for this formulation. Figure 3-7 shows the oil and water solubilization ratios for this surfactant formulation as a function of salinity. The salinities were achieved by mixing

SSW and SFB in different proportions, which mimic mixing during transport through the reservoir. Winsor type I, III and II phase behaviors were observed as the salinity was increased. This formulation equilibrates fast and shows a high optimum solubilization ratio of about 16 at the optimum salinity of about 57,000 ppm as shown in Figure 3-7. A solubilization ratio of 16 corresponds to an ultralow IFT of about 1.2×10^{-3} dynes/cm using the Huh equation. This formulation has excellent tolerance of divalent cations such as calcium and magnesium. The aqueous solutions were clear and stable up to 58,000 ppm TDS for more than 32 days at the reservoir temperature of 100 °C. This surfactant formulation was used in both static imbibition and fractured coreflood experiments. Chen (2014) measured the contact angle on a calcite plate with this formulation and found most of oil left the plate after it was immersed in the surfactant solution, which indicates the wettability of the plate was altered by this formulation by solubilizing the oil inside the micelles.

Imbibition test results

The objective of the static imbibition test was to investigate the wettability alteration by an ultra-low IFT surfactant formulation, and also compare the oil recovery with that of the dynamic imbibition process. In this study, one reservoir core plug 1.5 inches × 3.09 inches was saturated with the formation brine and then flooded with the surrogate oil to reach residual water saturation. The core was then immersed in the surrogate oil and aged at the reservoir temperature for about a month. After the aging process, the reservoir core was immersed in the formation brine to verify the wettability by observing the contact angle. As shown in Figure 3-8, oil droplets on top of the core tend to wet the solid. It demonstrates that the oil-wetness of the core was restored after aging. Then the reservoir core was placed inside an imbibition cell surrounded by the

surfactant solution at the optimal salinity. The surfactant formulation slowly imbibed into the core and expelled some amount of oil. The imbibition oil recovery reached 33.3 % OOIP in 17 days, reducing the oil saturation to 0.39 as shown in Figure 3-9. In this experiment, most of oil was observed to be produced from the top surface of the vertical core, which indicates that buoyancy is the most important driving force in this experiment.

CT scan analysis

The images of the reservoir core plugs after they were fractured (Figure 3-10) show they are very vuggy and heterogeneous. A CT scan of the second core was conducted before and after the core was fractured. The images in Figure 3-11 also show that the reservoir core is extremely heterogeneous and vuggy before fractures were made. Some vugs are connected and some are isolated. Some parts of the core have higher vug density than other parts. The size of the vugs also varies a lot. The images in Figure 3-12 show the core after it was fractured corresponding to the same cross-sections shown in Figure 3-11. Some vugs are connected with fractures and some are not.

Coreflood results

The brine permeability was 6 md before the core was fractured. After it was fractured, the permeability of the core was 1970 md. The permeability contrast between fractures and matrix is similar to that of the actual fractured reservoir. Polymers were not used for mobility control because of the low matrix permeability of about 6 md would make it very difficult to efficiently transport high molecular weight polymer. Also, the hard brine and high temperature would require the use of more expensive polymers compared to conventional HPAM. The surfactant solution was injected from the bottom

at a low velocity (0.2 ft/D) both to take advantage of buoyancy and to allow more time for imbibition and wettability alteration.

The water flood was conducted using formation brine at about 12 ft/D for ~ 0.13 PV, and stopped when the produced oil to water ratio was low. The waterflood recovered 16.8% oil, and the oil saturation after waterflood was 0.412. After the water flood, surfactant solution was injected to displace the oil at 100 °C. The formulation consisted of 0.5 wt% C_{28}-25PO-25EO-carboxylate and 0.5 wt% C_{15-18}-IOS. A 0.25 PV surfactant slug was injected into the core, and then followed by a brine drive. The initial (formation) brine had a salinity of about 117,000 ppm TDS with a divalent cation concentration of about 4,000 ppm. The salinity of the surfactant slug was 57,000 ppm TDS with a divalent cation concentration of about 2,300 ppm. The novel Guerbet alkoxy carboxylate and IOS surfactant mixture can tolerate such high temperature, salinity and hardness, and still produce ultra-low IFT and aqueous stability. After surfactant slug, about 1.46 PV brine was injected with a salinity of 10,000 ppm TDS. The chemical flood was stopped after about 1.71 PV of injection at an oil cut of about 5 %.

The oil recovery data are shown in Figure 3-13. The cumulative oil recovery was 65.9% of the remaining oil after the water flood, and the oil saturation decreased from 0.412 to 0.140. Compared with the static imbibition experimental results, the coreflood showed higher oil recovery and the oil was produced at a faster rate. Because of the high permeability fractures, low injection rate and low viscosity of the injected surfactant solution, the pressure drop was close to zero during the entire flood as shown in Figure 3-14.

The surfactant formulation developed in this coreflood reduced the IFT to ultra-low values on the order of 0.001 dyne/cm, and consequently the capillary pressure in the presence of surfactant was reduced to essentially zero. How does the surfactant flow into

the low permeability matrix if the capillary pressure is nearly zero? A plausible explanation is that the transverse pressure drop between the fractures and the matrix is sufficient to induce surfactant transport into the matrix. Once the surfactant is in the matrix, it changes the wettability and reduces the IFT and both mechanisms increase the oil relative permeability. The oil can then flow upward due to buoyancy until it reaches a fracture and then it can flow in the fracture until it is produced.

Figure 3-15 shows the produced surfactant concentration and salinity for this coreflood. No chromatographic separation or preferential retention was observed between the two surfactants. The total surfactant retention was 0.086 mg/g of rock with the individual contribution of 0.044 mg/g of C_{15-18}-IOS and 0.042 mg/g of C_{28}-25PO-25EO-carboxylate. The early effluent salinity was that of the initial brine, which decreased to the surfactant slug salinity, and then further decreased to the brine drive salinity. The surfactant was effective to produce oil at very high salinities corresponding to the Type II region. The brine drive had a low enough salinity for surfactant to transition from Type II into Type III region, and eventually to transition into Type I region. The coreflood was successful in spite of the fact that (1) the core was extremely vuggy, fractured, and heterogeneous, (2) no mobility control (i.e. polymer) was used, and (3) only a small amount of surfactant was injected.

SUMMARY

Surfactant formulations consisting of novel large-hydrophobe Guerbet alkoxy carboxylate and IOS surfactants were developed for a carbonate reservoir under high salinity and temperature. The surfactant both reduces the IFT to ultra-low values and alters the wettability of the rock toward more favorable water-wet conditions. Both static and dynamic core experiments were performed. In the dynamic coreflood experiment, the

oil saturation was reduced to 0.14 using only a small amount of surfactant with no polymer. The surfactant retention was only 0.086 mg/g rock. The results are excellent taking into account that (1) the core was extremely vuggy and fractured, (2) no mobility control was used, and (3) only a small surfactant slug was injected. The oil recovery from the dynamic coreflood was higher than that for a similar static imbibition experiment. The UTCHEM simulator was used by Lu et al. (2012) to match the coreflood data by using an extremely heterogeneous random permeability distribution to model the vuggy fractured core as opposed to attempting to model the fractures directly. Matching the experimental data is an important first step before using the simulator to predict field performance on a much larger scale than the coreflood experiment.

Table 3-1: SSW and SFB Compositions

Brine	Na^+ (ppm)	Ca^{2+} (ppm)	Mg^{2+} (ppm)	SO_4^{2-} (ppm)	Cl^- (ppm)	TDS (ppm)
SSW	12,188	480	1342	3250	21,133	38,393
SFB	41,473	3880	145	500	70,971	116,969

Table 3-2: Comparison of Static Imbibition and Fractured Coreflood Results

Experiment	Static imbibition	Fractured coreflood
Core Name	Reservoir core	Reservoir core
Type	Carbonate	Carbonate
Length (cm)	7.86	27.4
Diameter (cm)	3.78	10.2
Pore Volume (ml)	7.25	216.0
Porosity	0.082	0.097
Brine Permeability (md)	42.9	6 (before fractured) 1970 (after fractured)
S_{oi}	0.586	0.495
S_{orw}	-	0.412
Oil Recovery (%)	33.3	64.9
S_{orc}	0.390	0.140

Table 3-3: Summary of Fractured Coreflood Experiment

Temperature (°C)	100
Initial salinity (ppm)	116,969
Surfactant Slug	
Surfactant concentration (wt%)	1
PV injected	0.25
PV×C (%)	25
Viscosity (cp)	0.33
Salinity (ppm)	57,000
Velocity (ft/day)	0.2
Brine Drive	
PV injected	1.46
Viscosity (cp)	0.33
Salinity (ppm)	10,000
Velocity (ft/day)	0.2
Results	
Recovery (%)	64.9
Final residual oil saturation, S_{orc}	0.140
Surfactant retention (mg/g)	0.086

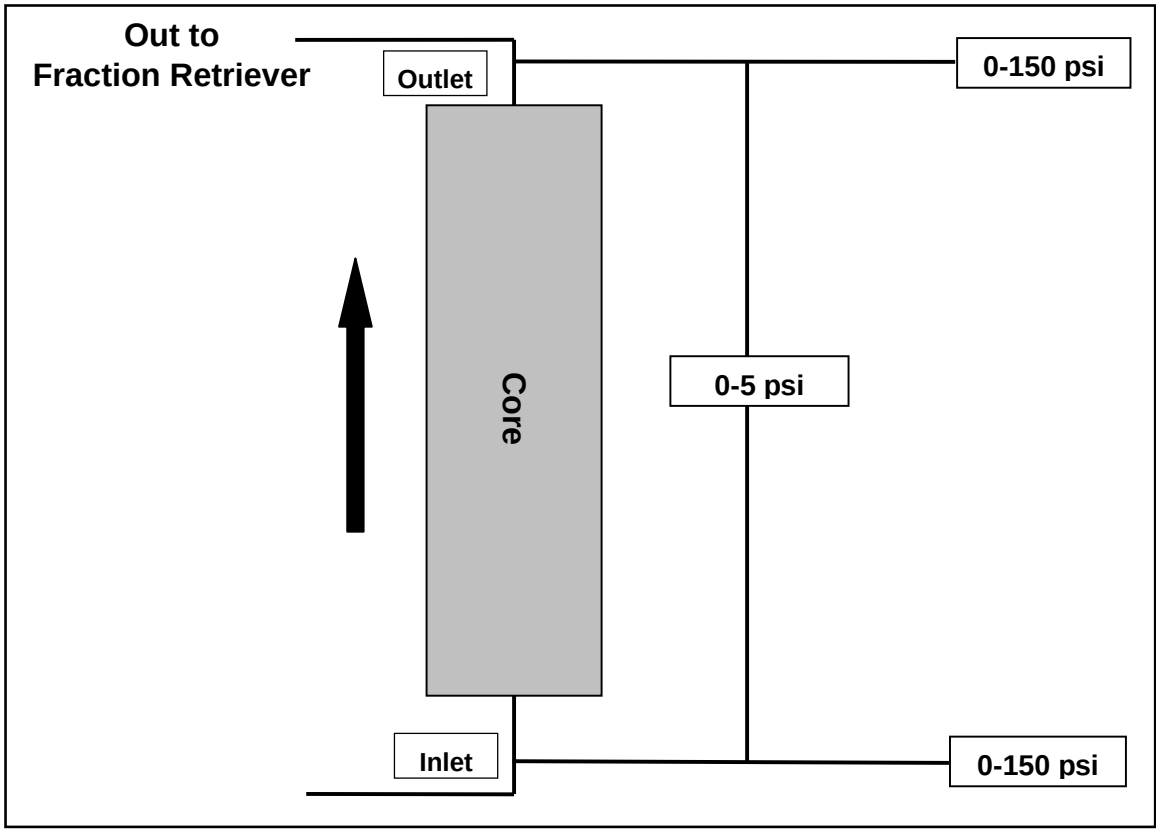

Figure 3-1: Schematic of coreflood setup.

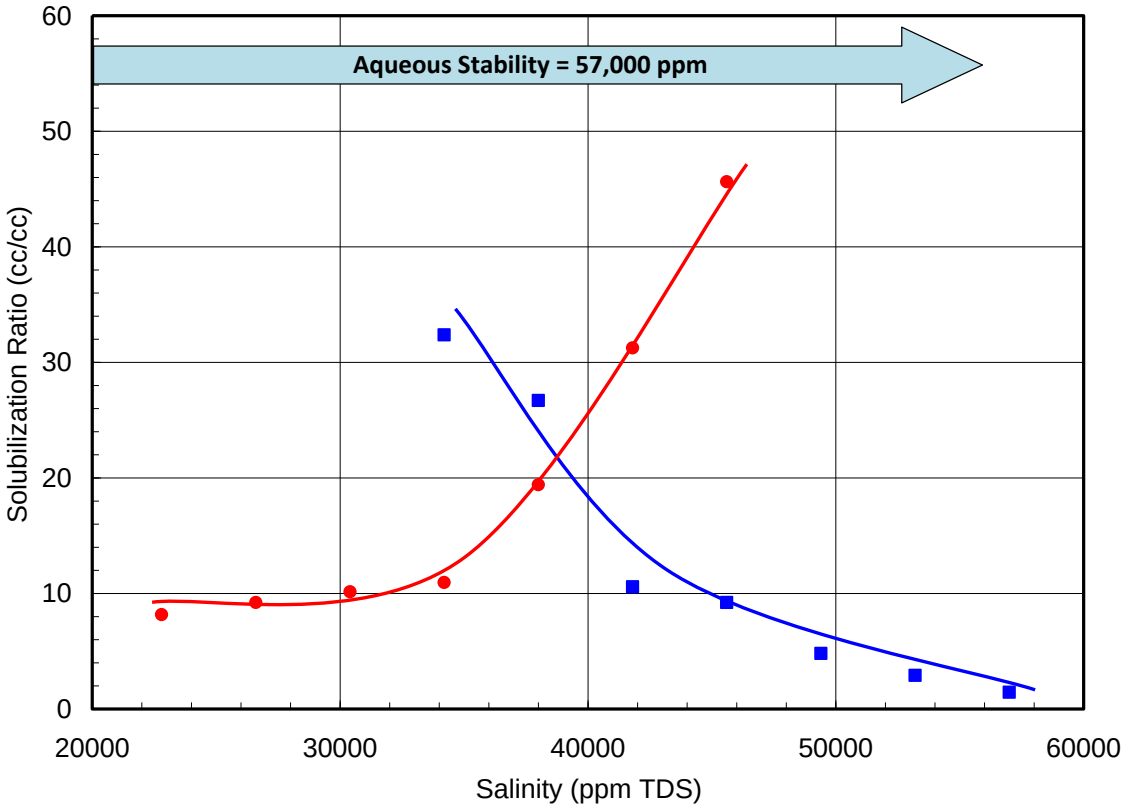

Figure 3-2: Phase behavior of 0.5 wt% C_{24}-25PO-56EO-carboxylate and 0.5 wt% C_{19-23}-IOS at 100°C with 50 vol% oil after 97 days.

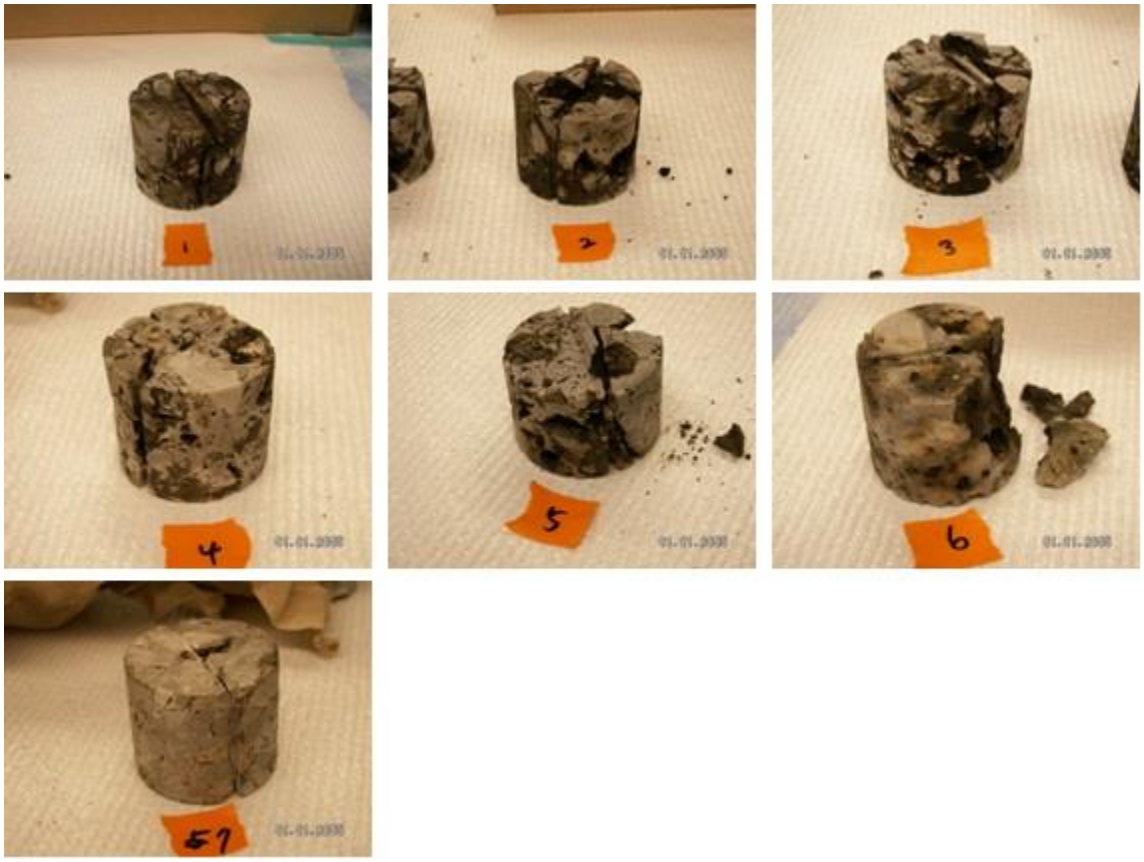

Figure 3-3: Photographs of 2-inch fractured reservoir core plugs.

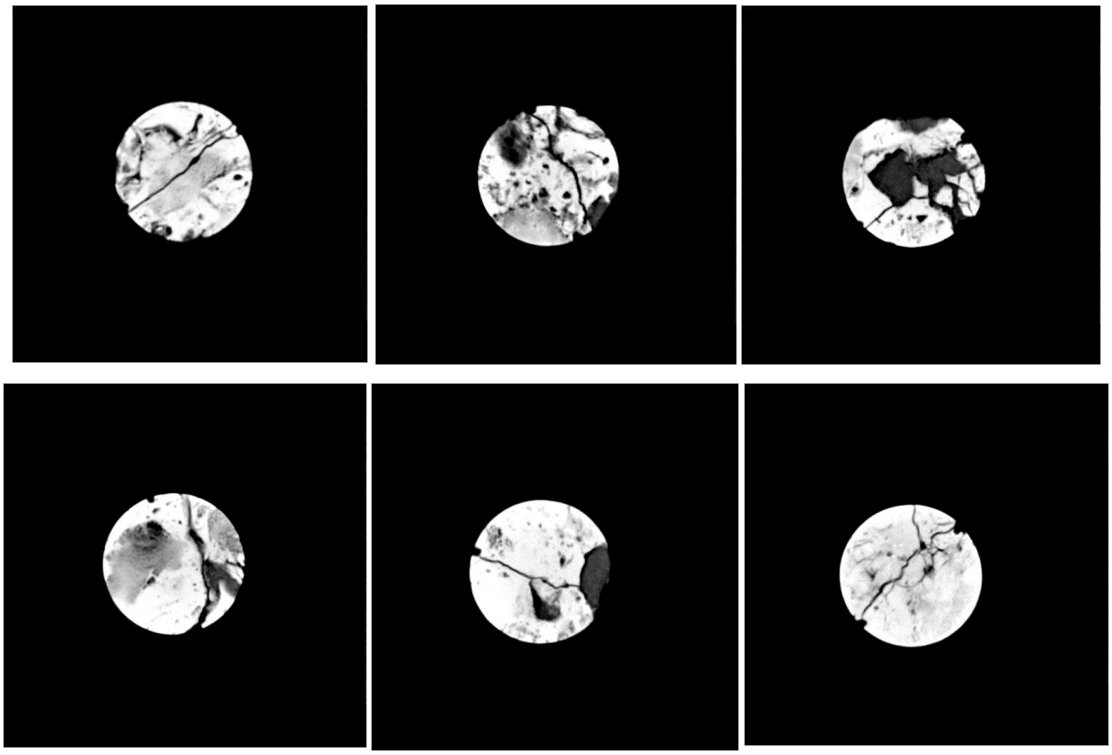

Figure 3-4: CT images of 2-inch fractured reservoir core.

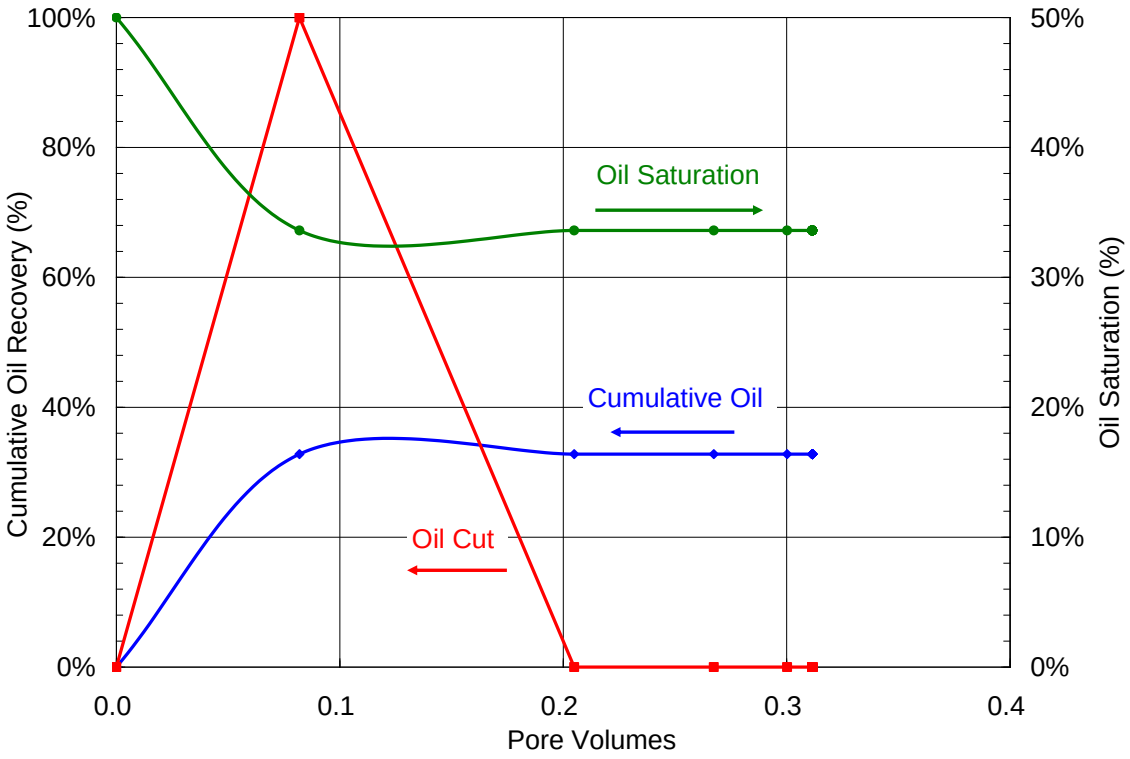

Figure 3-5: Oil recovery from waterflood of the first fractured reservoir coreflood at 100°C.

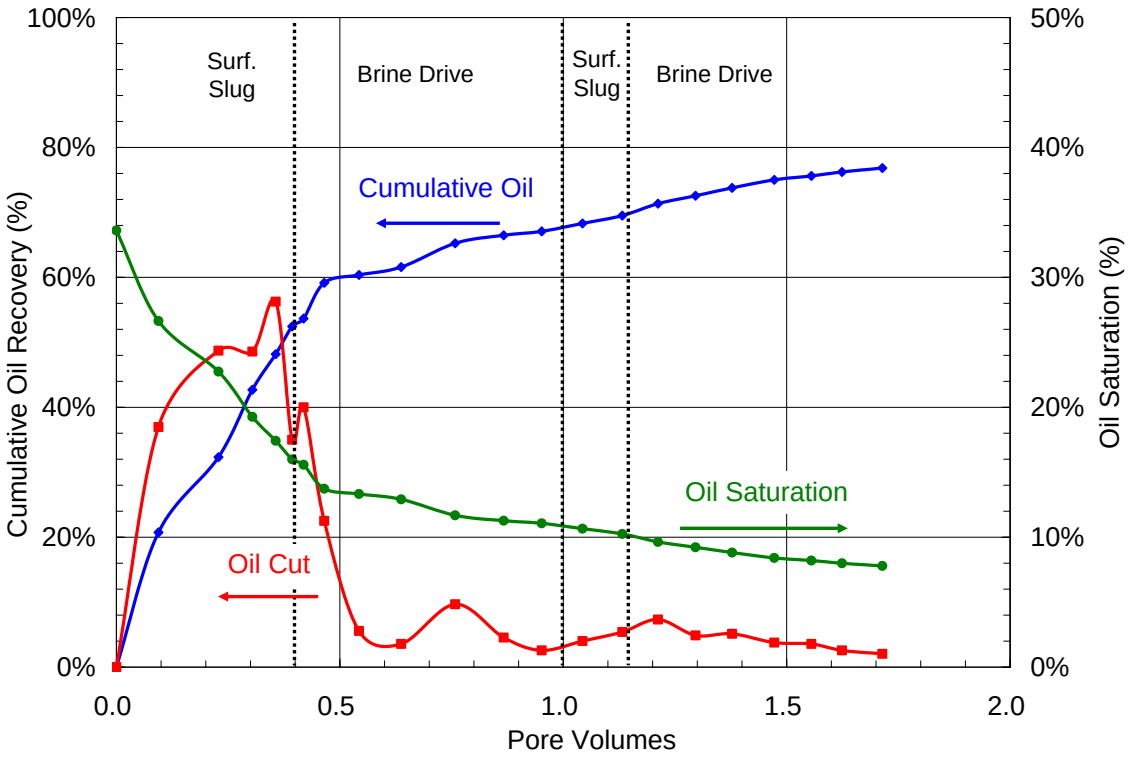

Figure 3-6: Oil recovery from the first fractured reservoir coreflood at 100 °C.

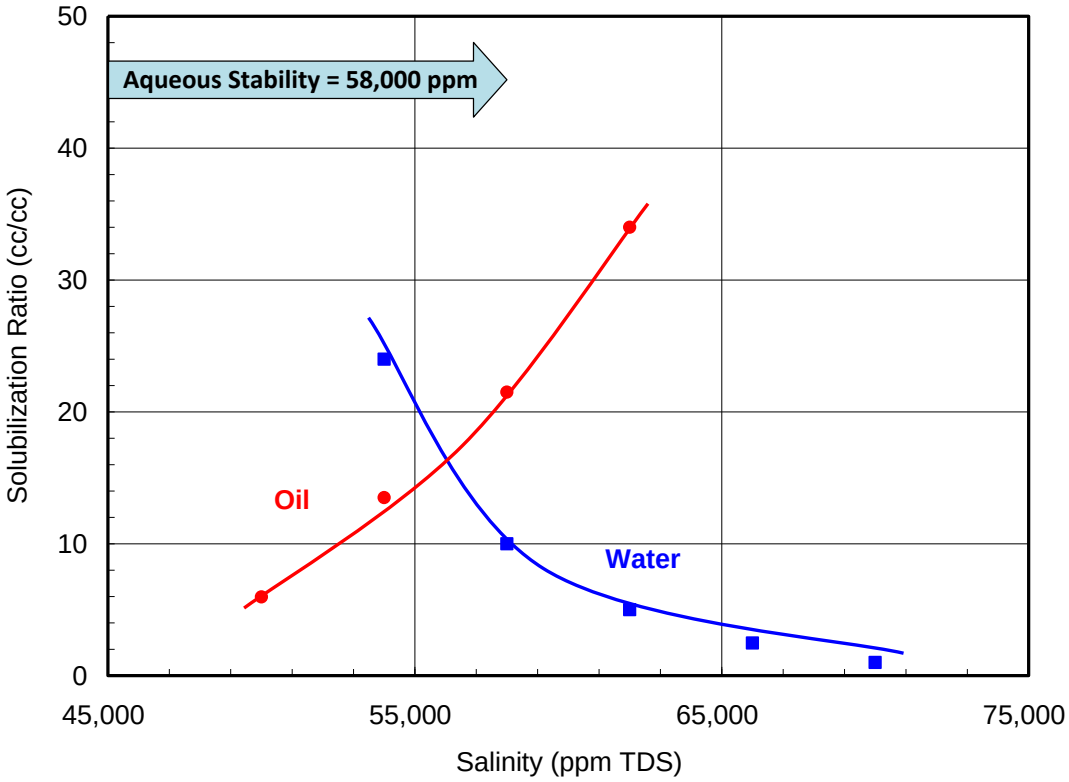

Figure 3-7: Phase behavior of 0.5 wt% C_{28}-25PO-25EO-carboxylate and 0.5 wt% $C_{15\text{-}18}$-IOS at 100 °C with 50 vol% oil after 32 days.

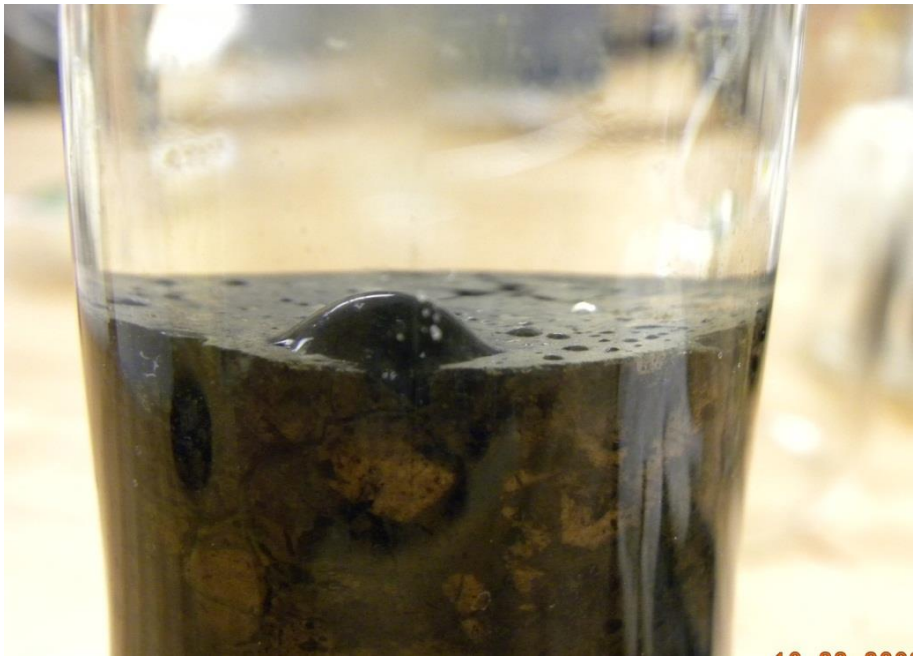

Figure 3-8: The reservoir core immersed in formation brine after aging.

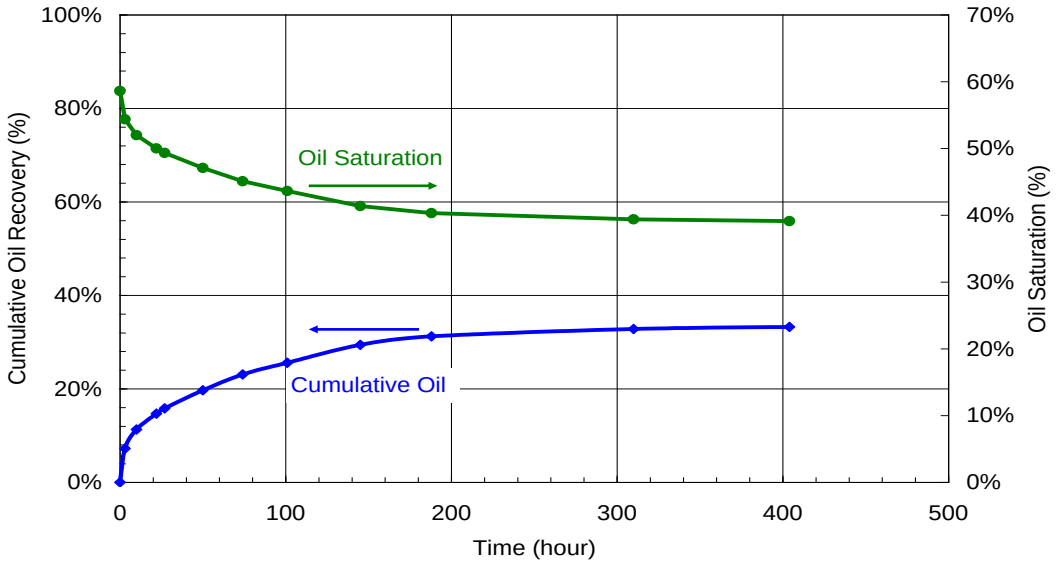

Figure 3-9: Oil recovery and oil saturation from static imbibition experiment at 100 °C.

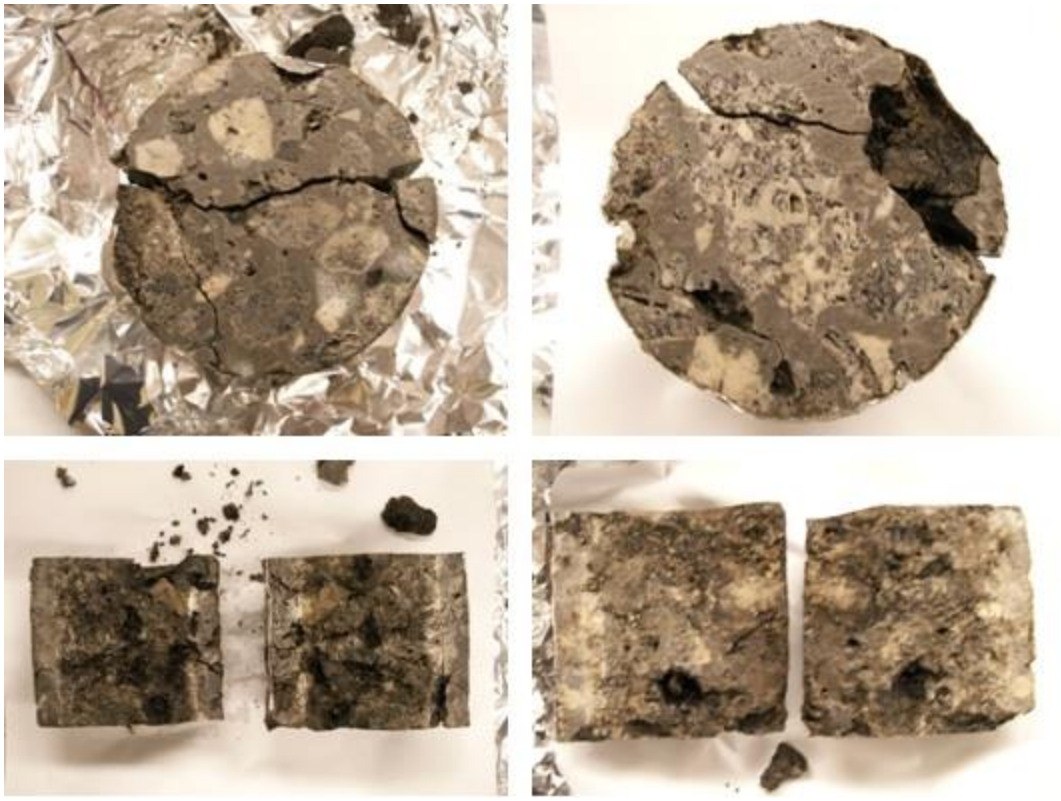

Figure 3-10: Photographs of 4-inch fractured reservoir core plugs.

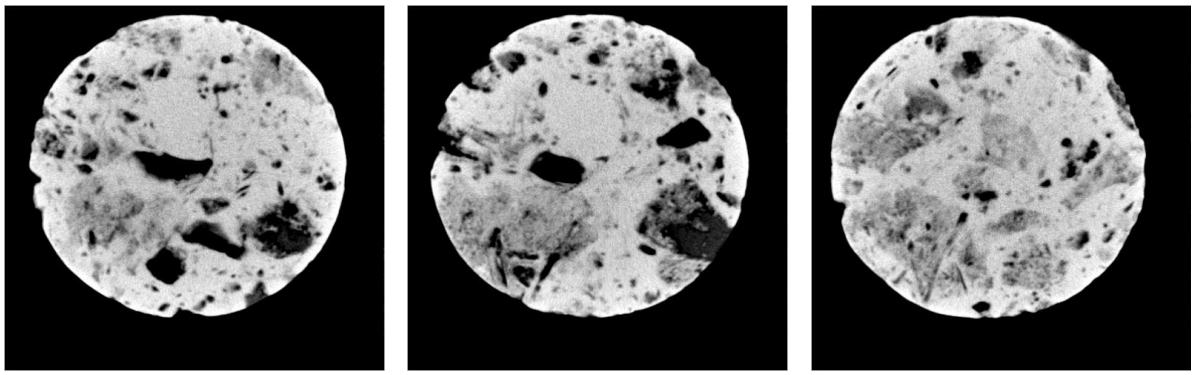

Figure 3-11: CT images of the 4-inch reservoir core before it was fractured.

Figure 3-12: CT images of the 4-inch reservoir core after it was fractured.

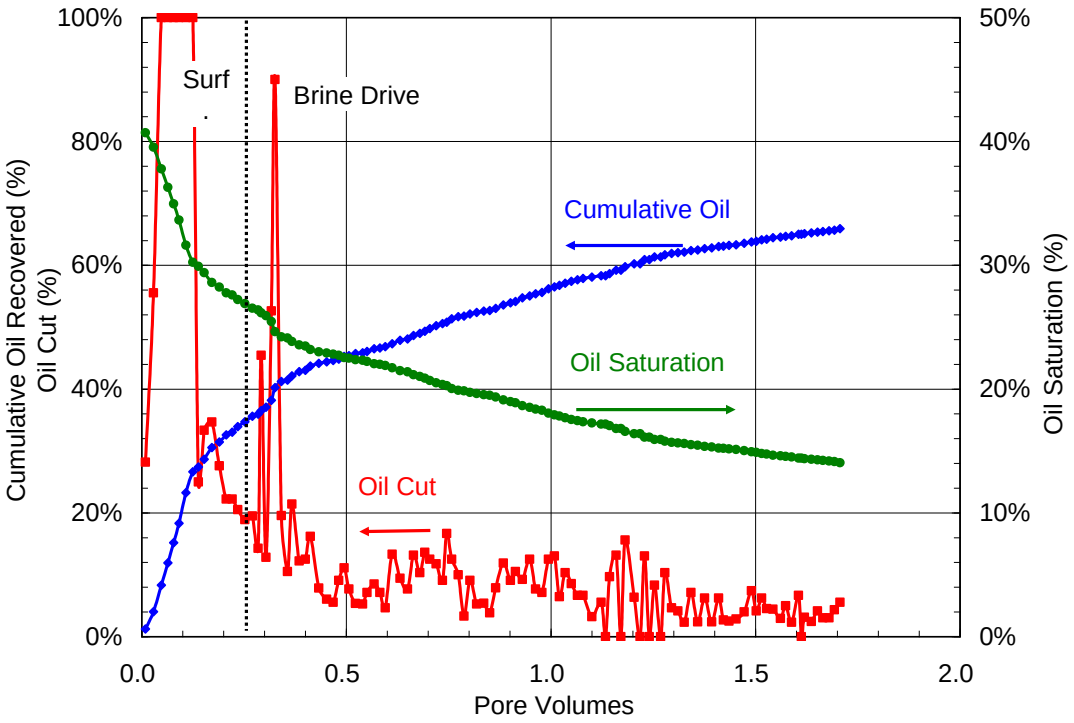

Figure 3-13: Oil recovery for the second fractured reservoir coreflood at 100 °C.

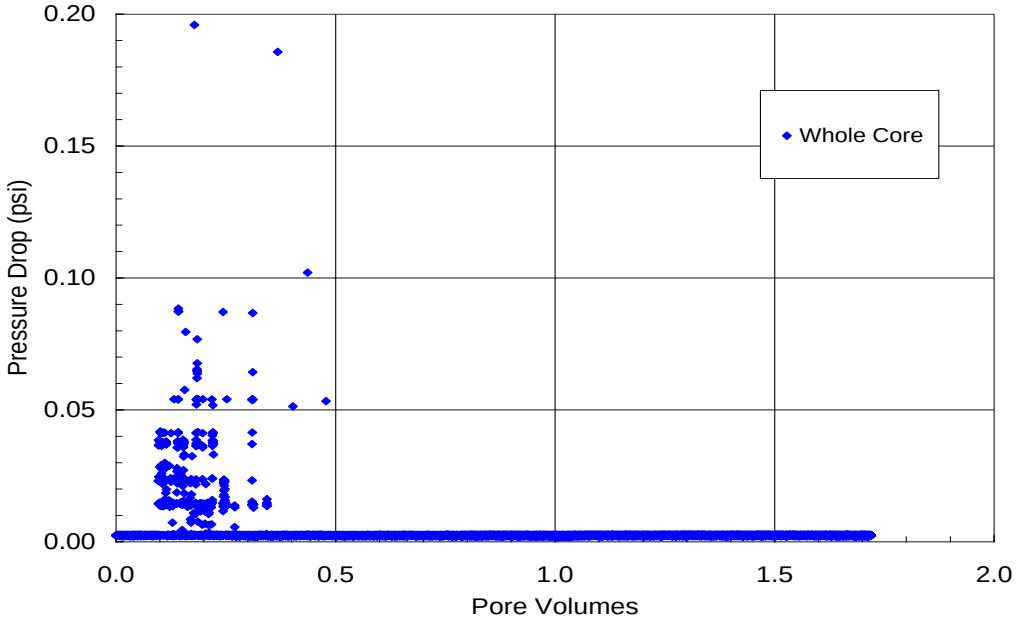

Figure 3-14: Pressure drop during the second fractured reservoir coreflood.

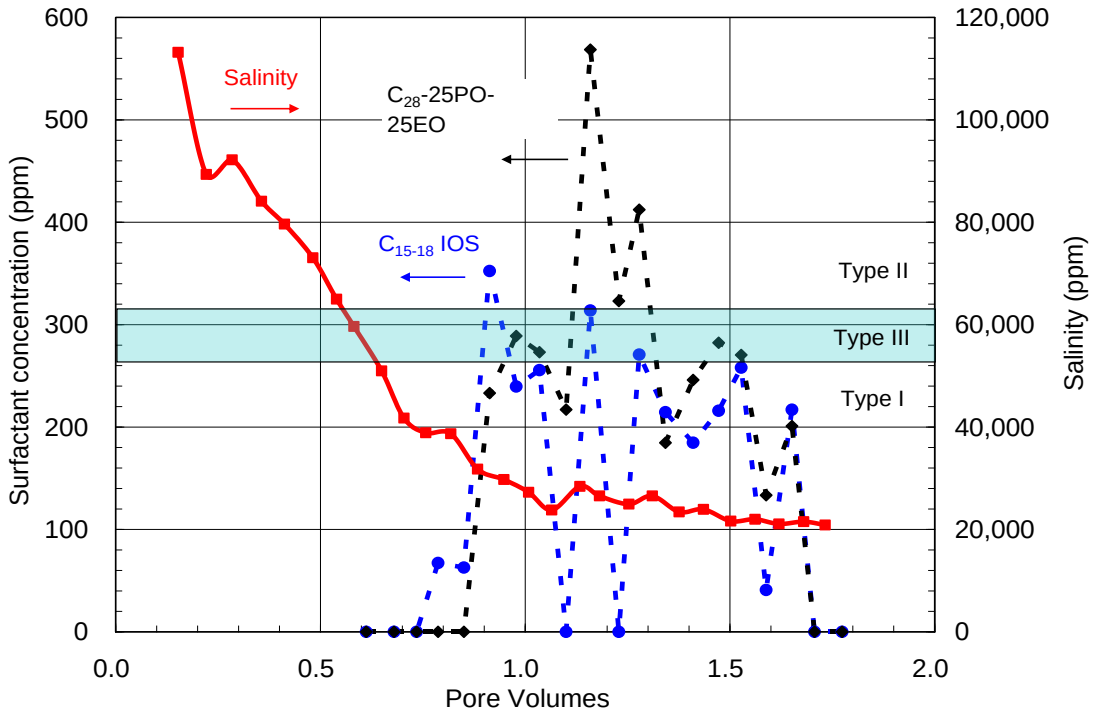

Figure 3-15: Measured surfactant concentration and salinity in the effluent samples from the second fractured reservoir coreflood.

Chapter IV: Gravity-Stable Surfactant Floods

INTRODUCTION

The hydrodynamic stability of both miscible and immiscible displacements in porous media has been studied for many years. Many investigators have reported both experimental and theoretical results for the effects of gravity and viscosity on the stability of miscible displacements (Hill, 1952; Perrine, 1961 and 1963; Dumore, 1964; Tan and Homsy, 1987 and 1988; Homsy, 1987; Hickernell and Yortsos, 1986; Manickam and Homsy, 1995) and immiscible displacements (Engelberts and Klinkenberg, 1951; Chuoke et al., 1959; Terwilliger et al., 1951; Sheldon et al., 1959; Fayers and Sheldon, 1959; Raghavan and Marsden, 1971; Nayfeh, 1972; Peters and Flock, 1981; Glass and Yarrington, 1996; Stephen et al., 2001; Meheust et al., 2002; Ould-Amer and Chikh, 2003; Riaz and Tchelepi, 2004).

Surfactants can generate ultra-low IFT and displace almost all the residual oil after waterflooding a core (for recent experimental examples, see Yang et al., 2010; Adkins et al., 2010; Barnes et al., 2012; Bataweel et al., 2012; Puerto et al., 2012; Adkins et al., 2012; Lu et al., 2012; Tabary et al., 2013), but even at ultra-low IFT surfactant floods are still not miscible displacements. The understanding of the gravitational stability of surfactant floods is lacking in the literature. Directly applying classical stability theory to ultra-low IFT surfactant floods is not appropriate and leads to inaccurate predictions. Thus, it is very important to understand the behavior of surfactant floods stabilized by gravity and propose a suitable theory for such applications.

A series of surfactant displacement experiments were carried out to determine the critical velocity for a gravity stable surfactant flood and these results were then compared with a new stability theory that takes into account the microemulsion phase (Lu et al., 2014c). The stability theory and experimental results imply that it is possible to design an

efficient surfactant flood without any mobility control if the surfactant solution is injected at a stable velocity. A new approach was investigated for increasing the critical velocity by optimizing the microemulsion viscosity. The goal is to increase the rate at which a stable flood can be achieved.

There are many advantages to conducting a gravity-stable surfactant flood compared to a surfactant flood that uses polymer for mobility control. Polymers add to the cost, complexity and uncertainty of the process. Polymer stability over long time periods corresponding to reservoir floods is a concern at high temperature. Polymer transport is a concern in low permeability reservoirs when using high-molecular weight polymers. Gas can be injected with the surfactant solution to create an in-situ foam for mobility control, but this process is much more complex and uncertain than using polymers for mobility control. Foam processes also require a source of high-pressure gas among other disadvantages.

The common use of horizontal wells has made the design and operation of gravity-stable surfactant floods much more attractive. Such floods can be done at a higher velocity than possible with vertical wells in a dipping reservoir. The use of horizontal wells has other advantages as well such as higher volumetric sweep efficiency. Nevertheless, the velocity for a gravity-stable surfactant flood will still be too low for practical floods unless the vertical permeability is high. Furthermore, there cannot be any permeability barriers between the horizontal injector at the bottom of the zone and the horizontal producer at the top of the zone. However, optimizing the microemulsion viscosity enables gravity-stable surfactant floods using horizontal wells to be done at reasonable rates and in reservoirs with a much lower permeability than previously thought possible.

STABILITY THEORY

Stability theory for water displacing oil in a homogeneous, uniform porous medium without a transition zone can be found in Lake (1989). The critical velocity is given by Eq. 1.

$$v_c = \frac{\Delta\rho g k k_{rw}^0}{\phi\mu_w\left(M^0 - 1\right)}\sin\alpha \tag{1}$$

where

$$\Delta\rho = \rho_w - \rho_o$$

and

$$M^0 = \frac{k_{rw}^0\mu_o}{\mu_w k_{ro}^0}.$$

Now consider a vertical column of a homogeneous porous medium at residual oil saturation after waterflooding. An aqueous surfactant solution is injected from the bottom of the column at a constant velocity. Assume that only oil and aqueous phases flow through the porous medium. The aqueous phase containing surfactant displaces an oil bank (oil and water flowing together ahead of the surfactant), so when applying Eq. 1 the mobility ratio should be the mobility of the aqueous phase divided by the mobility of the oil bank. The total relative mobility of the oil bank is defined as the total mobility of the flowing oil and water phases at the saturations in the oil bank:

$$\lambda_{OB} = \lambda_{ro} + \lambda_{rw} = \frac{k_{ro}}{\mu_o} + \frac{k_{rw}}{\mu_w}$$

The mobility ratio should be defined in terms of the total mobility of the oil bank as shown below:

$$v = \frac{\Delta\rho g k k_{rw}^0}{\phi\mu_w\left(M_{OB} - 1\right)}\sin\alpha \tag{2}$$

where

$$M_{OB} = \frac{\lambda_{rw}}{\lambda_{OB}} = \frac{\frac{k_{rw}^0}{\mu_w}}{\frac{k_{ro}}{\mu_o} + \frac{k_{rw}}{\mu_w}}.$$

In reality, a microemulsion forms between the oil bank and the injected surfactant solution and should be taken into account since its density and viscosity are different than the water and oil. Assume a uniform microemulsion at its optimum salinity so the oil and water concentrations in the microemulsion are equal. Then the microemulsion density will be close to the average of the water and oil densities. For a light oil, the microemulsion viscosity at optimum salinity is typically about ten times larger than the oil viscosity. However, it should be measured under each specific condition since it varies over a wide range for different microemulsions.

As illustrated in Figure 4-1, there are four regions in the column: starting from the top and going down, there is water at residual oil saturation (assuming the column has been water flooded to zero oil cut), oil bank with both oil and water flowing upward, microemulsion pushing the oil bank upward, and aqueous surfactant solution pushing the microemulsion upward. Taking into account the microemulsion, the mobility ratio at the interface between the microemulsion and oil bank should be defined as shown below:

$$v = \frac{(\rho_{me} - \rho_o) g k k_{rme}}{\phi \mu_{me} (M_{OB/me} - 1)} \sin\alpha \tag{3}$$

where

$$M_{OB/me} = \frac{\lambda_{rme}}{\lambda_{OB}} = \frac{\frac{k_{rme}}{\mu_{me}}}{\frac{k_{ro}}{\mu_o} + \frac{k_{rw}}{\mu_w}}.$$

Similarly, the critical velocity at the interface between the microemulsion and the aqueous surfactant solution is:

$$v = \frac{(\rho_s - \rho_{me})\, g k k_{rs}}{\phi \mu_s (M_{me/s} - 1)} \sin\alpha \qquad (4)$$

where

$M_{me/s} = \frac{k_{rs}\mu_{me}}{\mu_s k_{rme}}$.

The minimum of these two velocities is the critical velocity for a surfactant flood.

EXPERIMENTAL MATERIALS AND PROCEDURE

Surfactants and Materials

Anionic Surfactants

C_{13}-13PO-sulfate, $C_{15\text{-}18}$-IOS, and $C_{20\text{-}24}$-IOS surfactants were obtained from Stepan Company.

Co-solvents

Isobutyl alchohol (IBA), and triethylene glycol mono butyl ether (TEGBE) were received from Aldrich Chemicals.

Electrolytes and Brines

Sodium chloride, and sodium carbonate were obtained from Fisher Chemical.

Oils

Three oils were used in this study (Table 4-1).

Microemulsion phase behavior tests

Good surfactant formulations were identified using surfactant phase behavior tests for three oils at two temperatures, 38 and 58 °C (Table 4-2). Surfactant formulations

that produced ultra-low IFT and reached equilibrium in a few days were selected for microemulsion viscosity measurements and surfactant floods. The aqueous surfactant solution was observed for stability and clarity at experimental temperature to determine if it was stable up to at least optimum salinity.

Microemulsion samples preparation and viscosity measurements

The microemulsion samples used for the viscosity measurements were selected at the optimum salinity of each formulation as determined by phase behavior experiments. At least 8.5 ml of microemulsion is needed to make a viscosity measurement using the ARES LS-1 rheometer. Therefore, large tubes were used to prepare the microemulsion samples. The capped tubes were then mixed and placed in the oven at desired temperatures. When the sample was equilibrated, a syringe with a long needle was used to extract the microemulsion samples needed for the viscosity measurements.

Surfactant floods

The sandpack experiments were conducted in Kontes glass chromatography columns of 4.8 cm inside diameter. F-95 grade Ottawa sand was used to pack the column. The sandpacks were vacuumed and then saturated with NaCl brine. A tracer test was then performed to estimate the pore volume the sandpack. A higher salinity brine was injected as the tracer. The tracer data were also used to verify the sandpacks did not exhibit undesirable characteristics such as high dispersion or heterogeneity i.e. that they were good packs that were nearly homogeneous. Next the brine permeability was measured. Then several pore volumes of oil were injected downward from the top of the column in a favorable direction with respect to gravity. The original brine was then injected upward from the bottom of the column to establish residual oil saturation to water, Sorw. Then the surfactant solution at the optimum salinity was injected upward from the bottom of

the column until the end of the flood except for sandpack flood #8. Sandpack flood #8 was done with a surfactant slug injection followed by a brine drive. The effluent samples during the surfactant flood were collected in a fraction collector using volumetrically calibrated test tubes. Some of the sandpacks were used for more than one surfactant flood. Before reusing, the sand was cleaned by injecting isopropyl alcohol (IPA) and then NaCl brine until no surfactant was detected in the effluent.

Two epoxy-molded Bentheimer sandstone cores were also made and used in the floods. The coreflood procedure is the same as the sandpack floods. All the corefloods were run vertically in the convection oven at desired temperatures.

RESULTS AND DISCUSSION

First Series of Experiments for Oil #1 with High Microemulsion viscosity

Phase behavior and microemulsion viscosity results

The surfactant formulation developed for oil #1 was a mixture of 0.5 wt% C_{13}-13PO-sulfate, 0.5 wt% C_{20-24}-IOS, 2.0 wt% IBA, and 0.5 wt% Na_2CO_3. The large hydrophobe C_{20-24}-IOS is balanced by a more hydrophilic C_{13}-13PO-sulfate. The co-solvent IBA improved aqueous stability and microemulsion formation. The aqueous solutions were clear and stable up to 30,350 ppm TDS for more than 54 days at the reservoir temperature of 38°C. This formulation equilibrates fast and shows a high optimum solubilization ratio of about 22 at the optimum salinity of about 21,000 ppm TDS as shown in Figure 4-2. The estimated IFT at optimum salinity is about 6.2×10^{-4} dynes/cm based on the solubilization ratio of 22 (Huh, 1979). The trapping number (Pope et al., 2000) at this ultra-low IFT is on the order of 0.01, which is sufficient to displace all of the oil from the sand. For the special case of a vertical displacement, the trapping number is the scalar sum of the capillary and Bond numbers. In these experiments, the

capillary number was small compared to the Bond number i.e. its value was dominated by the buoyancy term.

The microemulsion sample at optimum salinity was prepared and the microemulsion viscosity was measured at 38 °C. The in-situ shear rate of the surfactant flood was estimated to be around 1 s^{-1}. The microemulsion viscosity at 1 s^{-1} and optimum salinity is about 24 cp, or about 5 times the oil viscosity (Figure 4-3).

Surfactant flood results

Experimental results for all of the surfactant floods are summarized in Table 4-4. Surfactant floods #1, #2 and #3 were conducted with this surfactant formulation with oil #1 in the same sandpack at different frontal velocities of 0.2, 0.4, and 0.8 ft/day, respectively. The tracer breakthrough data (Figure 4-4) show that the sandpack was nearly homogeneous.

Figures 4-5 to 4-7 show photographs of all three sandpack floods at different times during the surfactant flood. Four different sections and interfaces between them can be seen in the photographs. The four sections, from the top to the bottom of the column, are residual oil, oil bank, microemulsion and aqueous surfactant solution, respectively. The surfactant displacement is nearly stable at a frontal velocity of 0.2 ft/day and unstable at 0.4 and 0.8 ft/day. For each flood, the volume of the microemulsion transition zone increases with injected pore volumes and is larger at higher velocity due to more fingering. The interfaces between the oil bank and microemulsion and between the microemulsion and aqueous surfactant solution at 0.2 ft/day are sharper and more horizontal compared to floods at 0.4 and 0.8 ft/day. The fingers for the high velocity floods are more pronounced at the lower interfaces because the viscosity of the aqueous

surfactant solution is nearly as low as brine and much lower than the viscosity of the microemulsion.

Figures 4-8 through 4-10 show the surfactant flood results including cumulative oil recovery, oil cut, and oil saturation at velocities of 0.2, 0.4, and 0.8 ft/day, respectively. The surfactant floods displaced nearly all of the oil. The parameters and details of the three sandpack experiments are summarized in Table 4-3.

At 0.2 ft/day, the oil recovery at surfactant breakthrough and the average oil cut in the oil bank were high. Both decreased as the velocity increased due to the viscous fingering and also less oil was recovered from the oil bank and more from the produced microemulsion.

Calculation of Stable Velocity for Gravity Stable Surfactant Floods

The velocities required to achieve a gravity stable surfactant flood in the sandpack were calculated using the modified stability theory. The parameters used in the calculations are listed in Table 4-3. The critical velocity calculated from Eq. (1) is 1.69 ft/day with k^0_{rw} assumed to be 1.0 since almost all of the oil was displaced by the surfactant solution. The critical velocity calculated using Eq. (2) and the mobility ratio between the microemulsion and the oil bank is 0.45 ft/day.

If the microemulsion phase is taken into account, there are three phases and two interfaces during the displacement. Therefore, two velocities at two interfaces can be calculated, and the smaller one is the stable velocity. The microemulsion viscosity at optimum salinity is estimated to be ~24 cp at shear rate of 1 s^{-1}. The relative permeability of both the microemulsion phase and the aqueous phase was assumed to be 1.0 because of the ultra-low IFT (high trapping number). In this case, the mobility ratio between the microemulsion and the oil bank is 0.46 using an estimated total relative mobility of the

oil bank (λ_{OB}) equal to 0.091. This implies an unconditionally stable displacement at any velocity for the microemulsion phase displacing the oil bank. Next, the critical velocity between the microemulsion phase and aqueous surfactant phase was calculated using Eq. (4) and found to be 0.18 ft/day. This is the predicted velocity needed to achieve a gravity stable surfactant flood in this sandpack. This value is in much better agreement with the experiments than the value calculated using either Eq. (1) or (2).

Similar calculations were done for the White Castle field pilot described by Falls et al. (1994). The parameters of this pilot are shown in Table 4-3. The critical velocity calculated by Eq. (1) is 0.30 ft/day. The critical velocity calculated from Eq. (2) using an estimated oil bank mobility of 0.08 per cp is 0.06 ft/day. The critical velocities calculated from Eq. (3) and (4) are 0.15 and 0.04 ft/day, respectively. The velocity needed for a gravity stable surfactant flood is thus 0.04 ft/day. Using data from Falls et al. (1994), the surfactant flood velocity in the pilot test was estimated to be about 0.24 ft/day, which is much greater than the predicted stable velocity of 0.04 ft/day based on Eq. (4). This implies the flood was unstable, which is consistent with the observations and interpretation given in Falls et al. (1994), since they did not take into account the microemulsion viscosity.

Sensitivity Studies

The sensitivity of the critical velocity to both the microemulsion viscosity and aqueous surfactant phase viscosity was investigated using Eqs. (3) and (4). Figure 4-11 shows the critical velocity for both interfaces. The apparent oil bank viscosity was estimated to be ~11 cp in this case. The critical velocity for the upper interface between the oil bank and the microemulsion is v1. The critical velocity for the lower interface between the microemulsion and the aqueous surfactant phase is v2. The displacement is

stable when the velocity is less than the smaller of the two critical velocities. The highest critical velocity is when the two curves cross i.e. when v1=v2, which in this case is at ~0.80 ft/D for a microemulsion viscosity of ~6 cp. This is the optimum velocity for minimizing the project life of a gravity stable surfactant flood.

Thus, an important new insight is that the microemulsion viscosity can be optimized to maximize the velocity for a stable surfactant flood. The experiments were done with an oil viscosity of 5.4 cp and a microemulsion viscosity of 24 cp. The surfactant flood can be done at a higher velocity and still be stable when the oil viscosity decreases because the mobility of the oil bank increases.

The calculations so far assume the viscosity of the aqueous surfactant solution is the same as water. If polymer is added to the surfactant solution, then the critical velocity will increase for the lower interface between the aqueous surfactant solution and the microemulsion as shown in Figure 4-12 for the experimental case with a microemulsion viscosity of 24 cp. The upper interface is unconditionally stable with such a viscous microemulsion.

Figure 4-12 shows that adding polymer is not very effective until the viscosity increases to nearly the value that would be stable even without gravity. These calculations show that optimizing the microemulsion viscosity is a more effective method of increasing the critical velocity than adding polymer.

Second Series of Experiments for Oil #2 with Medium Microemulsion viscosity

Phase behavior and microemulsion viscosity results

A second batch of oil #1 was used after the first batch was depleted. The second batch had a higher viscosity than the first batch, so oil #2 was made by diluting the second batch of oil #1 with 20 wt% cyclohexane to reduce its viscosity to 4 cp.

The same surfactants used for oil #1 were used for oil #2, but the co-solvent IBA was replaced by TEGBE to lower the microemulsion viscosity. The surfactant formulation #2 for oil #2 was 0.5 wt% C_{13}-13PO-sulfate, 0.5 wt% C_{20-24}-IOS, and 2.0 wt% TEGBE. The aqueous solutions were clear and stable to more than 35,000 ppm TDS for more than 19 days at the temperature of 38 °C. This formulation equilibrates fast and shows a good optimum solubilization ratio of about 25 at the optimum salinity of about 30,000 ppm TDS as shown in Figure 4-13. The estimated IFT at optimum salinity is about 4.8×10^{-4} dynes/cm. The microemulsion viscosity at optimum salinity was 10 cp at 38 °C. By using the same amount of TEGBE instead of IBA as co-solvent, the microemulsion viscosity at optimum salinity was lowered from ~24 to ~10 cp. The microemulsion viscosity data are shown in Figure 4-14. The microemulsion was observed to be Newtonian at low shear rates.

Surfactant flood results

Another sandpack was prepared and the tracer test results showed that it is was nearly homogeneous (Figure 4-15). Flood #4 was conducted in this sandpack with surfactant formulation #2. The sandpack properties are shown in Table 3. With this new sandpack, the apparent oil bank viscosity was estimated to be ~11 cp. The critical velocity vs. the microemulsion viscosity for this sandpack is plotted in Figure 4-16. The critical velocity at a microemulsion viscosity of ~10 cp is about 0.36 ft/D, and could be further increased to ~0.7 ft/D if the microemulsion viscosity could be lowered to about 6 cp. However, attempts to further reduce the microemulsion viscosity with this oil were not successful. .

Surfactant flood #4 was done at 0.35 ft/D. Figure 4-17 shows photograph at different times during the surfactant flood. The oil recovery results for flood #4 are

shown in Figure 4-18. Practically all the oil was recovered by this surfactant flood. The results showed that the displacement was stable at 0.35 ft/D and demonstrated the critical velocity can be increased by decreasing the microemulsion viscosity.

To further test the gravity stable theory in different cores, surfactant flood #5 was performed in a Bentheimer sandstone core with formulation #2 at 38 °C. The tracer test results are shown in Figure 4-19. The Bentheimer sandstone core is more heterogeneous than the sandpack. With the properties of this core (Table 3), the apparent oil bank viscosity was estimated to be ~ 22 cp.

Figure 4-20 shows the sensitivity of the critical velocities to the microemulsion viscosity. The optimized critical velocity in this coreflood is about 0.25 ft/D with a microemulsion viscosity of about 10 cp. The optimum microemulsion viscosity is about 10 cp in this case. Either higher or lower microemulsion viscosity than 10 cp would lower the critical velocity. Based on this viscosity, surfactant flood #5 was done at a velocity of 0.2 ft/D. The coreflood results are shown in Figure 4-21. The core was cut after the surfactant flood to examine the performance of the flood shown in Figure 4-22. The oil shown in the photograph was from the oil trapped in the pressure line when the core was cut. All of the water flood residual oil was displaced from the core, so the surfactant flood at 0.2 ft/D was considered stable.

Figure 4-16 shows that the optimum critical velocity in the sandpack can be achieved by decreasing the microemulsion viscosity to around 6 cp. However, with an oil viscosity of 4 or 5 cp and a temperature of 38 °C, the microemulsion viscosity could not be further reduced. The lowest microemulsion viscosity obtained under these conditions was about 10 cp.

Third Series of Experiments for Oil #3 with Low Microemulsion viscosity

Phase behavior and microemulsion viscosity results

To obtain a lower microemulsion viscosity, the experimental temperature was increased from 38 °C to 58 °C, and oil #3 with a viscosity of 1 cp at 58 °C was used. Oil #3 was made by diluting the second batch of oil with 50 wt% toluene. Surfactant formulation #3 developed for this oil was 0.5 wt% C_{13}-13PO-sulfate, 0.5 wt% C_{15-18}-IOS, and 2.0 wt % TEGBE. The phase behavior results are shown in Figure 4-23. The optimum solubilization ratio is about 18 at optimum salinity of about 22,000 ppm with the aqueous stability of more than 75,000 ppm at 58 °C. The estimated IFT at optimum salinity is about 9.3×10^{-4} dynes/cm. The co-surfactant of C_{20-14}-IOS in formulation #2 was replaced by C_{15-18}-IOS in this formulation (#3) to obtain good solubilization ratios as well as to reduce the microemulsion viscosity. The microemulsion viscosity at optimum salinity was about 3.5 cp at 58 °C, and the microemulsion shows Newtonian behavior as shown in Figure 4-24.

Surfactant flood results

A third sandpack was made for surfactant flood #6. Its properties are summarized in Table 3. The tracer test data are shown in Figure 4-25. The critical velocities vs. the microemulsion viscosity were plotted in Figure 4-26 with the estimated apparent oil bank viscosity of ~5 cp. The highest critical velocity is about 1.5 ft/D at a microemulsion viscosity of about 3.5 cp.

Taking into account uncertainties during the surfactant flood, the surfactant solution was injected at a frontal velocity of 1.0 ft/D in flood #6. Figure 4-27 shows photographs of this sandpack flood at different times during the flood. The oil recovery results for flood #6 are shown in Figure 4-28. The results showed that the flood was

stable at 1.0 ft/D, and the critical velocity was successfully increased by further decreasing the microemulsion viscosity using the less viscous oil.

Bentheimer sandstone coreflood #7 was also conducted with oil #4 at 58 °C. The core properties are shown in Table 3. The tracer data are shown in Figure 4-29. The critical velocity estimated with an apparent oil bank viscosity of ~11 cp is shown in Figure 4-30. The critical velocity can be optimized to ~0.46 ft/D at the microemulsion viscosity of about 8 cp. Formulation #3 was slightly adjusted to contain less co-solvent to increase the microemulsion viscosity. The tuned surfactant formulation #4 was 0.5 wt% C_{13}-13PO-sulfate, 0.5 wt% C_{15-18}-IOS, and 1.5 wt % TEGBE. This formulation had an optimum solubilization ratio of ~25 at optimum salnity of about 20,000 ppm with an aqueous stability of more than 75,000 ppm at 58 °C (Figure 4-31). The estimated IFT at optimum salinity is about 4.8×10^{-4} dynes/cm. The microemulsion viscosity at optimum salinity was about 8.0 cp at 1 s^{-1} at 58 °C (Figure 4-32).

Using this formulation, Bentheimer sandstone coreflood #7 was performed at 0.40 ft/D. The coreflood results are plotted in Figure 4-33. The core was opened after the surfactant flood. A photograph of the cut core is shown in Figure 4-34. A small amount of oil was left in the core after surfactant flood. The final oil recovery was above 90.0 % with the final oil saturation less than 5.0 %.

To further optimize the surfactant flood, flood #8 was repeated in a new sandpack with an injection of a surfactant slug followed by a brine drive. The same surfactant formulation #3 and oil #3 were used for the sandpack flood #8 at 58 °C. The tracer test results show the sandpack is homogeneous (Figure 4-35). A 0.5 PV (PV×C=50) surfactant slug was injected at the optimum salinity of 22,000 ppm followed by a brine drive of 14,000 ppm salinity at 1.0 ft/D. The photographs of the sandpack during the

flood are shown in Figure 4-36. Oil recovery results obtained from this sandpack flood are shown in Figure 4-37.

An additional flood #9 was performed in the same sandpack as flood #8 using the same formulation in the same injection mode of 0.5 PV surfactant slug followed by brine drive, but at a higher frontal velocity of 4.0 ft/D to compare with flood #8. Figure 4-38 shows that the flood was very unstable. The oil recovery results shown in Figure 4-39 also indicate that the flood was not stable. The oil production lasted almost 2 pore volumes. The oil cut in the oil bank was lower than flood #8, and more oil was produced as an emulsion.

The experimental velocities are plotted against theoretical stable velocities for all surfactant floods above in Figure 4-40. The red data points are velocities of unstable surfactant floods (flood #2, 3 and 9), and blue data points are velocities of stable surfactant floods (flood #1, 4, 5, 6 and 7). The linear regression line is plotted for velocities of stable floods, and the equation and R-squared value are shown in the same fugure. The slope of the straight line is very close to 1, the straight line intercepts at the origin, and R^2 is almost 1. This indicates the experimental velocities and theoretical velocities are in very good agreement. The modified theory can therefore be used to predict the stable velocity of a surfactant flood.

SUMMARY

Three series of experiments were performed including phase behavior tests, microemulsion viscosity measurements, and surfactant floods in both sandpacks and Bentheimer sandstone cores. Surfactant formulations were developed for each flood with ultra-low IFT and good aqueous stability.

The new stability theory is in good agreement with the experimental results. The stability theory can be used to predict the critical velocities very well compared to the experimental data. The critical velocity of surfactant flood #1 in a 5500 md sandpack with formulation #1 was experimentally identified to be 0.20 ft/D at a microemulsion viscosity of ~24 cp at 38 °C. By replacing IBA with TEGBE as co-solvent in formulation #2, the microemulsion viscosity was reduced to ~10 cp and the critical velocity increased to 0.35 ft/D in a 5000 md sandpack (flood #4) at 38 °C. The performance of a stable flood with the same formulation was verified in a Bentheimer sandstone core of 2500 md (flood #5) at 0.20 ft/D and 38 °C.

A less viscous oil (oil #3) and higher temperature of 58 °C were selected to further lower the microemulsion viscosity. Formulation #3 was developed to obtain a microemulsion viscosity of ~4 cp. The critical velocity was then increased to 1.0 ft/D in a sandpack of 4200 md permeability (flood #6). To perform the stable surfactant flood in a 2300 md Bentheimer sandstone core (flood #7), formulation #4 with less co-solvent than formulation #3 was used with a microemulsion viscosity of ~8 cp. The stable flood was done at 0.40 ft/D in flood #7. Flood #6 was repeated in another sandpack of 4300 md permeability, but designed with an injection of 0.5 PV surfactant slug followed by a brine drive at a stable velocity of 1.0 ft/D.

The predictions made using the new stability theory were found to be in good agreement with the experimental core floods. These results show that it is possible to optimize the microemulsion viscosity to maximize the critical velocity for a stable surfactant flood. The increase shown for these experiments was very large. Such a large increase in velocity is highly favorable since it implies a much lower project life in the field.

These experiments have provided new insight into how a gravity stable surfactant displacement behaves and in particular the importance of the microemulsion phase and its properties, especially its viscosity. This insight opens up a new pathway for optimizing surfactant floods without mobility control. The experimental results presented here and the simulation results presented by Tavassoli *et al*. (2013) indicate that it is possible to design an efficient surfactant flood without any mobility control if the surfactant solution is injected at a stable velocity in horizontal wells at the bottom of the formation and the oil captured in horizontal wells at the top. This approach is practical only if the vertical permeability of the geological zone is high. Under favorable reservoir conditions, gravity stable surfactant floods may be attractive alternatives to surfactant-polymer floods. Some of the world's largest oil reservoirs are deep, high-temperature, high-permeability, light-oil reservoirs and thus candidates for gravity stable surfactant floods under favorable reservoir conditions.

Table 4-1: Oil Properties

Oil #	Temperature (°C)	Surrogate Oil	Density (g/cm^3)	Viscosity (cp)
1	38	dead oil	0.80	5.4
2	38	20 wt% cyclohexane and 80 wt% dead oil	0.80	4.0
3	58	50 wt% toluene and 50 wt% dead oil	0.82	1.0

Table 4-2: Surfactant Formulations

Formulation #	Temperature (°C)	Oil #	Surfactant #1	Surfactant #2	Co-solvent
1	38	1	0.5 wt% C_{13}-13PO-sulfate	0.5 wt% C_{20-24}-IOS	2.0 wt % IBA
2	38	2	0.5 wt% C_{13}-13PO-sulfate	0.5 wt% C_{20-24}-IOS	2.0 wt % TEGBE
3	58	3	0.5 wt% C_{13}-13PO-sulfate	0.5 wt% C_{15-18}-IOS	2.0 wt % TEGBE
4	58	3	0.5 wt% C_{13}-13PO-sulfate	0.5 wt% C_{15-18}-IOS	1.5 wt % TEGBE

Table 4-3: Sandpack and White Castle Field Properties

Parameter	Sandpack Flood	White Castle Pilot
k (md)	5500	1000
ϕ	0.35	0.31
α	90°	45°
ρ_o (g/cm^3)	0.80	0.88
ρ_s (g/cm^3)	1.0	1.0
ρ_{me} (g/cm^3)	0.9	0.94
μ_o (cp)	5.4	2.8
μ_w (cp)	0.7	0.64
μ_s (cp)	0.7	0.64
μ_{me} (cp)	24	10 (estimated)
k^0_{rw}	1.0	1.0
k^0_{ro}	0.93	0.9 (estimated)
k_{rs}	1.0	1.0
k_{rme}	1.0	1.0
λ_{OB} (estimated)	0.091	0.08
v (ft/day) by Eq. 1	1.69	0.30
v (ft/day) by Eq. 2	0.45	0.06
v (ft/day) by Eq. 3	unconditionally stable	0.15
v (ft/day) by Eq. 4	0.18	0.04
Actual v (ft/day)	0.2	0.24 (estimated)

Table 4-4: Summary of Surfactant Floods

Experiment #	#1	#2	#3	#4	#5	#6	#7	#8	#9
Temperature (°C)	38	38	38	38	38	58	58	58	58
Oil #	1	1	1	2	2	3	3	3	3
Core Name	Ottawa Sand	Ottawa Sand	Ottawa Sand	Ottawa Sand	Bentheimer Sandstone	Ottawa Sand	Bentheimer Sandstone	Ottawa Sand	Ottawa Sand
Length (cm)	24.4	24.4	24.4	25.1	29.5	25.9	29.6	25.9	25.9
Diameter (cm)	4.8	4.8	4.8	4.8	5.0	4.8	5.0	4.8	4.8
Pore Volume (ml)	160	160	160	169	133	169	133	169	169
Porosity	0.350	0.350	0.350	0.372	0.234	0.361	0.233	0.361	0.361
Brine Permeability (md)	5500	5500	5500	5000	2500	4200	2300	4300	4300
Initial Oil Saturation, S_{oi} (%)	82.89	84.70	83.17	81.1	71.4	73.8	67.2	74.0	72.8
Residual Oil Saturation After waterflood, S_{orw} (%)	16.16	12.58	14.02	15.1	32.7	16.5	28.9	15.5	14.9
Water Viscosity (cp)	0.7	0.7	0.7	0.7	0.7	0.51	0.51	0.51	0.51
Estimated Apparent Oil Bank Viscosity (cp)	11	11	11	11	22	5	11	5	5
Microemulsion Viscosity (cp)	24	24	24	10	10	4	8	4	4
Microemulsion Density (g/cm^3)	0.90	0.90	0.90	0.91	0.91	0.87	0.87	0.87	0.87
Surfactant Solution									
Formulation #	1	1	1	2	2	3	4	3	3
Surfactant Concentration (wt%)	1.0	1.0	1.0	1.0	1.0	1.0	1.0	1.0	1.0
Viscosity (cp)	0.7	0.7	0.7	0.7	0.7	0.51	0.51	0.51	0.51
Density (g/cm^3)	1.0	1.0	1.0	1.0	1.0	1.0	1.0	1.0	1.0
Salinity (ppm)	21,000	21,000	21,000	30,000	30,000	22,000	20,000	22,000	22,000
Velocity (ft/day)	0.20	0.40	0.80	0.35	0.20	1.0	0.40	1.0	4.0
Brine Drive									
Salinity (ppm)								14,000	14,000
Velocity (ft/day)								1.0	4.0
Results									
Oil Recovery (%)	99.74	99.81	94.93	94.12	95.86	94.98	92.60	96.37	87.70
Final Oil Saturation, S_{orc}	0.0006	0.0003	0.0085	0.009	0.014	0.008	0.021	0.006	0.018

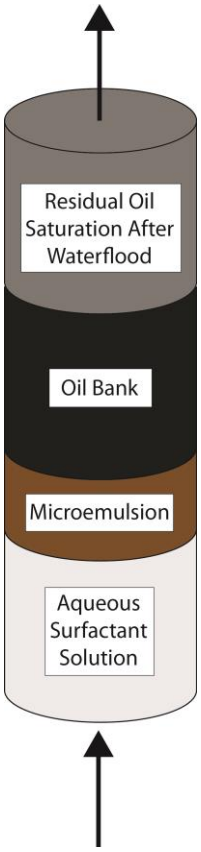

Figure 4-1: Illustration of four idealized flow regions.

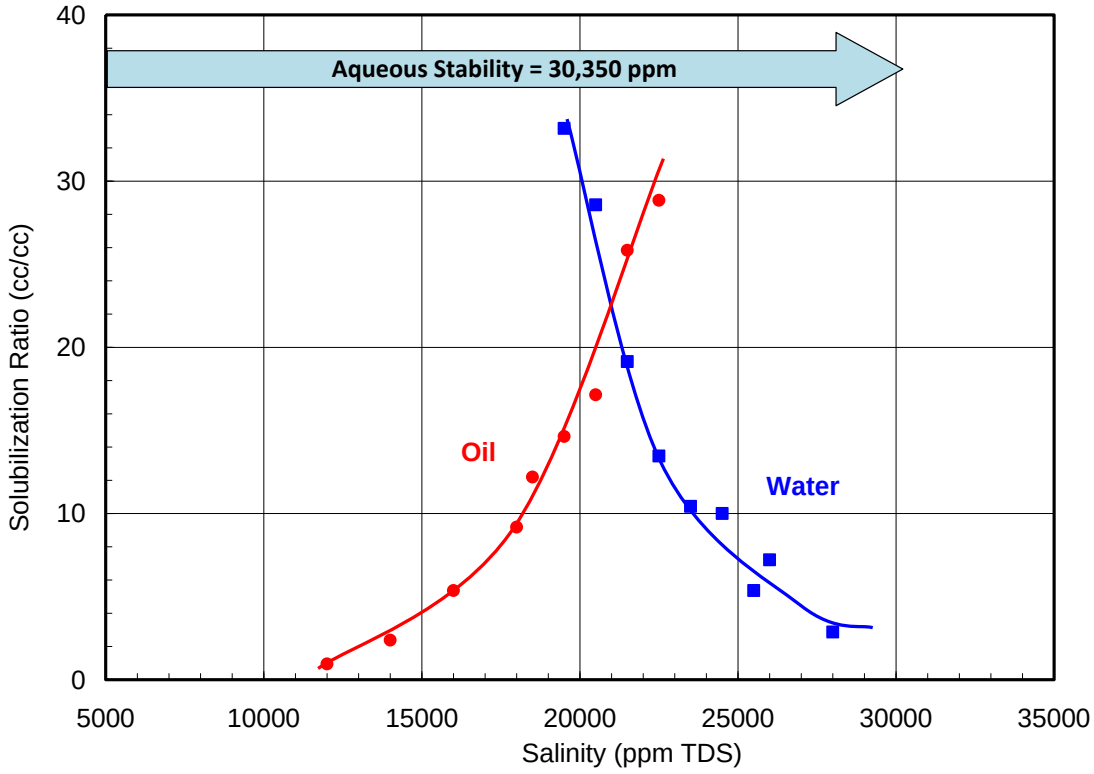

Figure 4-2: Phase behavior of 0.5 wt% C_{13}-13PO-sulfate, 0.5 wt% C_{20-24}-IOS, and 2.0 wt% IBA for oil #1 at 38 °C with 50 vol% oil after 54 days.

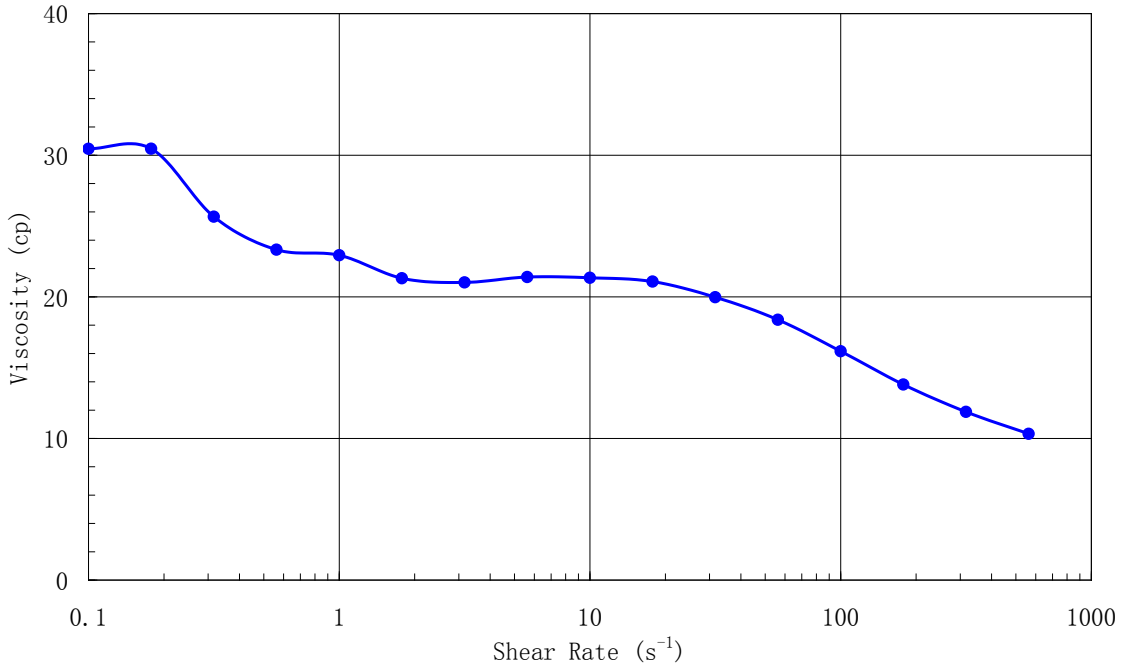

Figure 4-3: Microemulsion viscosity for formulation #1 at optimum salinity and 38 °C.

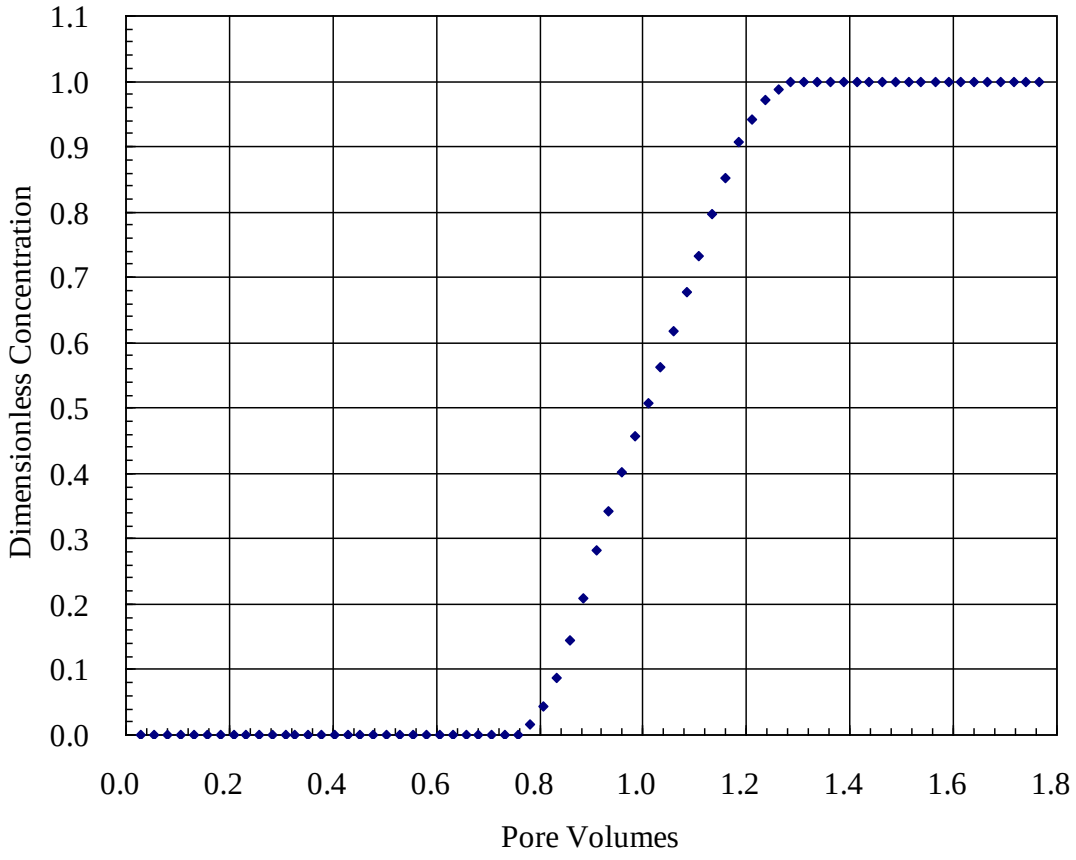

Figure 4-4: Tracer breakthrough data in sandpack for surfactant flood #1-3.

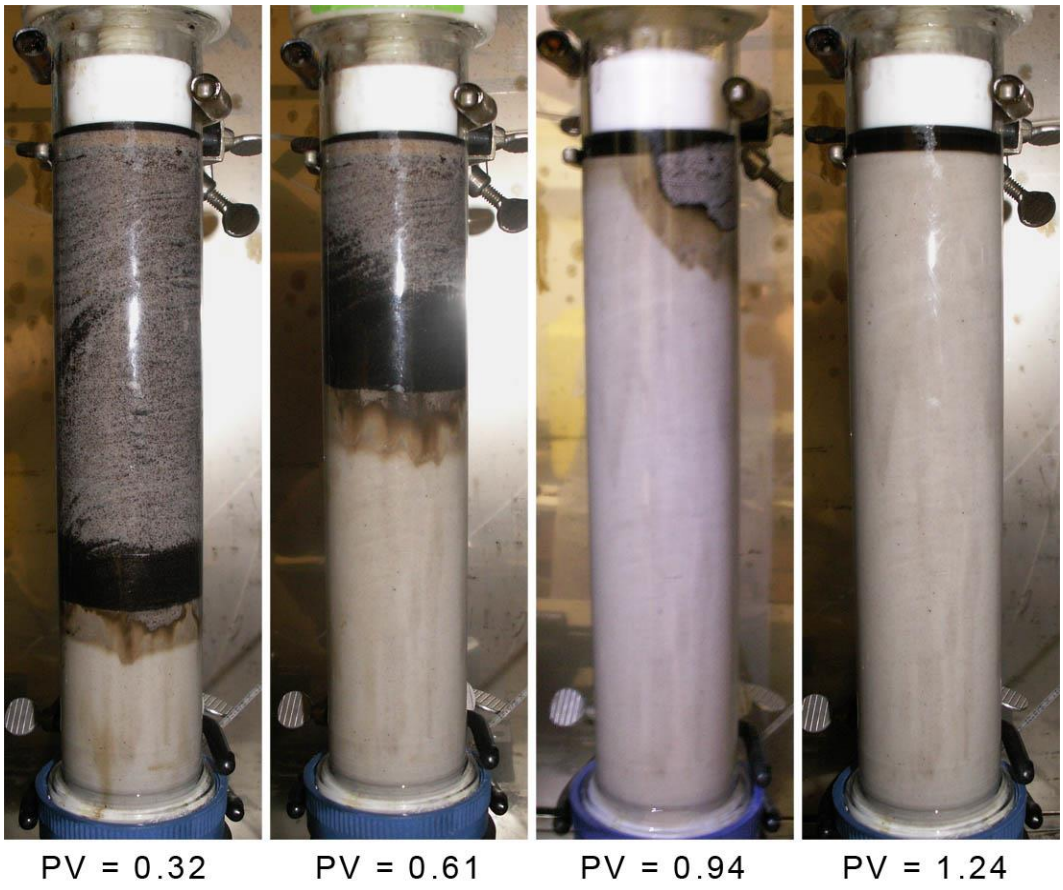

Figure 4-5: Photographs of surfactant flood #1.

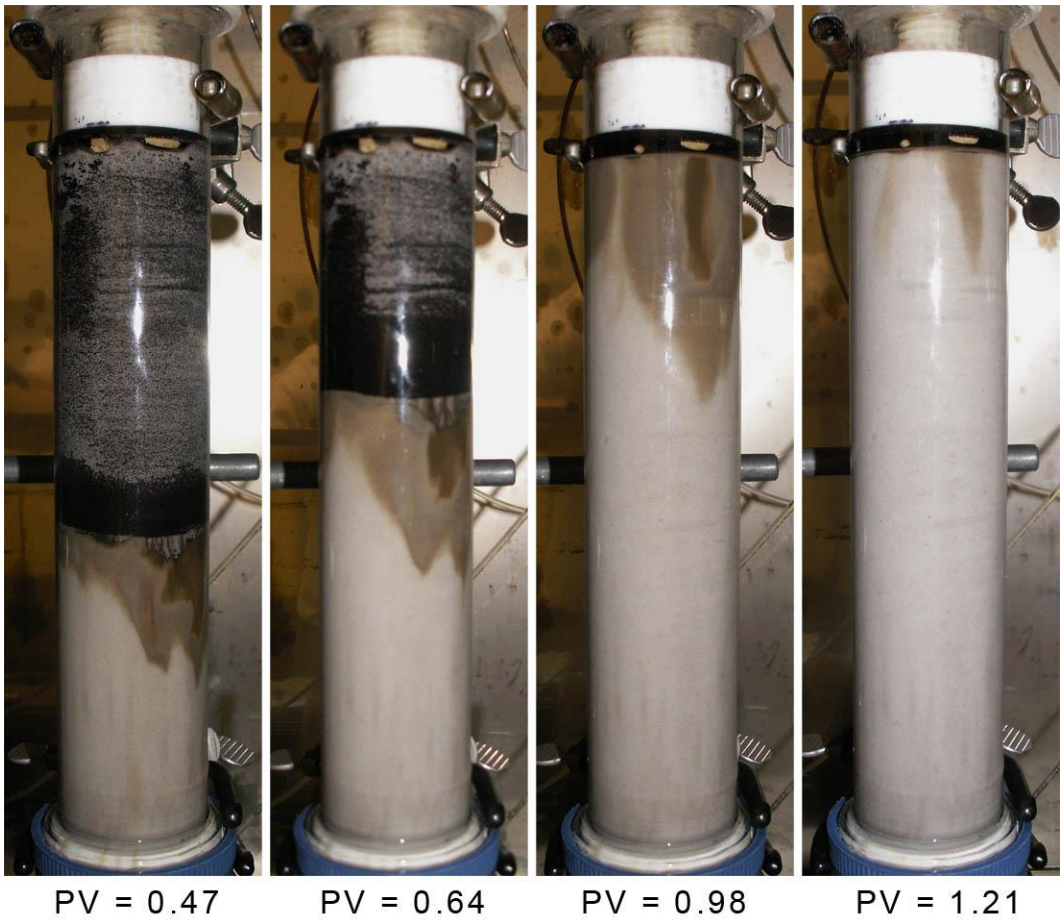

Figure 4-6: Photographs of surfactant flood #2.

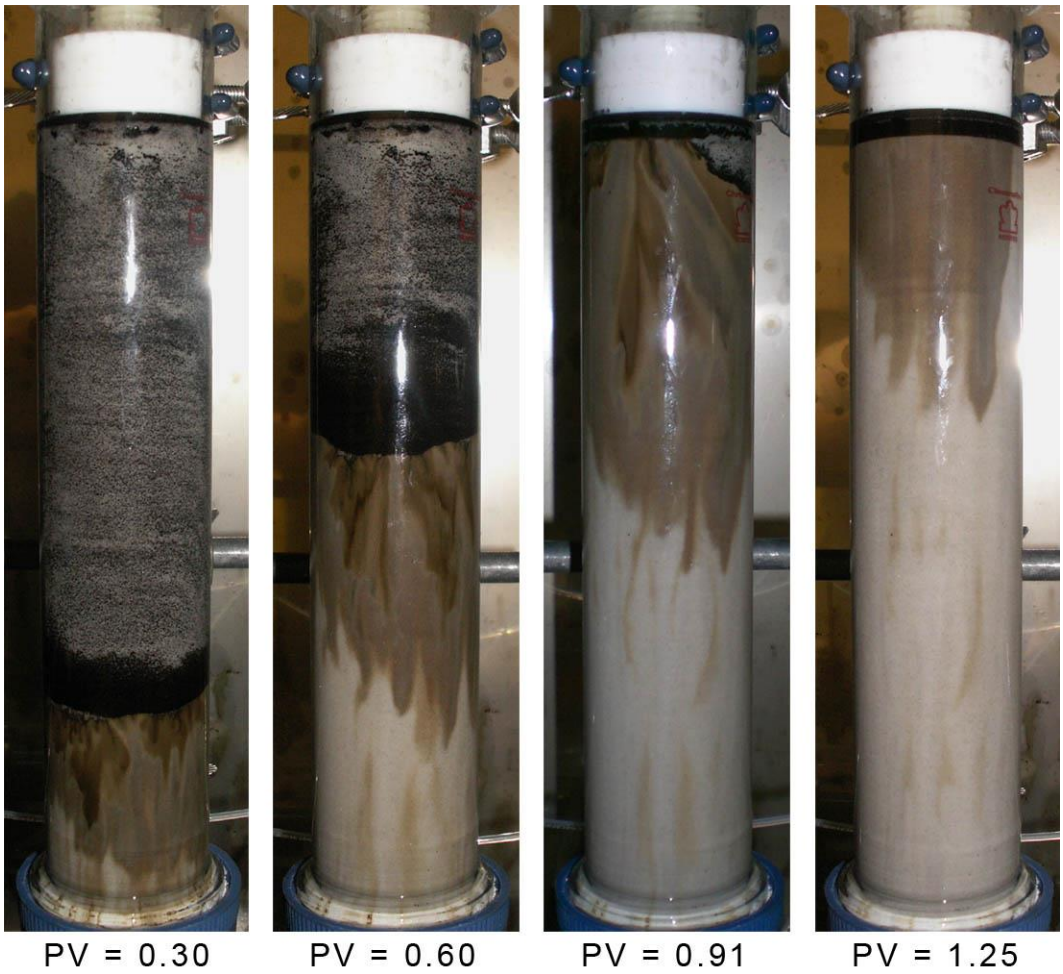

Figure 4-7: Photographs of surfactant flood #3.

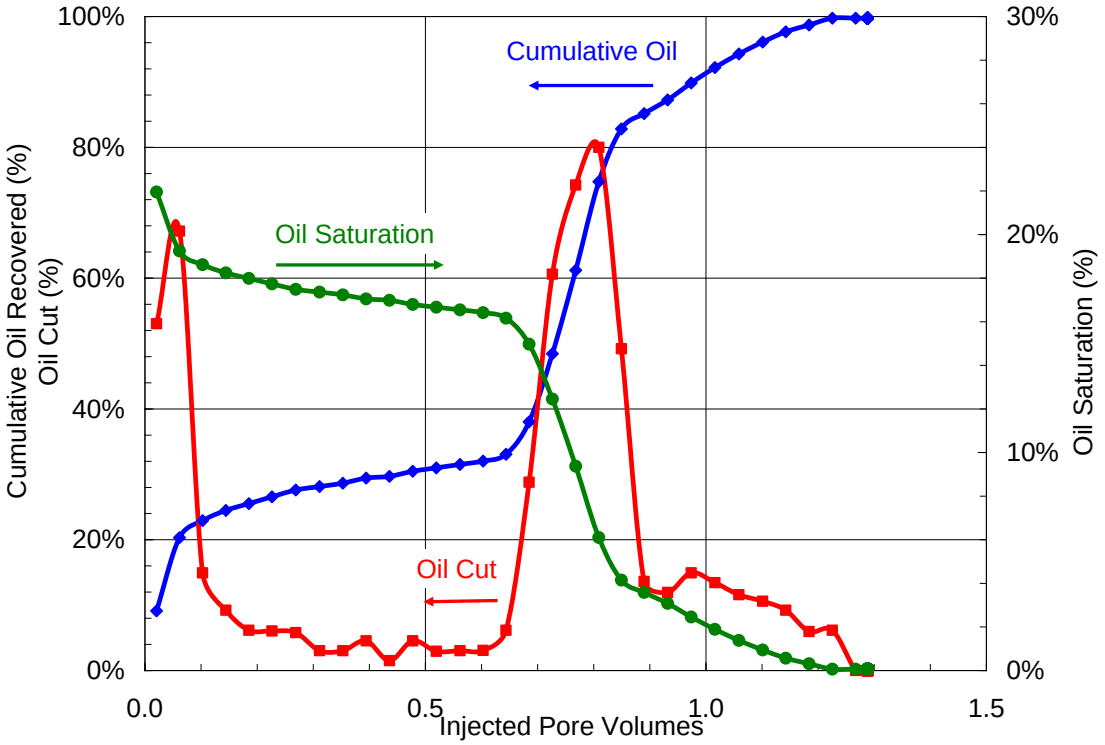

Figure 4-8: Measured oil recovery, oil cut, and oil saturation from surfactant flood #1 at 0.2 ft/day and 38 °C.

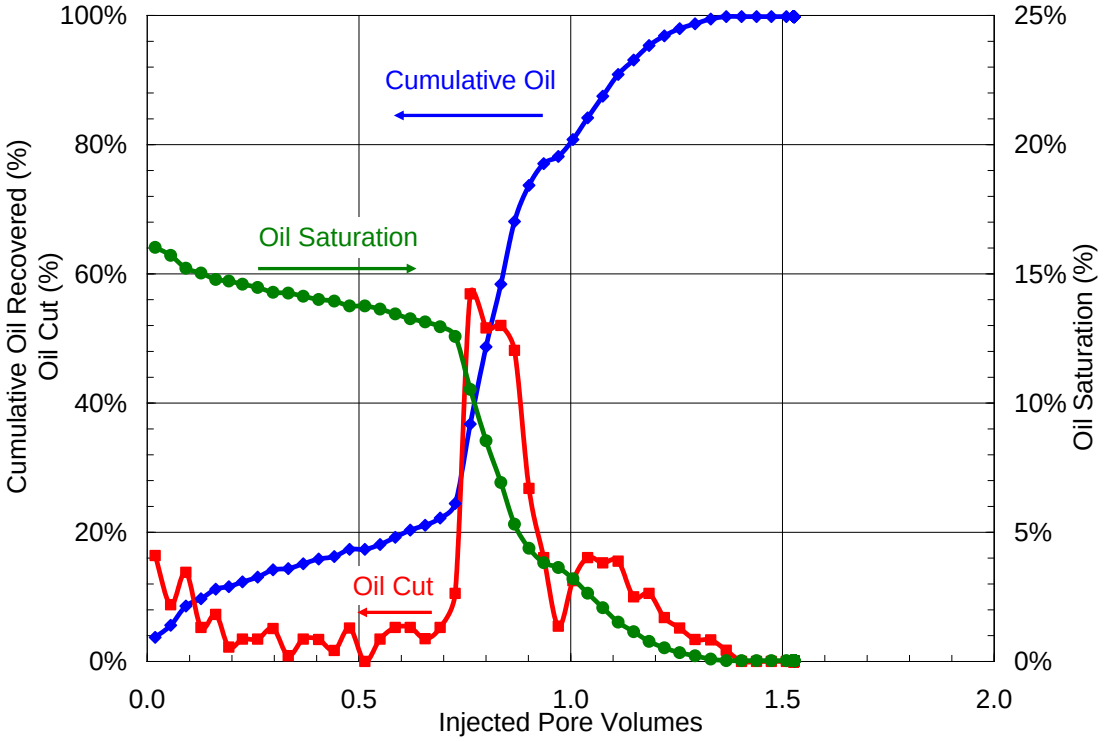

Figure 4-9: Measured oil recovery, oil cut, and oil saturation from surfactant flood #2 at 0.4 ft/day and 38 °C.

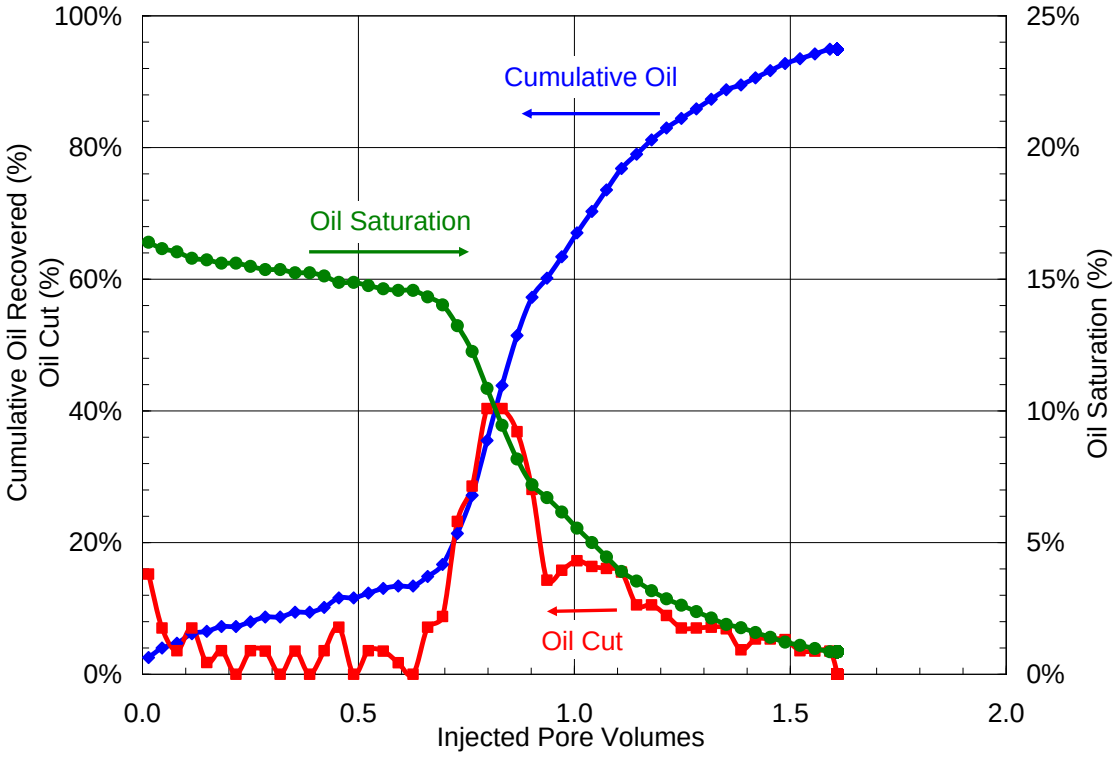

Figure 4-10: Measured oil recovery, oil cut, and oil saturation from surfactant flood #3 at 0.8 ft/day and 38 °C.

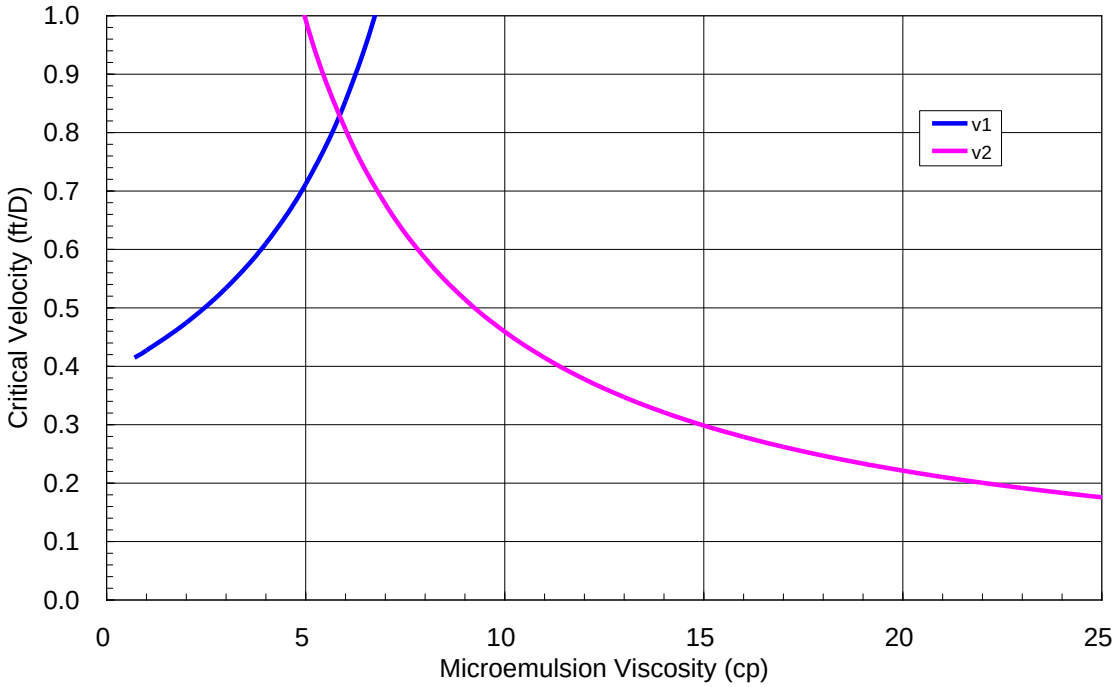

Figure 4-11: Critical velocity of upper interface (v1) and lower interface (v2) for sandpack flood #1.

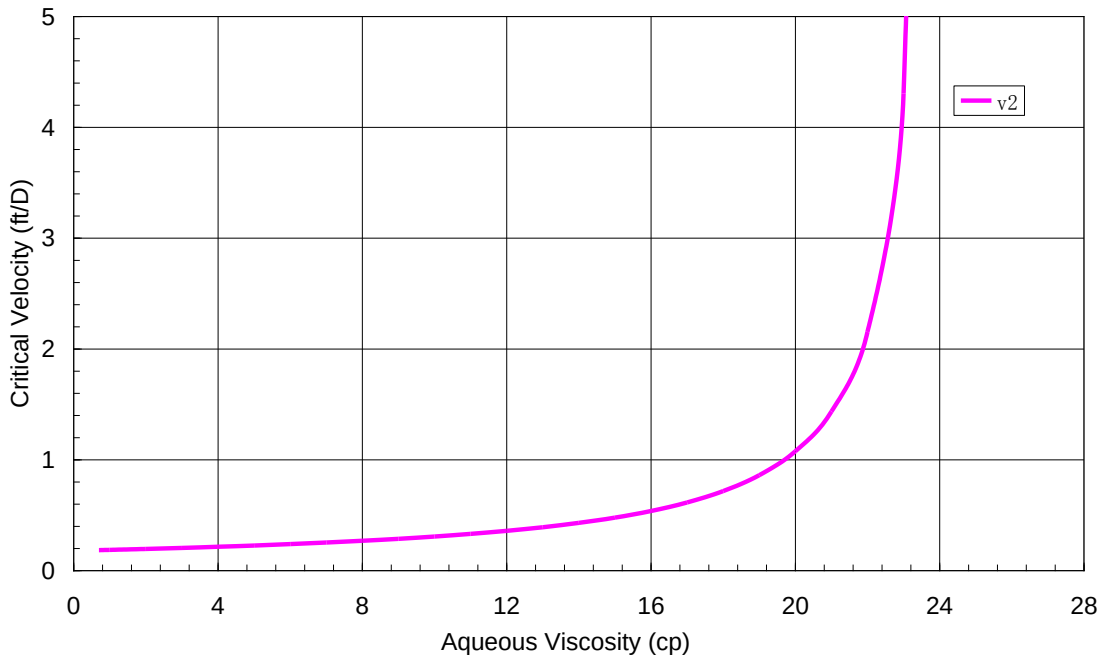

Figure 4-12: Critical velocity of lower interface for a fixed microemulsion viscosity of 24 cp for sandpack flood #1.

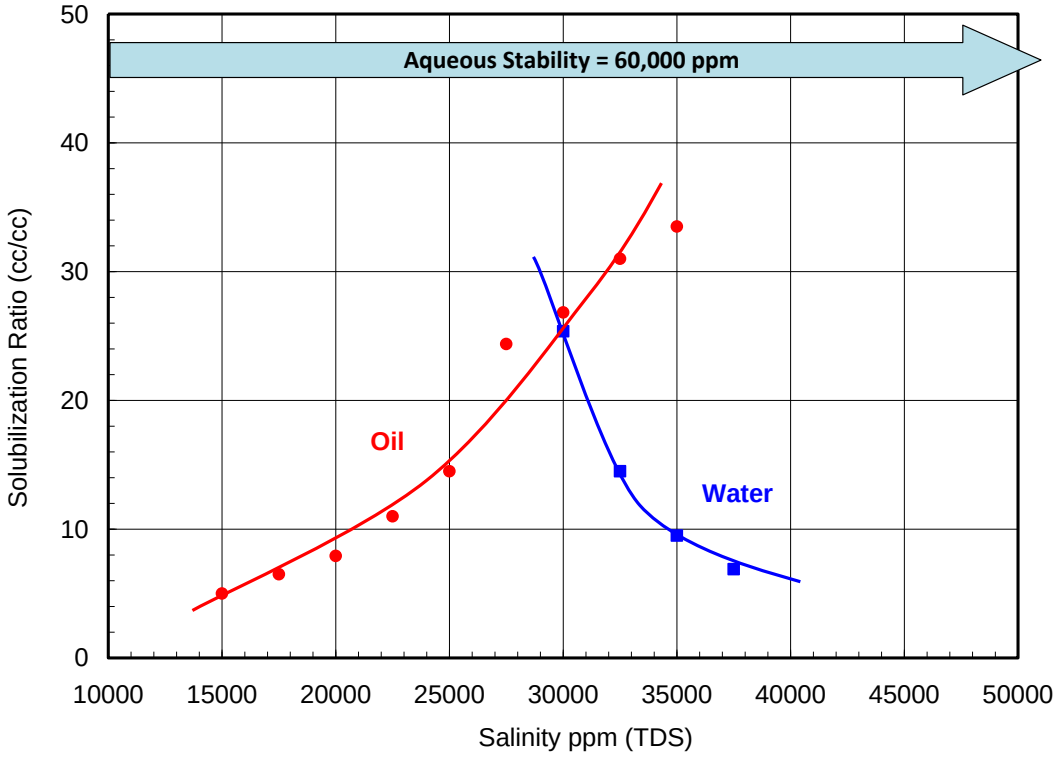

Figure 4-13: Phase behavior of 0.5 wt% C_{13}-13PO-sulfate, 0.5 wt% C_{20-24}-IOS, and 2.0 wt% TEGBE for oil #2 at 38 °C with 50 vol% oil after 19 days.

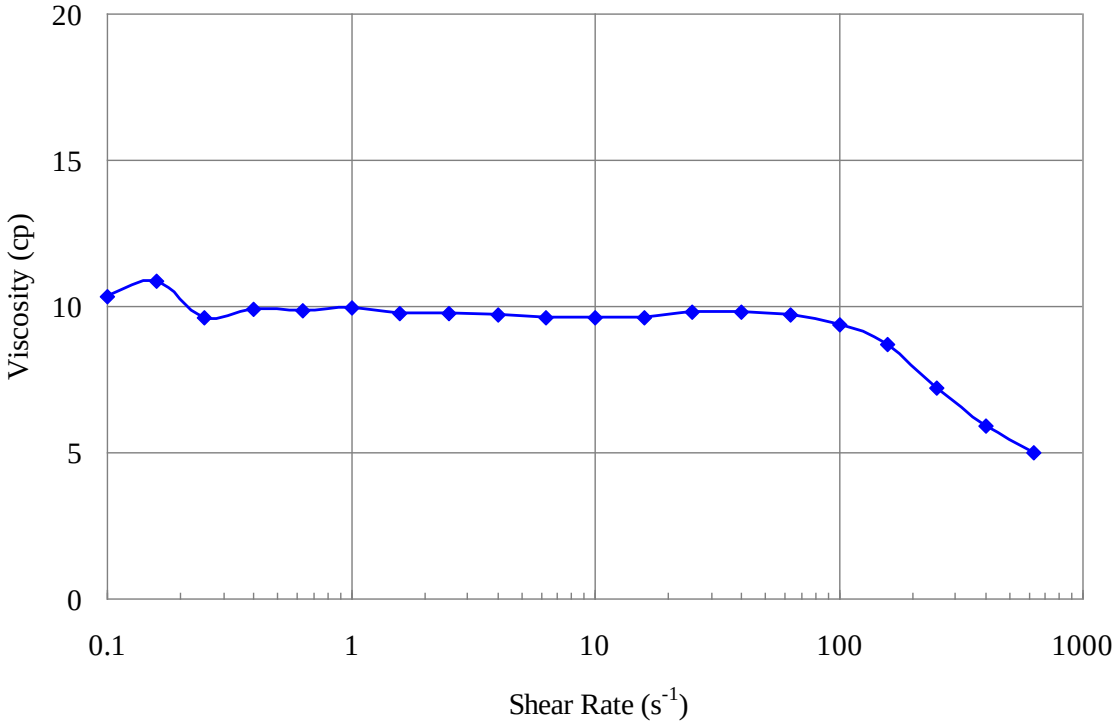

Figure 4-14: Microemulsion viscosity for formulation #2 at optimum salinity and 38 °C.

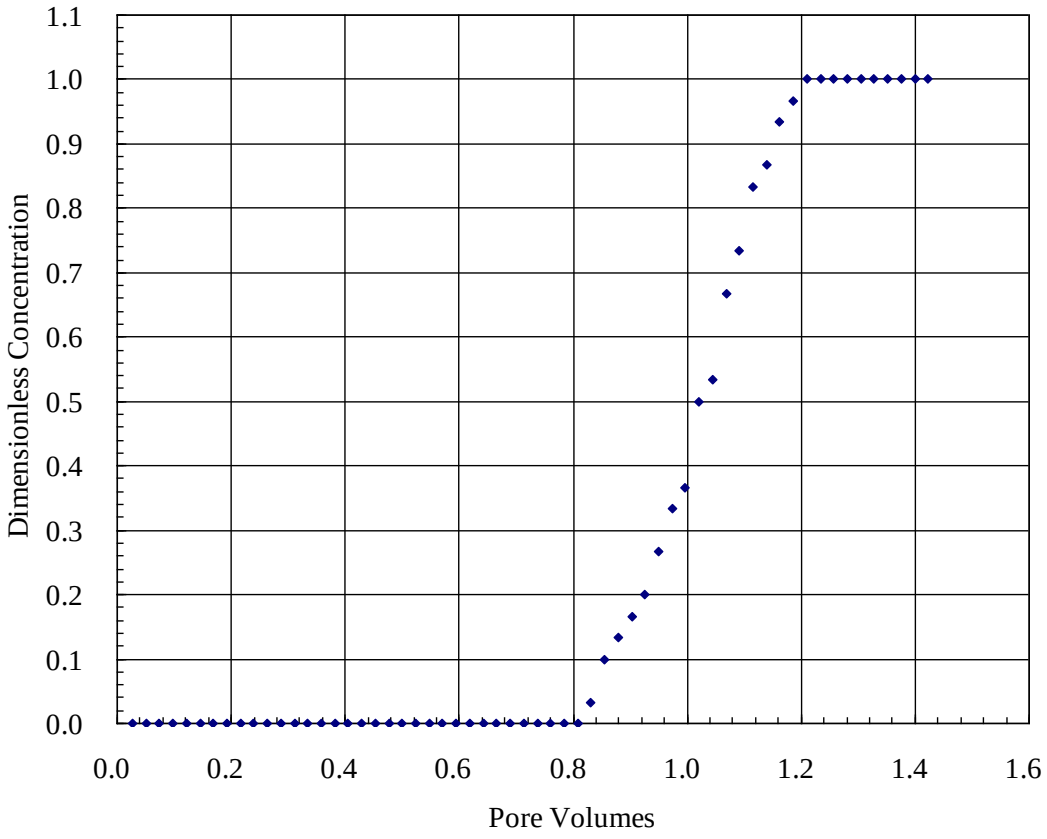

Figure 4-15: Tracer breakthrough data in sandpack #4.

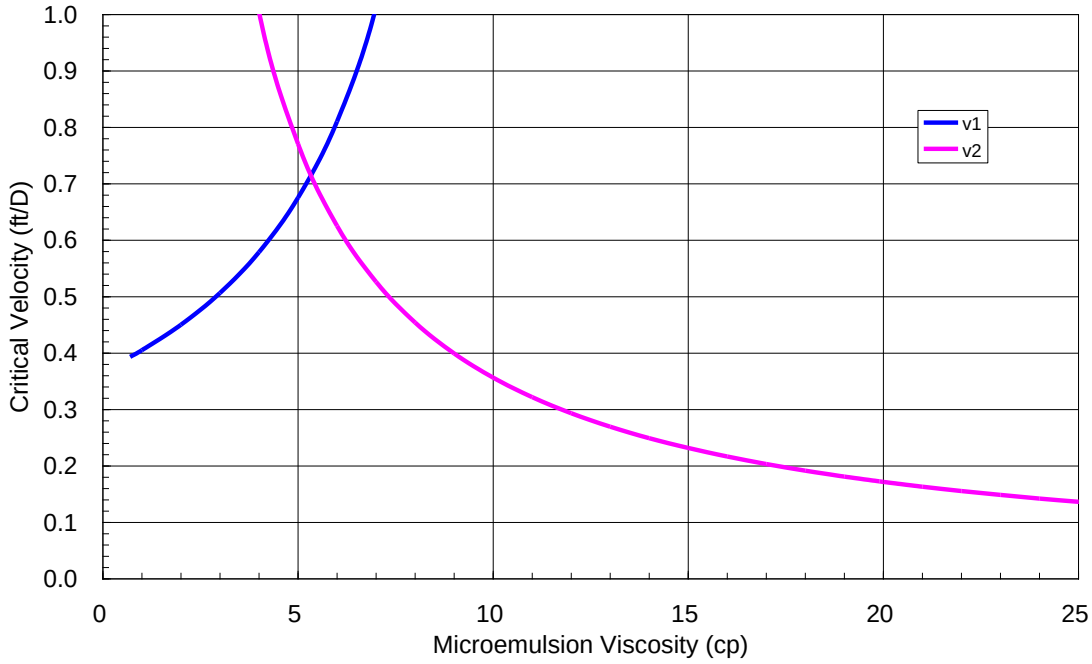

Figure 4-16: Critical velocity of upper interface (v1) and lower interface (v2) for sandpack flood #4.

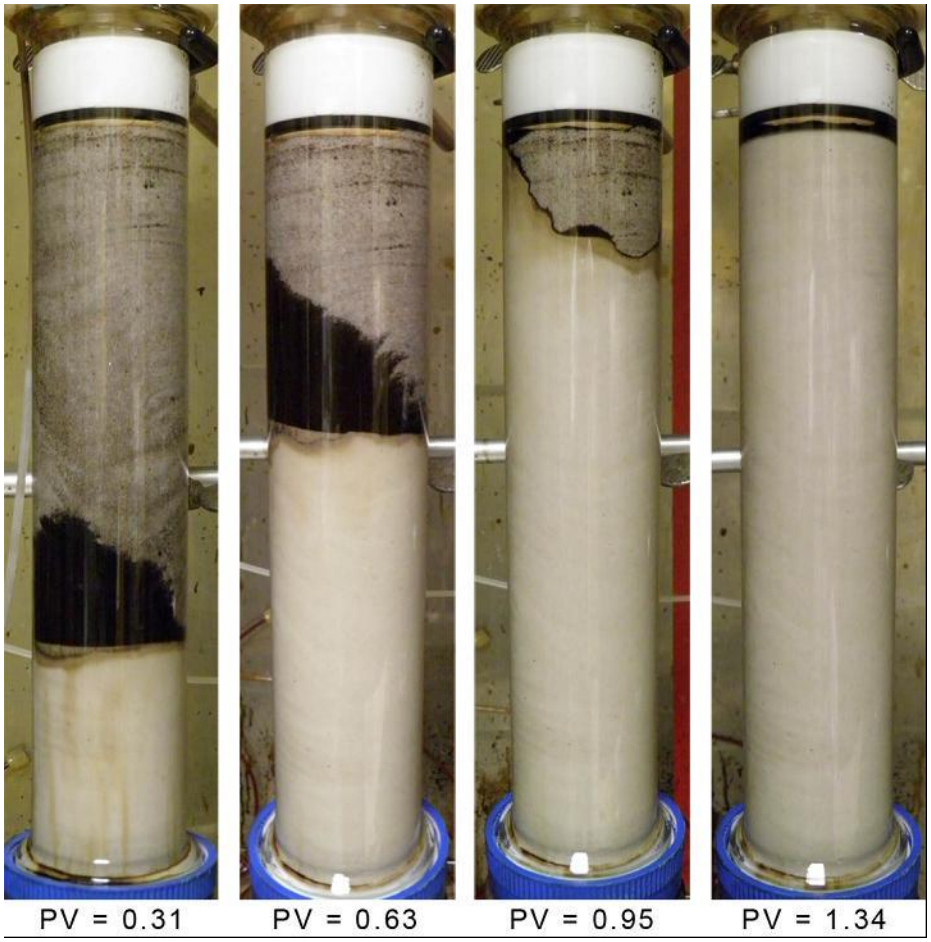

Figure 4-17: Photographs of surfactant flood #4.

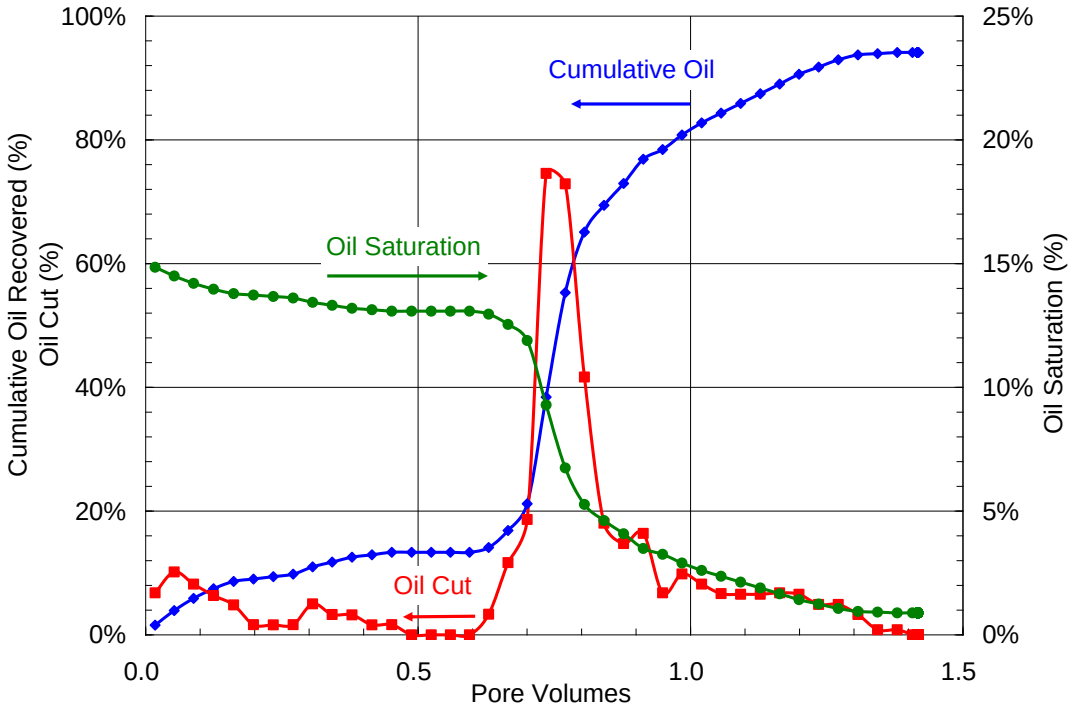

Figure 4-18: Measured oil recovery, oil cut, and oil saturation from surfactant flood #4 at 0.35 ft/day and 38 °C.

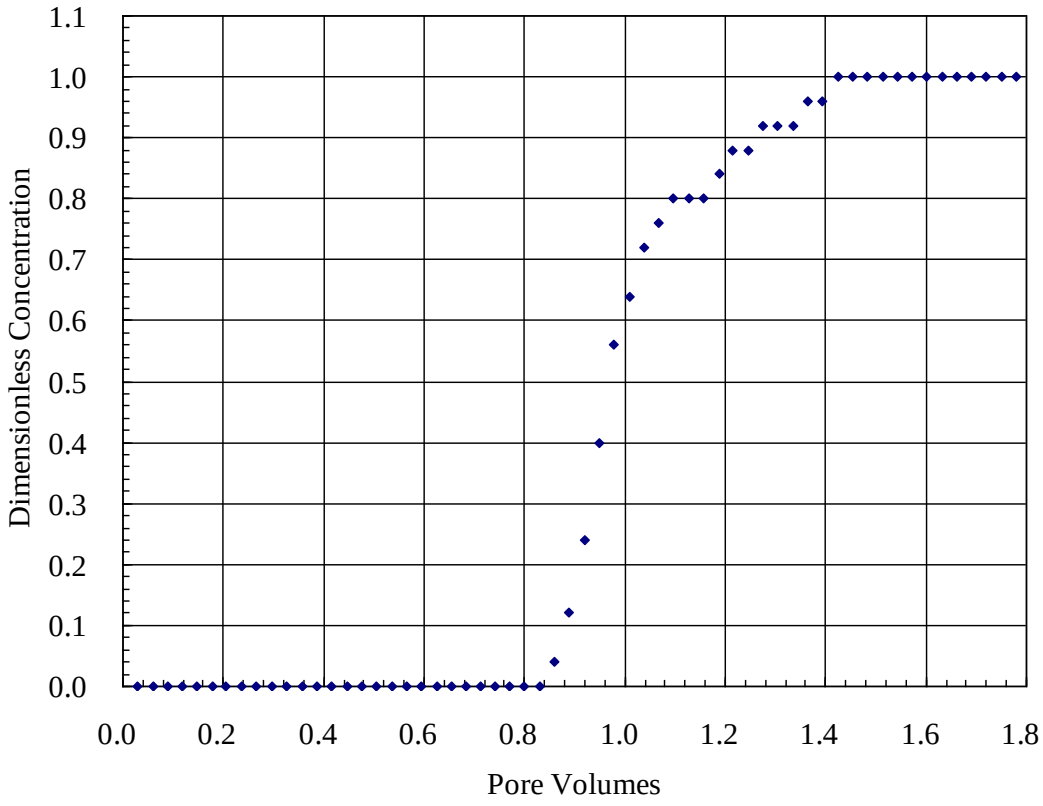

Figure 4-19: Tracer breakthrough data in a Bentheimer sandstone coreflood #5.

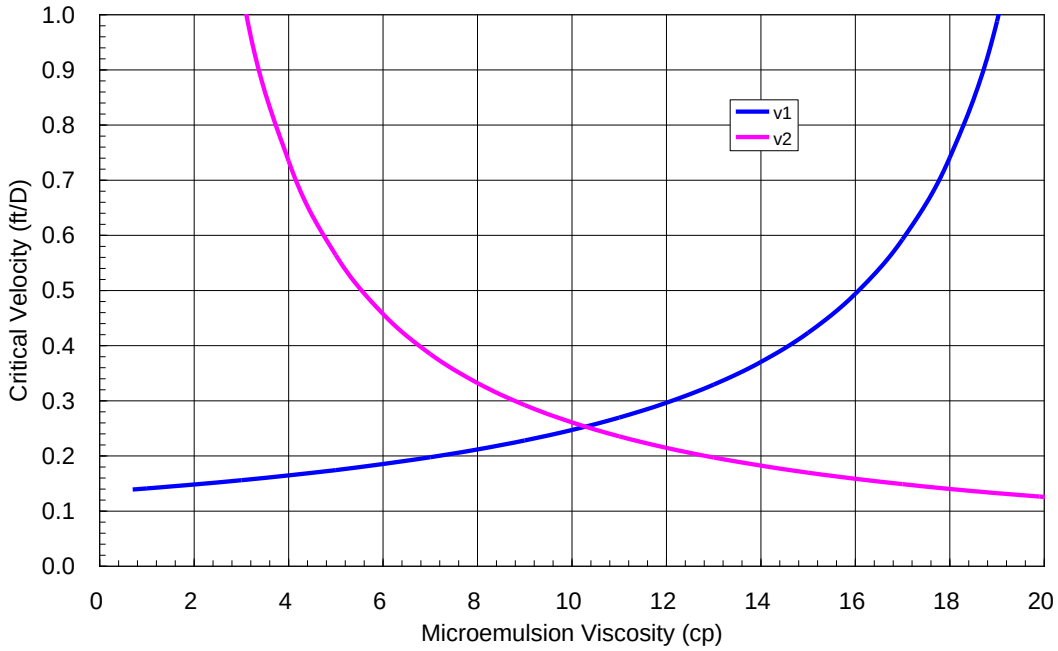

Figure 4-20: Critical velocity of upper interface (v1) and lower interface (v2) for coreflood #5.

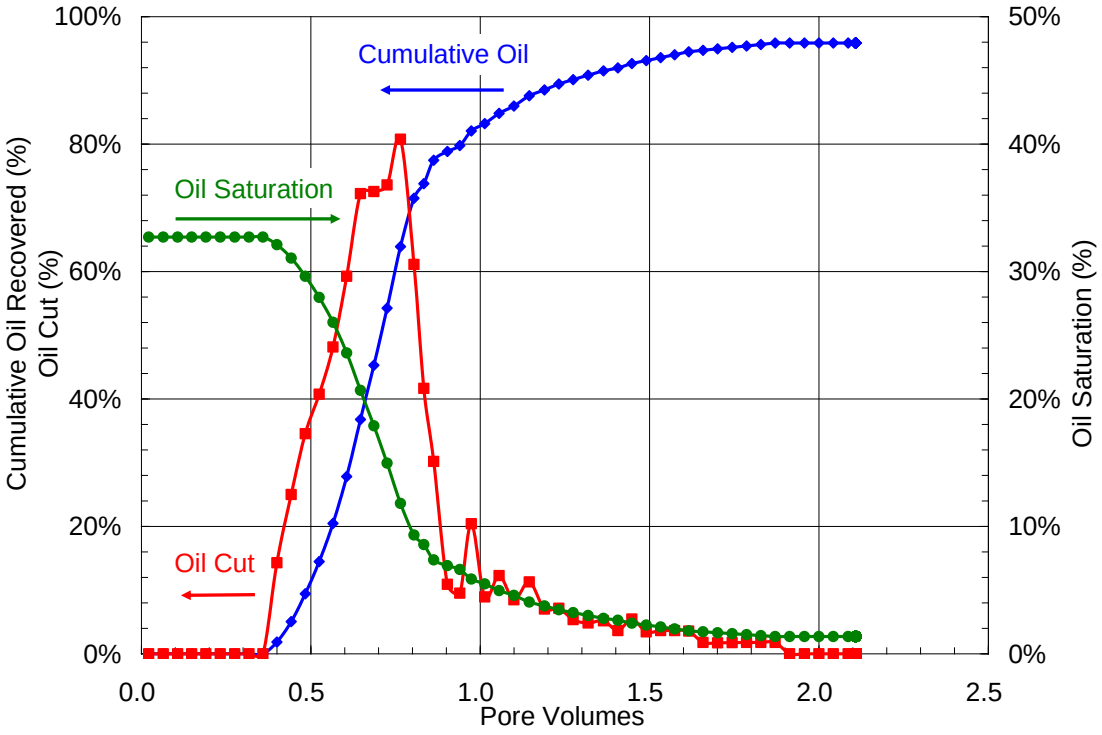

Figure 4-21: Measured oil recovery, oil cut, and oil saturation from surfactant flood #5 at 0.20 ft/day and 38 °C.

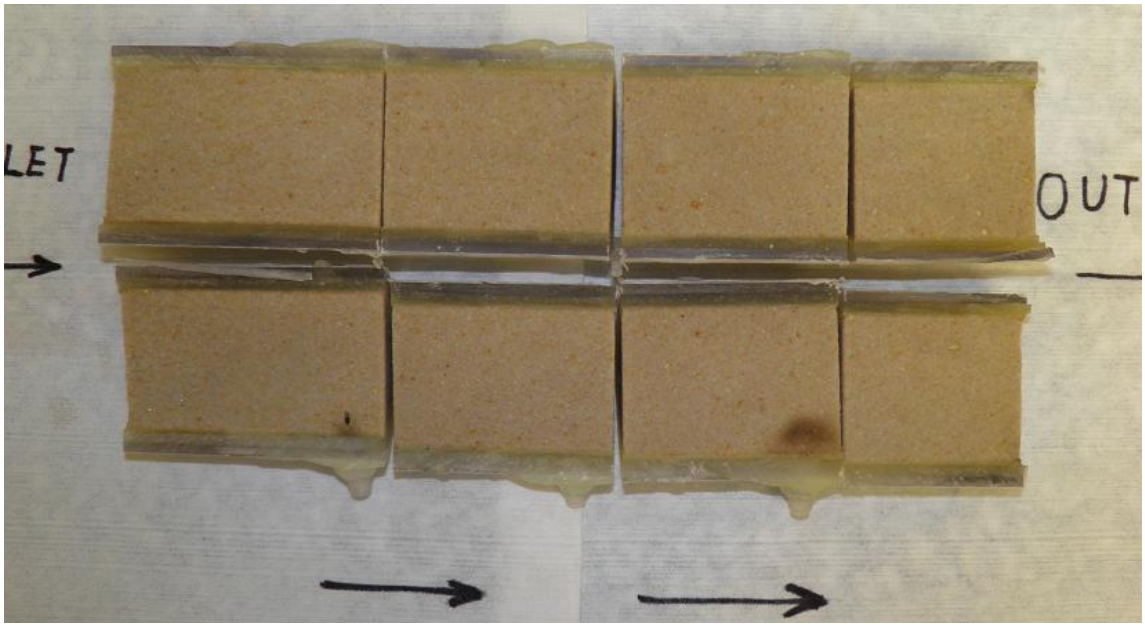

Figure 4-22: Photographs of the Bentheimer core after surfactant flood #5.

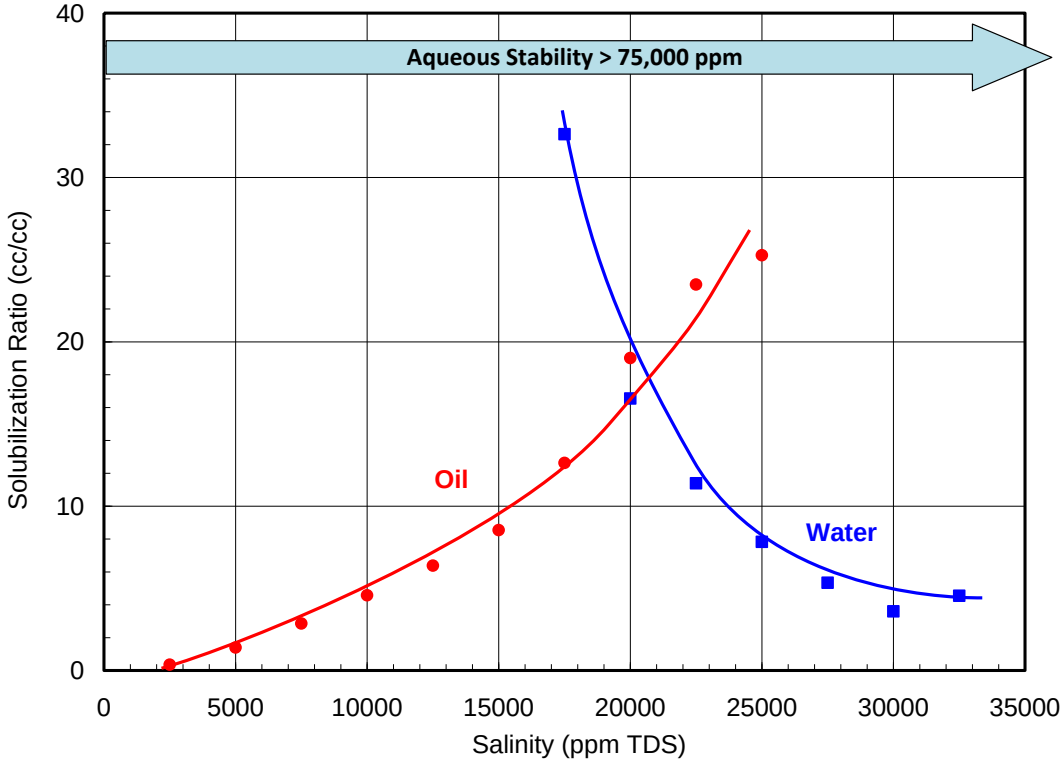

Figure 4-23: Phase behavior of 0.5 wt% C_{13}-13PO-sulfate, 0.5 wt% $C_{15\text{-}18}$-IOS, and 2.0 wt% TEGBE for oil #3 at 58 °C with 30 vol% oil after 45 days.

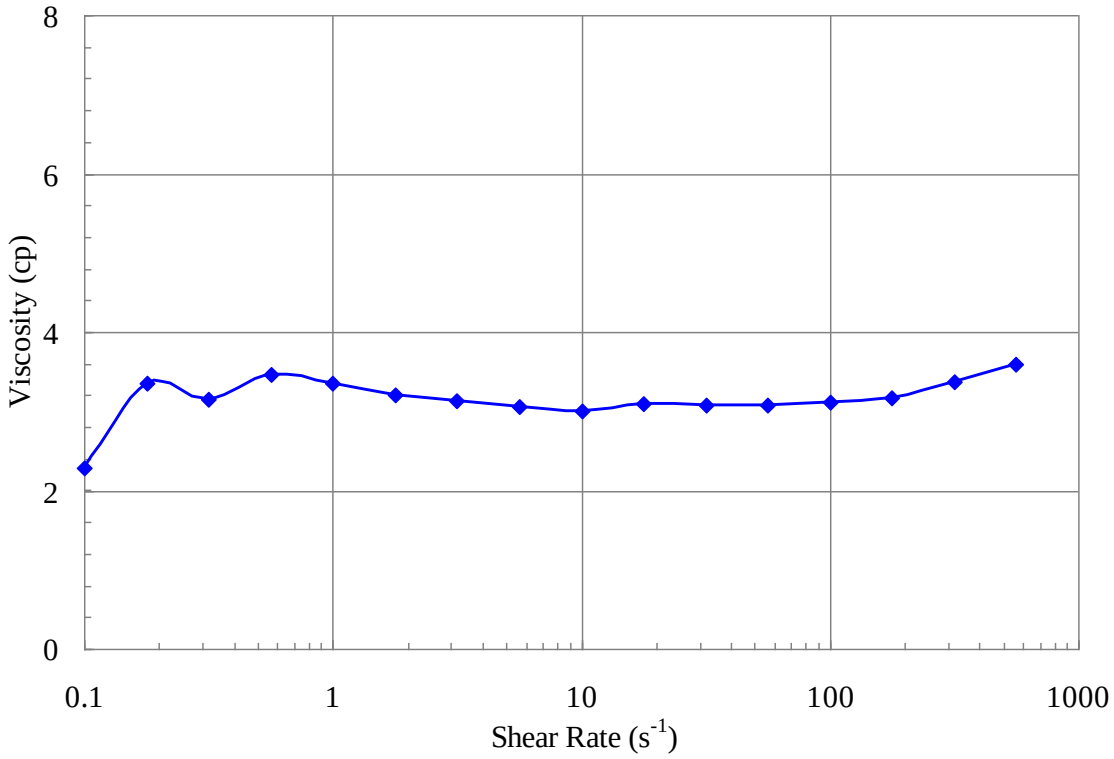

Figure 4-24: Microemulsion viscosity for formulation #3 at optimum salinity and 58 °C.

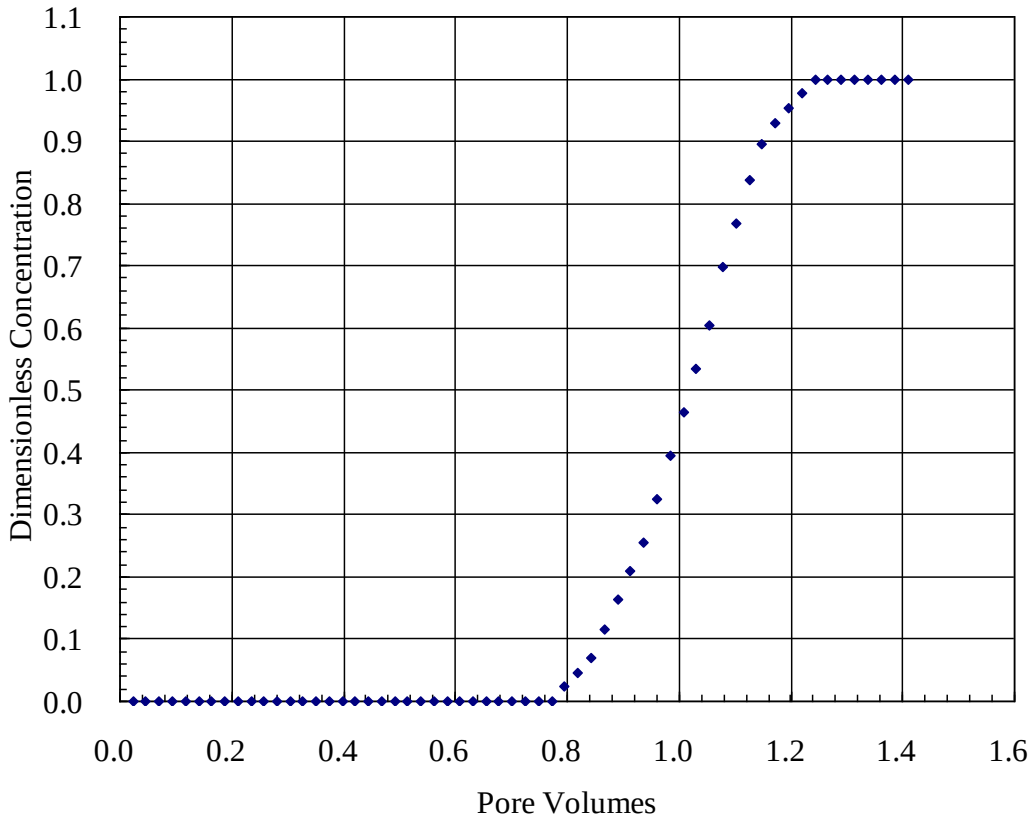

Figure 4-25: Tracer breakthrough data in sandpack #6.

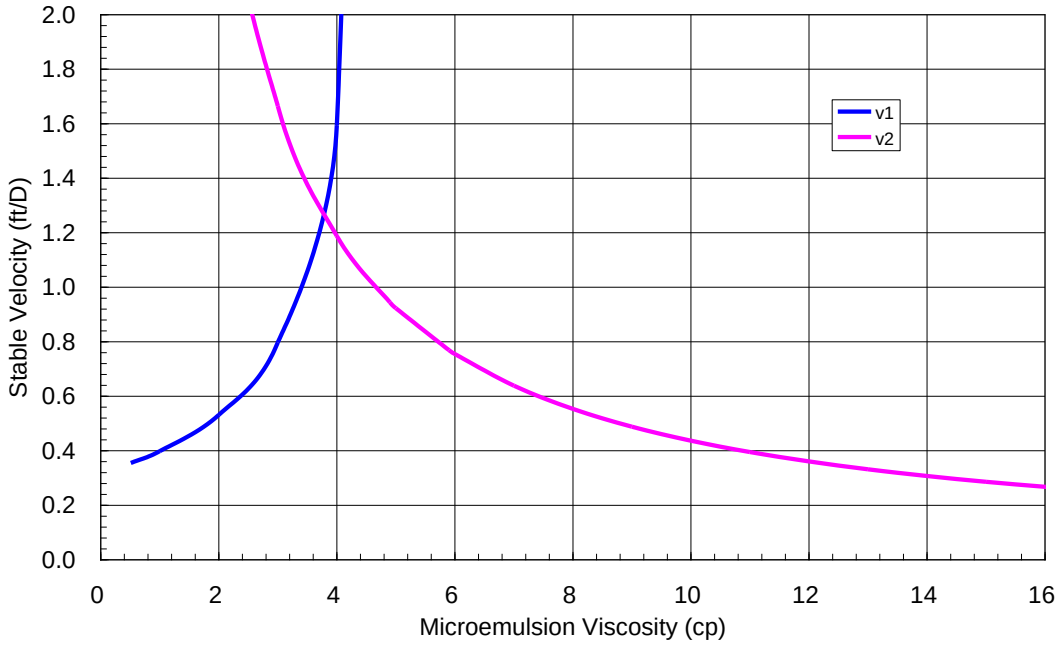

Figure 4-26: Critical velocity of upper interface (v1) and lower interface (v2) for coreflood #6.

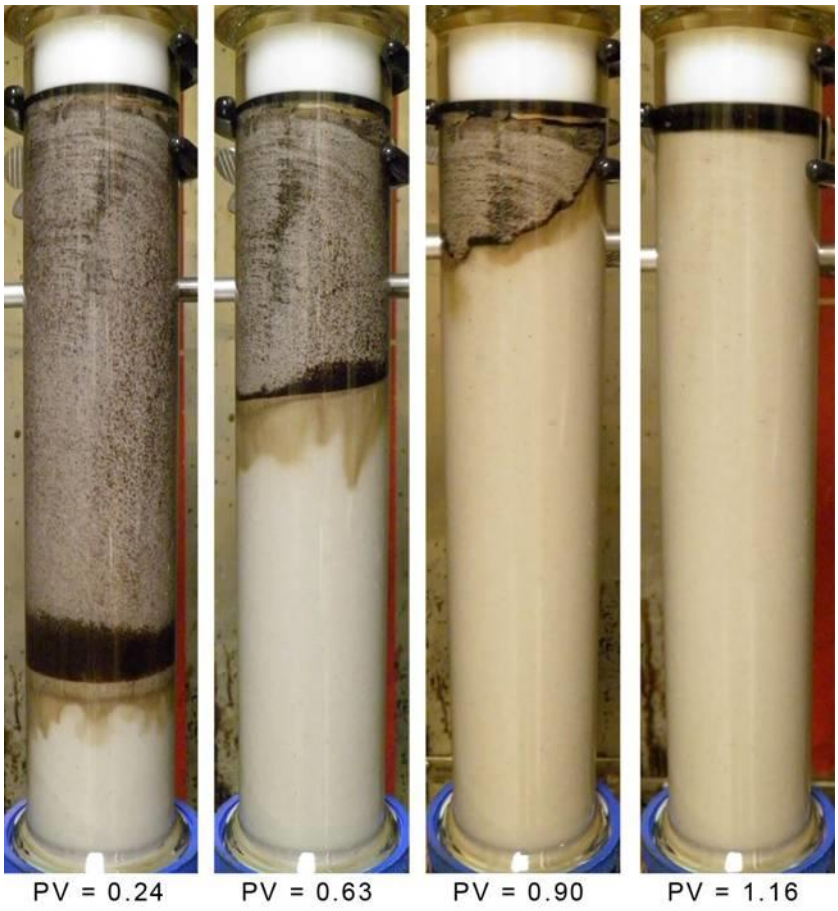

Figure 4-27: Photographs of surfactant flood #6.

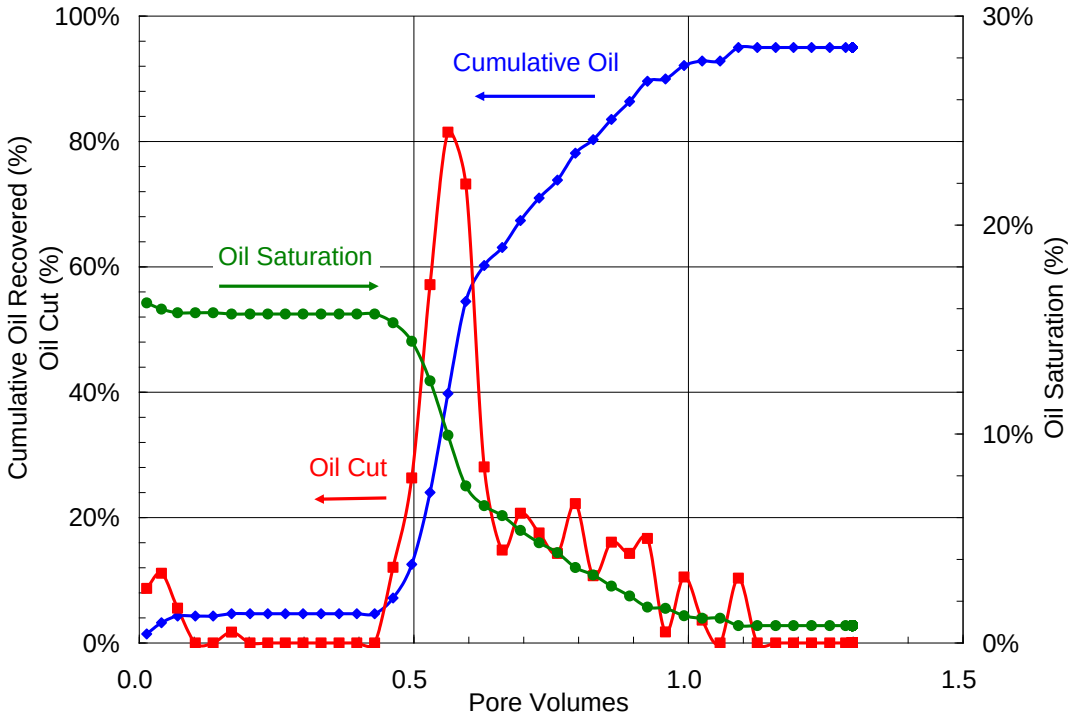

Figure 4-28: Measured oil recovery, oil cut, and oil saturation from surfactant flood #6 at 1.0 ft/day and 58 °C.

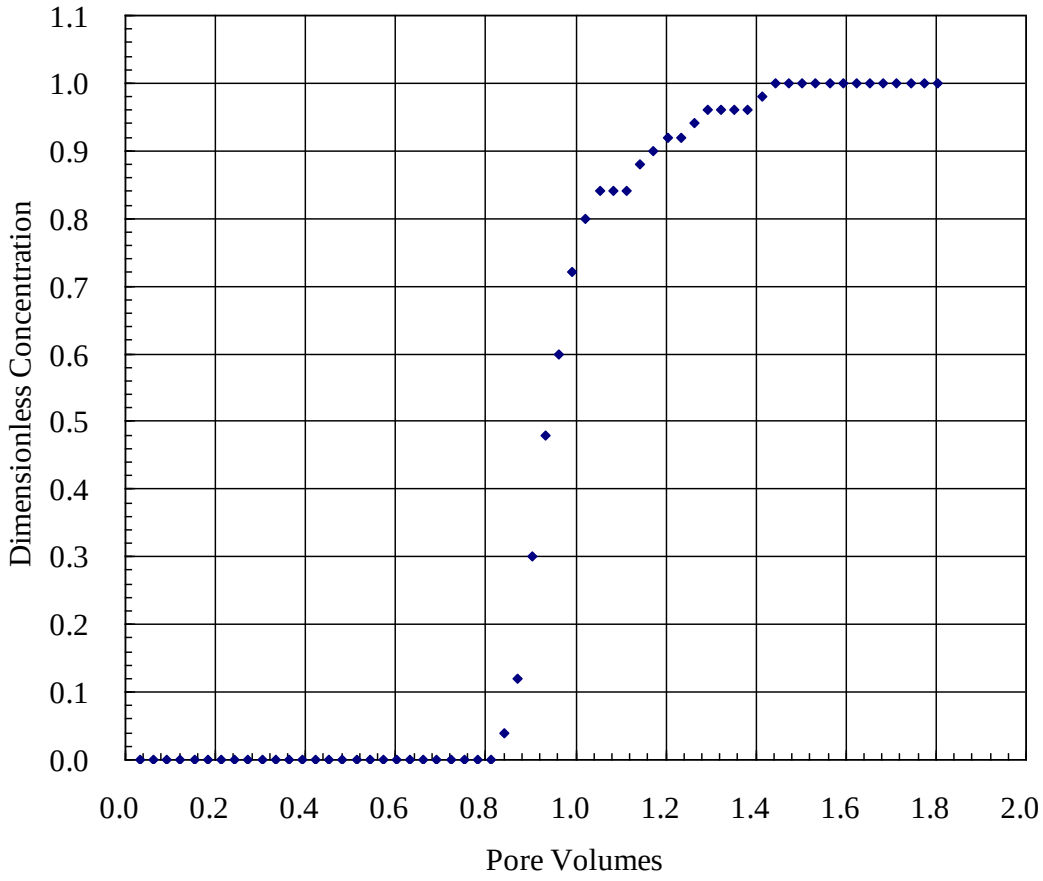

Figure 4-29: Tracer breakthrough data in Bentheimer sandstone coreflood #7.

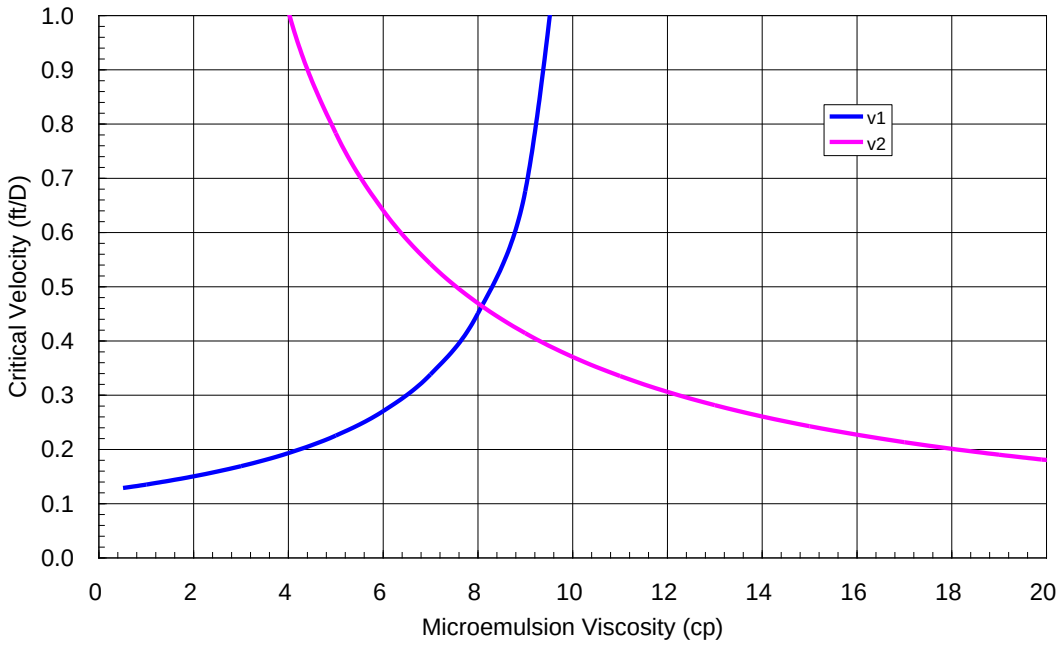

Figure 4-30: Critical velocity of upper interface (v1) and lower interface (v2) for coreflood #7.

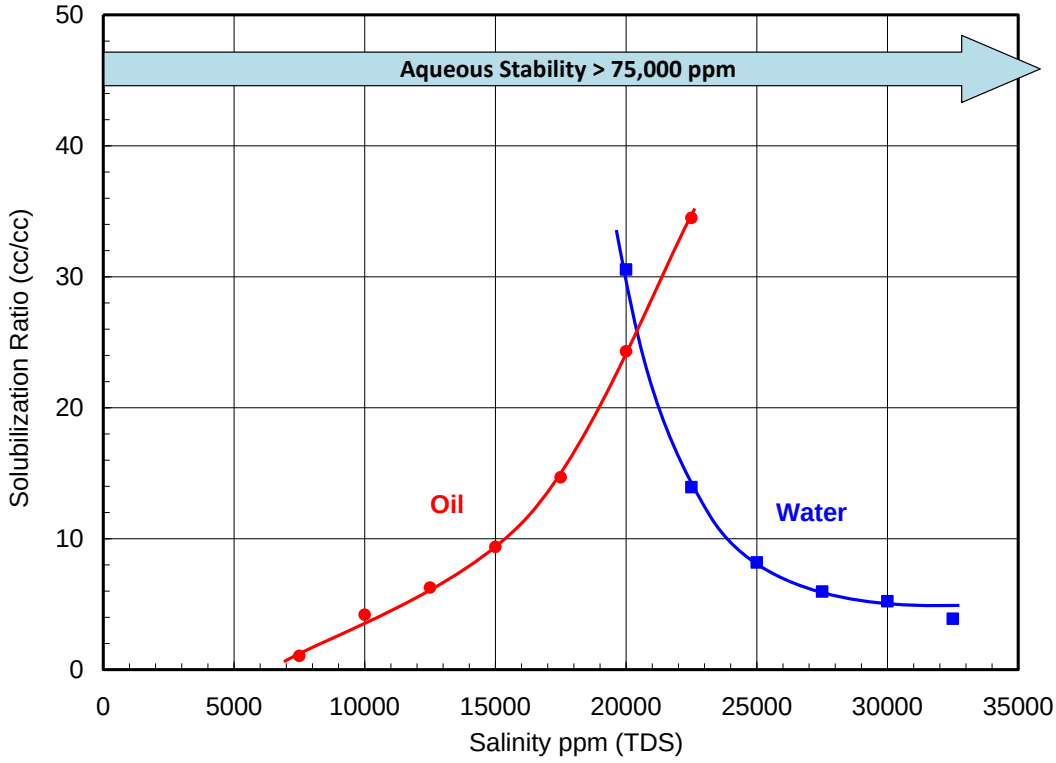

Figure 4-31: Phase behavior of 0.5 wt% C_{13}-13PO-sulfate, 0.5 wt% $C_{15\text{-}18}$-IOS, and 1.5 wt% TEGBE for oil #3 at 58 °C with 30 vol% oil after 31 days.

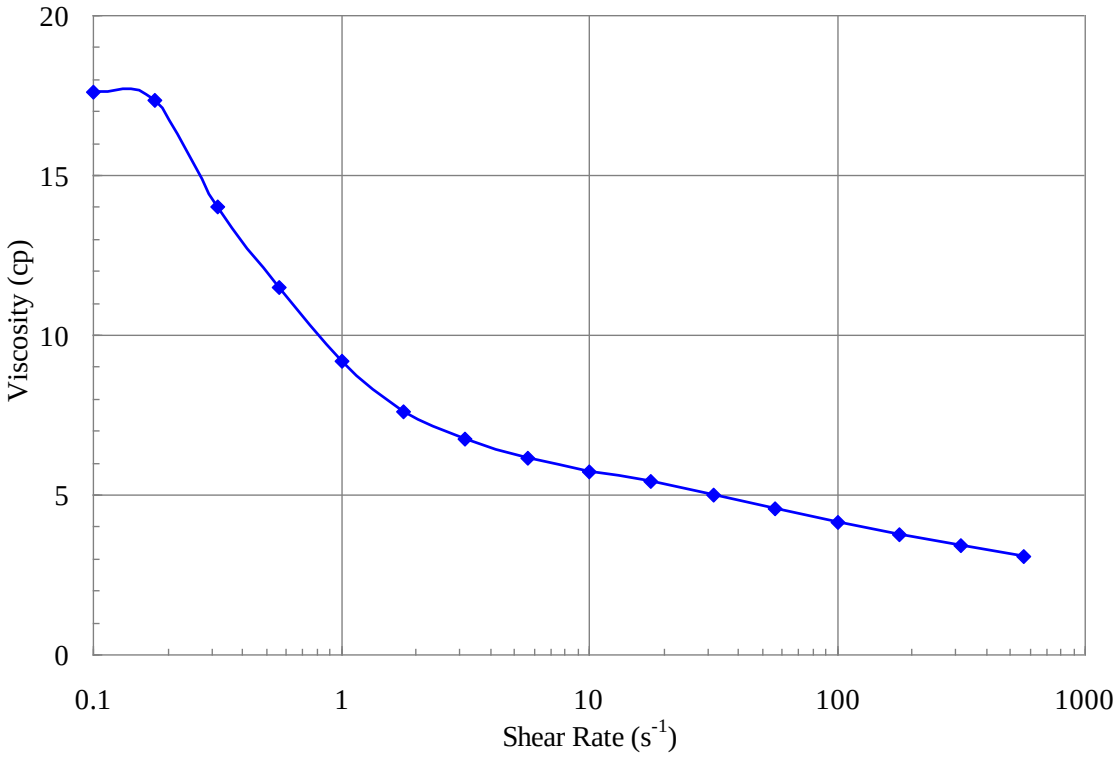

Figure 4-32: Microemulsion viscosity for formulation #4 at optimum salinity and 58 °C.

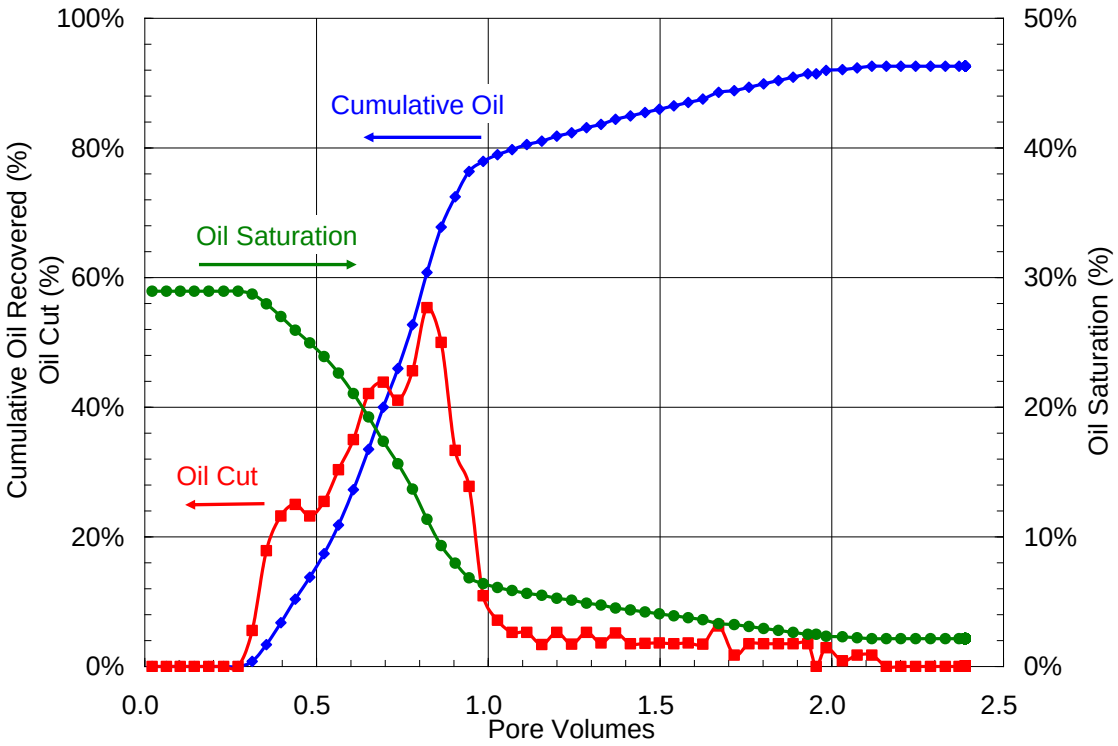

Figure 4-33: Measured oil recovery, oil cut, and oil saturation from surfactant flood #7 at 0.40 ft/day and 58 °C.

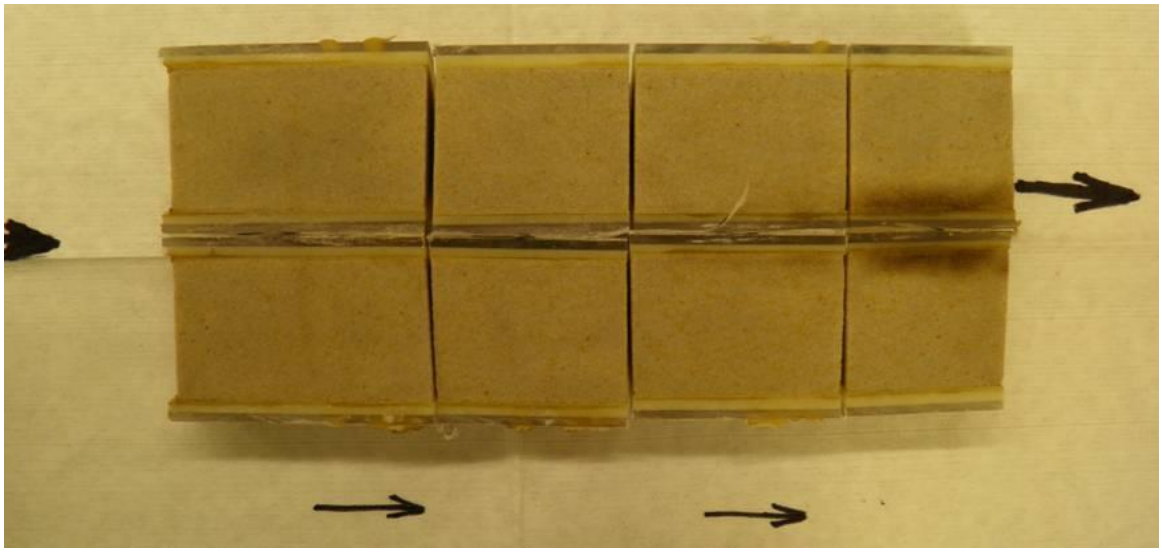

Figure 4-34: Photographs of Bentheimer core after surfactant flood #7.

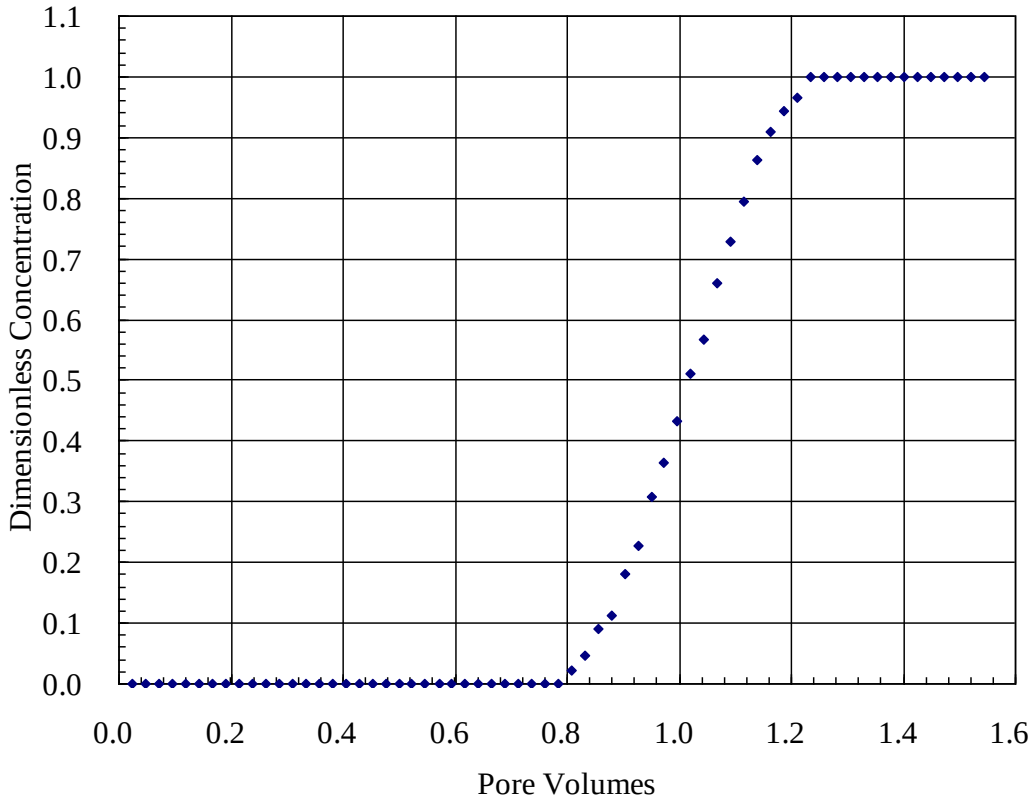

Figure 4-35: Tracer breakthrough data in sandpack #8.

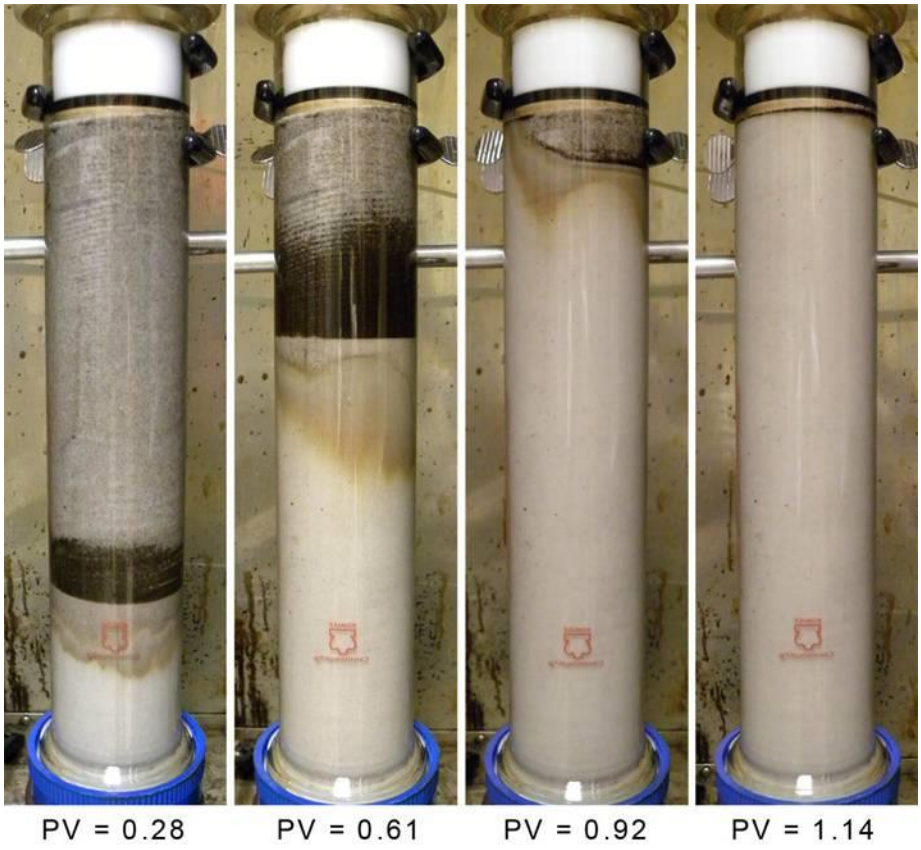

Figure 4-36: Photographs of surfactant flood #8.

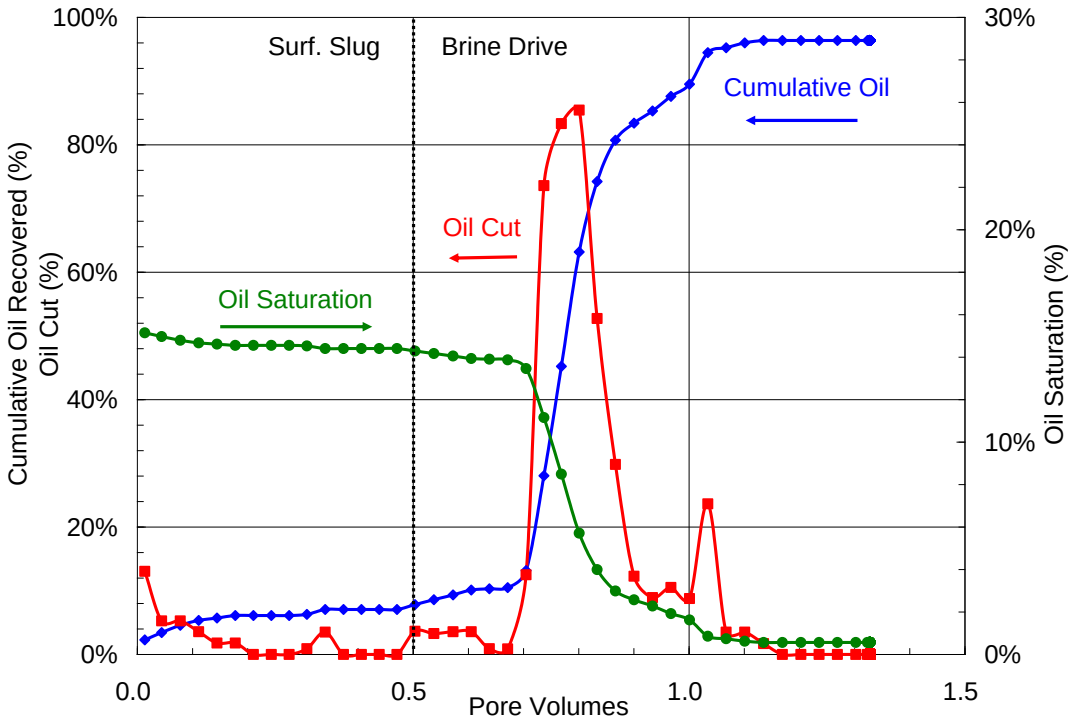

Figure 4-37: Measured oil recovery, oil cut, and oil saturation from surfactant flood #8 at 1.0 ft/day and 58 °C.

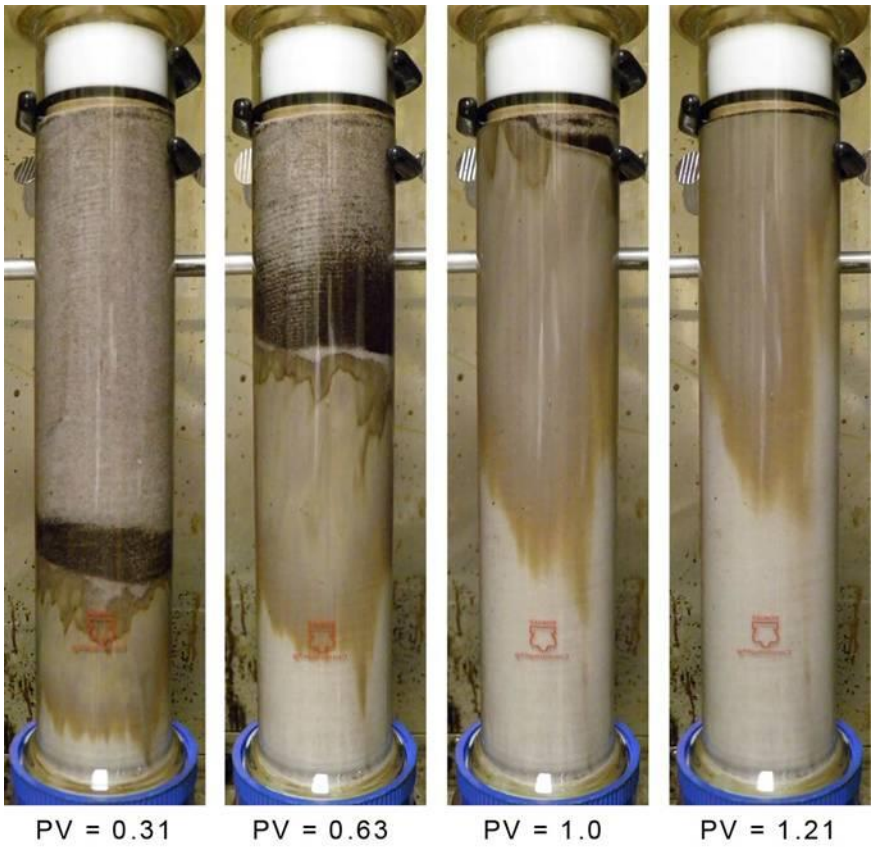

Figure 4-38: Photographs of surfactant flood #9.

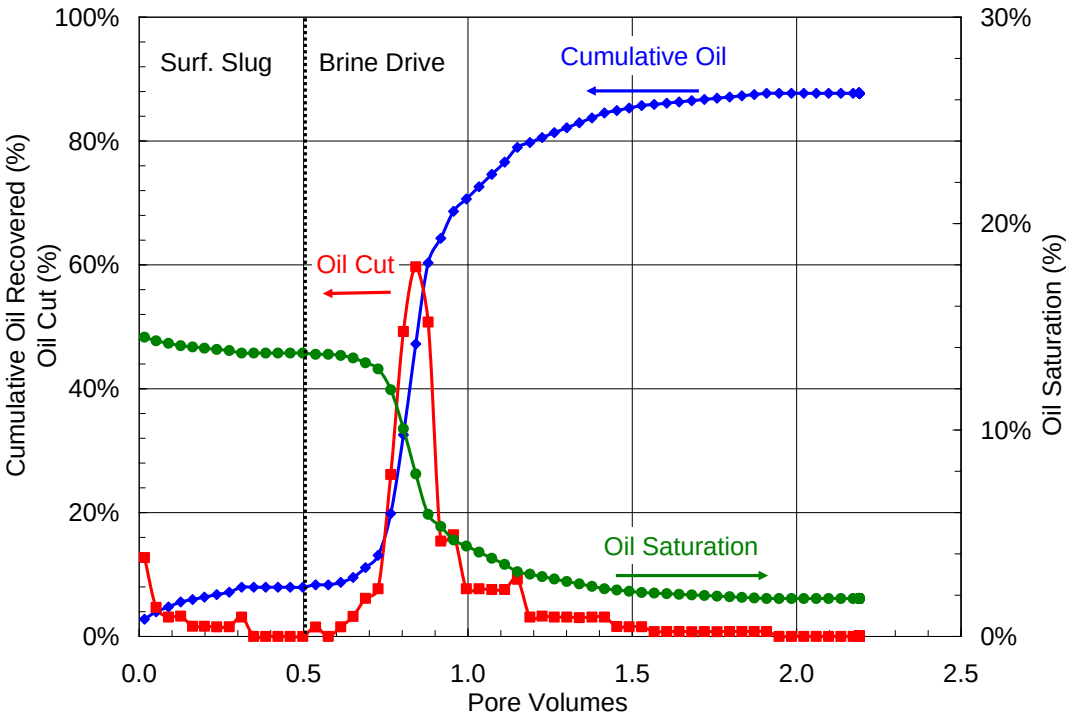

Figure 4-39: Measured oil recovery, oil cut, and oil saturation from surfactant flood #9 at 5.0 ft/day and 58 °C.

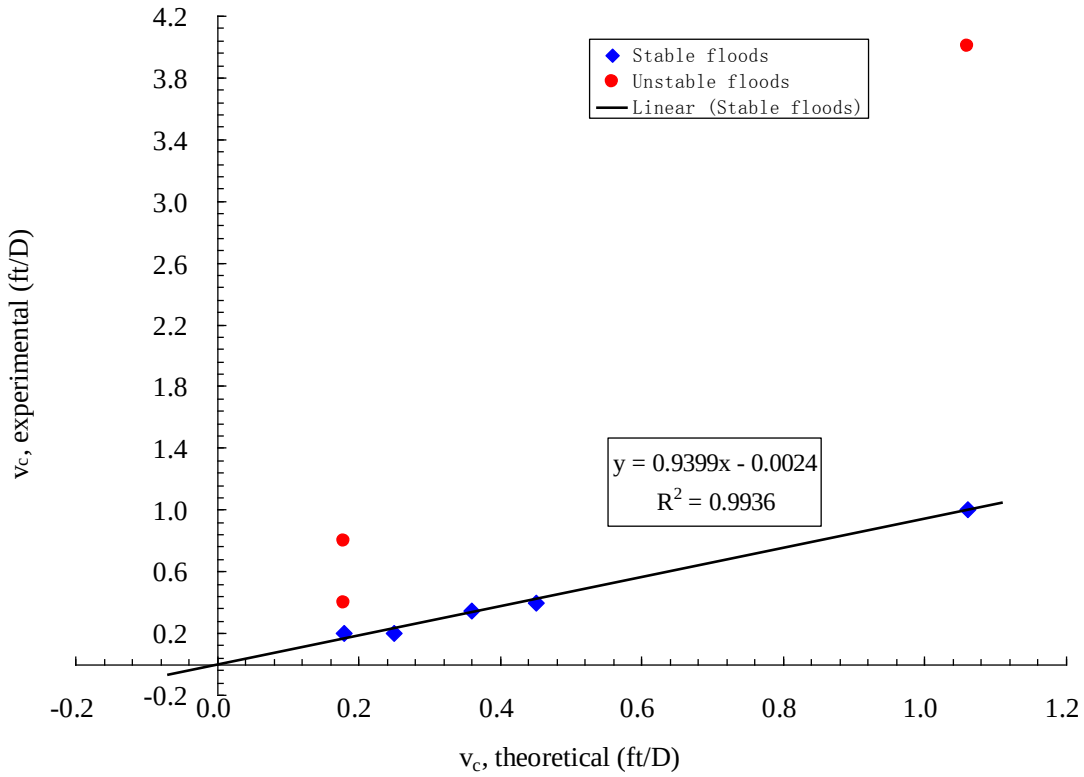

Figure 4-40: Experimental velocities as a function of theoretical stable velocities for all surfactant floods.

Chapter V: Anionic and Nonionic Surfactant Mixtures

INTRODUCTION

A large number of papers have been published on wettability alteration by cationic surfactants (Austad et al., 1998; Standnes et al., 2002), nonionic surfactants (Vijapurapu and Rao, 2004; Standnes et al., 2002; Xie et al., 2005) and anionic surfactants (Hirasaki et al., 2004; Seethepalli et al., 2004, Sharma and Mohanty, 2011; Chen and Mohanty, 2012). Cationic and nonionic surfactants are usually good candidates to alter the oil-wet rock towards more water-wet, but not efficient to reduce oil-water IFT. Anionic surfactants are very efficient to lower the IFT to ultra-low level, but do not effectively alter the wettability. In this study, we investigated the feasibility of achieving both wettability alteration and ultra-low IFT using the mixtures of anionic and amine ethoxylate nonionic surfactants.

EXPERIMENTAL MATERIALS AND PROCEDURES

Surfactants and Materials

Surfactants

Carboxylates were synthesized at the University of Texas at Austin. Internal olefin sulfonates (IOS) were obtained from Stepan Company and Shell Chemical Company. Ethomeen T/25 was from Akzo Nobel, and Tallow amine-12EO was received from Harcros Chemicals. The molecular structures of Ethomeen T/25 and Tallow amine-12EO are shown in Figure 5-1.

Co-solvents

Triethylene glycol mono butyl ether (TEGBE) was received from Aldrich Chemicals.

Polymers

The polymers Flopaam 3330s were received from SNF Floerger (Cedex, France).

Electrolytes and Brines

Sodium chloride, sodium carbonate, calcium chloride, magnesium chloride hexahydrate, and sodium sulfate were obtained from Fisher Chemical. Specific synthetic brines were made and used based on each specific reservoir application. The brine compositions are listed in Table 5-2.

Oils

Several dead crude oils and surrogate oils were used in this study (Table 5-1). Formulations are developed using surrogate oils rather than live oil to save time and cost, but the final test should be done with live oil at high pressure. The surrogate oil is made based in part on the equivalent alkane carbon number (EACN) of the dead oil (Cayias et al., 1976; Salager et al., 1979; Glinsmann, 1979; Puerto and Reed, 1983; Roshanfekr et al., 2012; Roshanfekr, 2010; Jang et al., 2014).

Microemulsion Phase behavior and Aqueous stability tests

The phase behavior of various mixtures was carefully observed over an extended period of time. The mixtures that formed low-viscosity microemulsions and displayed ultra-low IFT with both oil and water were selected for the further evaluation. Their aqueous stability was tested at both room temperature and reservoir temperature. The aqueous solutions were observed to ensure that no cloudiness and/or phase separation occurred up to the desired injection salinity, which is usually the optimum salinity. These phase behavior observations are the key to our approach to the development of high-performance chemical formulations. A large number of mixtures can be made and observed over a period of time with relatively little cost or effort to explore the effect of

surfactant type and concentration, co-surfactant type and concentration, co-solvent type and concentration, salinity, hardness, oil concentration, polymer type and concentration, temperature, etc. Both the interfacial tension and the viscosity can be observed by performing a quick emulsion test by briefly shaking the pipettes and then observing the coalescence of the emulsion to form separate oil, water and microemulsion phases. After reaching equilibrium, the phase volumes can be read and used to calculate interfacial tension using the Huh equation (Huh, 1979).

The aqueous solubility of each chemical formulation is tested by adding the aqueous solution from the phase behavior experiments to 20 mL glass ampules. Typically a scan that mirrors the phase behavior scan is produced. The ampules are blanketed with Argon and sealed using the propane-oxygen torch. The ampules are mixed using the Vortex Genie 2 until a homogenous solution is created. Observations of the aqueous solutions are recorded first at room temperature and next the ampules are equilibrated at reservoir temperature using the ovens. The aqueous solutions continue to be monitored after reaching reservoir temperature.

Coreflood experiments

The coreflood experiments were designed with favorable salinity gradients to maximize robustness of the corefloods (Glover et al. 1979; Pope et al., 1979; Hirasaki et al., 1983; Levitt et al., 2009; Solairaj et al., 2012). The cores were evacuated and then saturated with the synthetic formation brine followed by injection of brine to measure the brine permeability. The following flooding sequence was then used: 1. oil was injected at about 100 psi to establish residual water saturation and measure oil permeability at residual water saturation; 2. water was injected to establish residual oil saturation to water; 3. aqueous chemical solutions were injected to measure residual oil saturation to

chemical. Effluent samples were collected in graduated test tubes for fluid analysis. Differential pressure transducers were used to measure the pressure drop across several sections of the core and the entire core. All of the corefloods were done vertically in a convection oven at reservoir temperature.

Contact angle measurements

The contact angle was measured using cristobalite or calcite plates. The cristobalite and calcite represent minerals in sandstone and carbonate reservoirs, respectively. The plates with approximately 1.5x1.5x0.2 inch dimensions were polished to attain a fresh and smooth surface. The clean plates were first aged in the formation brine for 1 day and then aged in oil at 80 C for 7 days to render oil-wetness. The aged plates were immersed in formation brine to measure contact angles to verify the plates are oil-wet. Then the plates were put in the surfactant solutions, and the contact angles were observed for at least 2 days. Around 5-7 oil droplets were chosen on the polished part of the plate with well-characterized angles obtained from the high-resolution images of the contact angle. An average value is obtained from these observations.

RESULTS AND DISCUSSION

Phase behavior experiments were performed to study the behavior of the mixtures of anionic and non-ionic surfactants with oils at reservoir temperatures. Oil #1 is an inactive oil in a carbonate reservoir at 105 °C. The formulation developed for this oil is 0.5 wt% TSP-15PO-27EO-carboxylate, 0.4 wt% C_{19-23}-IOS, 0.3 wt% Ethomeen T/25, and 1.0 wt% TEGBE at 105 °C. Figure 5-2 shows the phase behavior results of this formulation after 82 days. This surfactant mixture was able to provide ultra-low IFT and good aqueous stability at high temperature in hard brine. The optimum solubilization

ratio is above 10 at optimum salinity of about 15,000 ppm. The surfactant solution was clear up to 20,000 ppm at 105 °C.

A second formulation was identified for oil #2, which is also inactive in a carbonate reservoir of 78 °C. The anionic and nonionic surfactant mixture for this oil is 0.45 wt% C_{28}-25PO-45EO-carboxylate, 0.3 wt% C_{19-23}-IOS, 0.25 wt% Tallow amine-12EO, and 0.5 wt% TEGBE in hard brine. Figure 5-3 shows the solubilization ratio at optimum salinity of ~52,500 ppm is about 13, which is indicating ultra-low interfacial tension. The surfactant aqueous stability is up to 75,000 ppm TDS.

Based on this phase behavior results, a coreflood was conducted in a Silurian dolomite core to test the surfactant formulation performance. A 0.5 PV surfactant slug containing 1.0 wt% surfactant (PV×C=50) was injected at the salinity of ~54,000 ppm followed by a polymer drive of 33,000 ppm salinity at frontal velocity of 2 ft/day. Figure 5-4 shows the oil recovery results for this coreflood. The final oil recovery was 90.1 % of water flood residual oil saturation and the final oil saturation was 0.038. Only a trace amount of surfactants was produced in the effluents which were not enough to be detected by HPLC. Thus all of the injected surfactant (0.32 mg surfactant per gram of rock) was retained. The coreflood showed the anionic-cationic surfactant formulation can generate ultra-low IFT to effectively recovery residual oil after a waterflood.

Contact angle measurements

Two additional anionic-nonionic surfactant formulations were developed for contact angle measurements. Oil #2 is an inactive oil in a carbonate reservoir at 78 °C. Oil #3 is an inactive oil in a sandstone reservoir at 55 °C.

The formulation for oil #2 is 0.65 wt% C_{28}-25PO-45EO-carboxylate, 0.2 wt% C_{15-18}-IOS, 0.45 wt% C_{19-28}-IOS, and 0.2 wt% Tallow amine-12EO at 78 °C. The phase

behavior results are shown in Figure 5-5. The optimum solubilization ratio is around 10 and the optimum salinity is about 67,000 ppm. The aqueous stability is at least 79,000 ppm TDS. Figure 5-6 shows a photograph of calcite plate in formation brine at 78 °C after being aged with oil for 7 days at temperature of 78 °C. A film of oil stuck to the top of the plate. The plate showed strongly oil-wet character in the formation brine. Then the plate was immersed in the surfactant solution at the optimum salinity of ~67,000 ppm to observe the contact angle. Because this surfactant solution mixture has a high solubilization ratio with this oil at optimum salinity, most of the oil on the plate was solubilized into the micelles. Almost no oil or very tiny oil droplets remained on the surface of the plate as shown in Figure 5-7, so the contact angle could not be measured.

Therefore, a surfactant solution of higher IFT was prepared for contact angle measurements. From phase behavior results shown in Figure 5-5, the solubilization ratio is about 5 at ~50,000 ppm corresponding to a much higher IFT compared to that at optimum salinity. Thus, the same surfactant formulation with a lower salinity of ~50,000 ppm was used to replace brine surrounding the plate. Again, most of the oil on the plate was solubilized (Figure 5-8), and the contact angles of the oil droplets left on the plate could not be measured.

Another anionic-nonionic surfactant formulation was also identified for oil #3. This formulation contained 0.35 wt% C_{24}-25PO-18EO-carboxylate, 0.35 wt% C_{19-28}-IOS, 0.3 wt% Ethomeen T25, and 1.0 wt% TEGBE at 55 °C. The optimum solubilization ratio is about 14 at the optimum salinity of about 75,000 ppm as shown in Figure 5-9. The cristobalite plate was oil wet after aging in oil at elevated temperature of 80 °C (Figure 5-10). The brine was replaced by the surfactant solution with an optimum salinity of ~ 75,000 ppm. As shown in Figure 5-11, most of oil was solubilized, which made contact angle measurements difficult. Next a surfactant solution with a lower salinity of ~ 48,000

ppm and thus a higher IFT (solubilization ratio of ~5) was used. The contact angle still could not be measured because the image as shown in Figure 5-12 was not clear.

When strong oil-wet plates were immersed in anionic-nonionic surfactant solutions with either ultra-low or high IFTs, almost none of the oil remained on the surface of the plates, so contact angles were not measurable. The wettability of the plates was altered from strong oil-wet to water-wet by these anionic-nonionic surfactant solutions.

SUMMARY AND CONCLUSIONS

Several anionic-nonionic surfactant formulations were identified for different oils at different reservoir conditions. All the formulations showed ultra-low IFT and good aqueous stability. The formulation for oil #2 was able to effectively displace residual oil after waterflooding a heterogeneous Silurian dolomite core. The anionic-nonionic surfactant formulations for oil #2 and #3 altered the oil-wet calcite or cristobalite plates to water-wet by the indicated by the observation that almost no oil remained on the surface of plates after immersed in surfactant solutions. However, more experiments are needed to evaluate the effects of such anionic-nonionic surfactant formulations on wettability alteration.

Table 5-1: Oil Properties

Oil #	Temperature (°C)	API	Total Acid Number (mg KOH/g oil)	Surrogate Oil	Surrogate Oil Viscosity (cp)
1	105	34	0.10	13 wt% toluene and 87 wt% dead oil	2.0
2	78	27	0.50	10 wt% toluene and 90 wt% dead oil	1.7
3	55	33	0.50	Dead oil	2.9

Table 5-2: Brine Compositions

Brine #	Na^+ (ppm)	Ca^{2+} (ppm)	Mg^{2+} (ppm)	K^+ (ppm)	SO_4^{2-} (ppm)	HCO_3^- (ppm)	Cl^- (ppm)	TDS (ppm)
PWI	8267	965	144	0	1175	329	13,844	24,758
FW	885	235	35	0	1273	305	774	3516
SSKOC	12708	0	0	343	3276	0	17,506	33,833
IB	50,798	842	255	0	3913	2001	76,518	134,327
HSNRW	404	150	5	0	740	132	177	1608

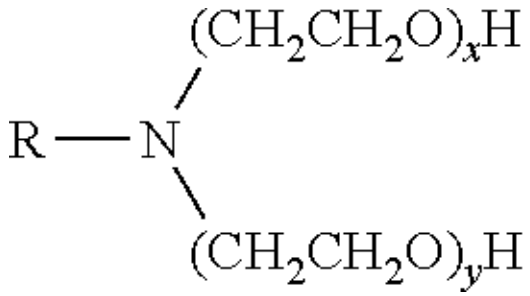

Figure 5-1: The molecule structure of Ethomeen® T/25 and Tallow amine-12EO. R is alkyl substituent-tallow alkyl, ethylene oxide added molar number x + y is 15 for Ethomeen T/25, and 12 for Tallow amine-12EO.

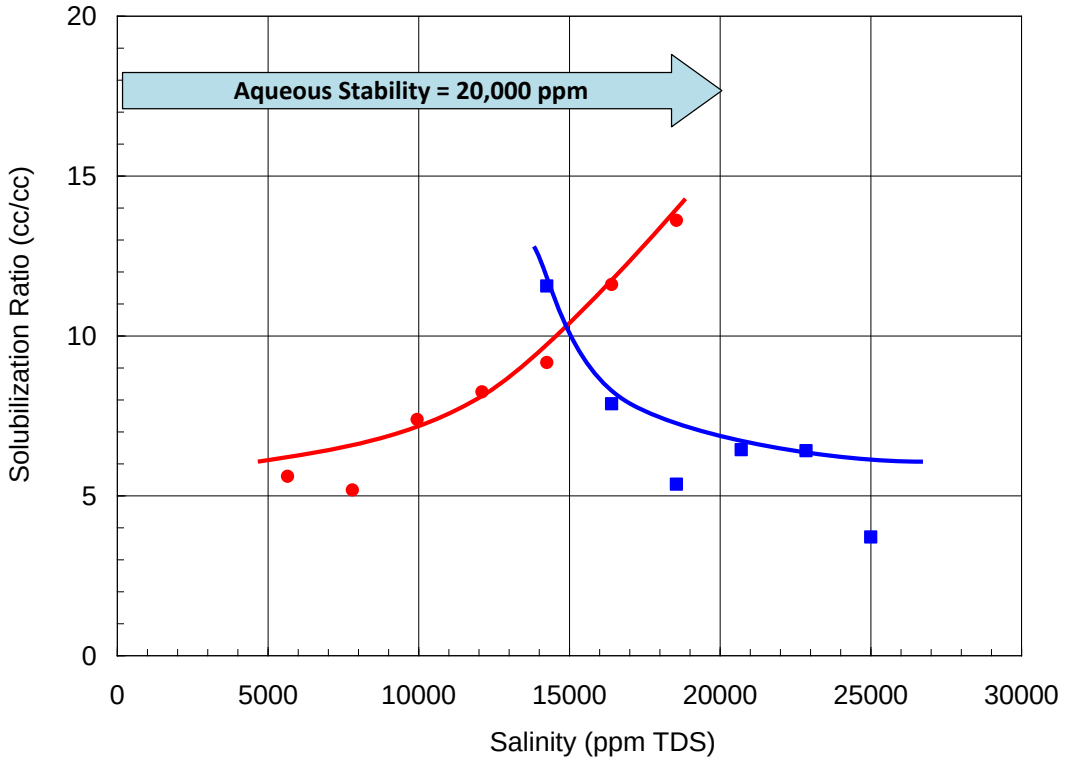

Figure 5-2: Phase behavior of 0.5 wt% TSP-15PO-27EO-carboxylate, 0.4 wt% C_{19-23}-IOS, 0.3 wt% Ethomene T25, 1.0 wt% TEGBE for oil #1 at 105 °C with 50 vol% oil concentration after 82 days.

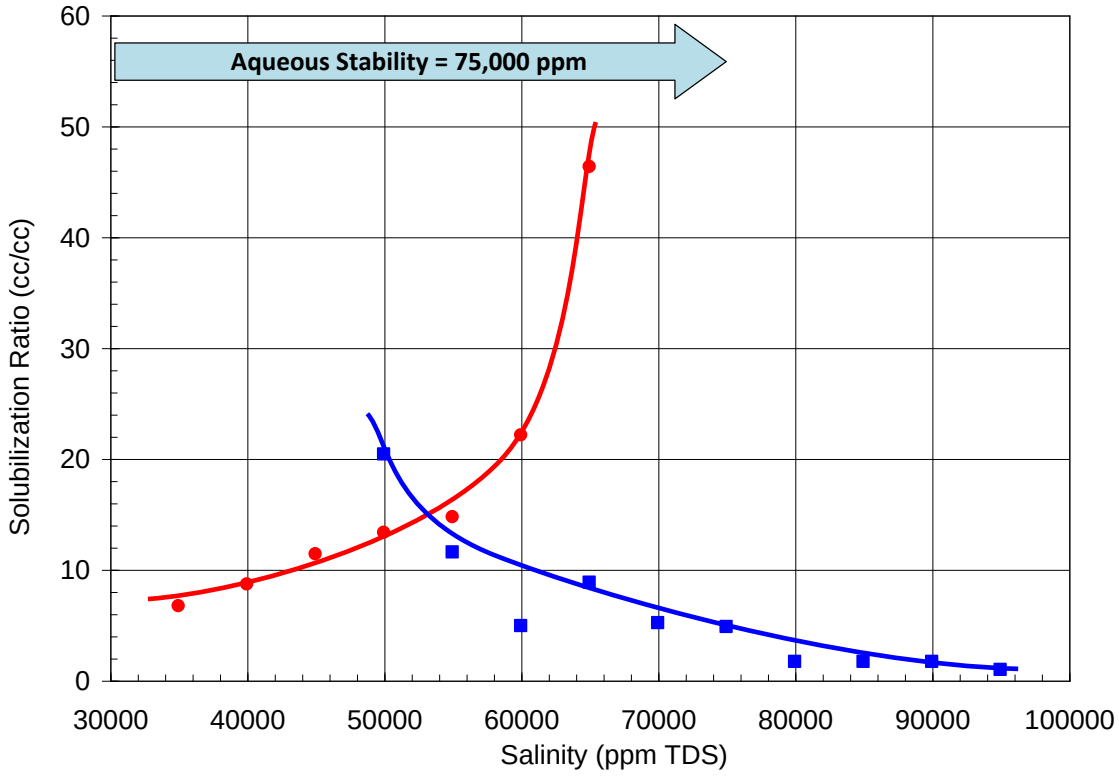

Figure 5-3: Phase behavior of 0.45 wt% C_{28}-25PO-45EO-carboxylate, 0.3 wt% C_{19-23}-IOS, 0.25 wt% Tallow amine-12EO, 0.5 wt% TEGBE for oil #2 at 78 °C with 30 vol% oil concentration after 7 days.

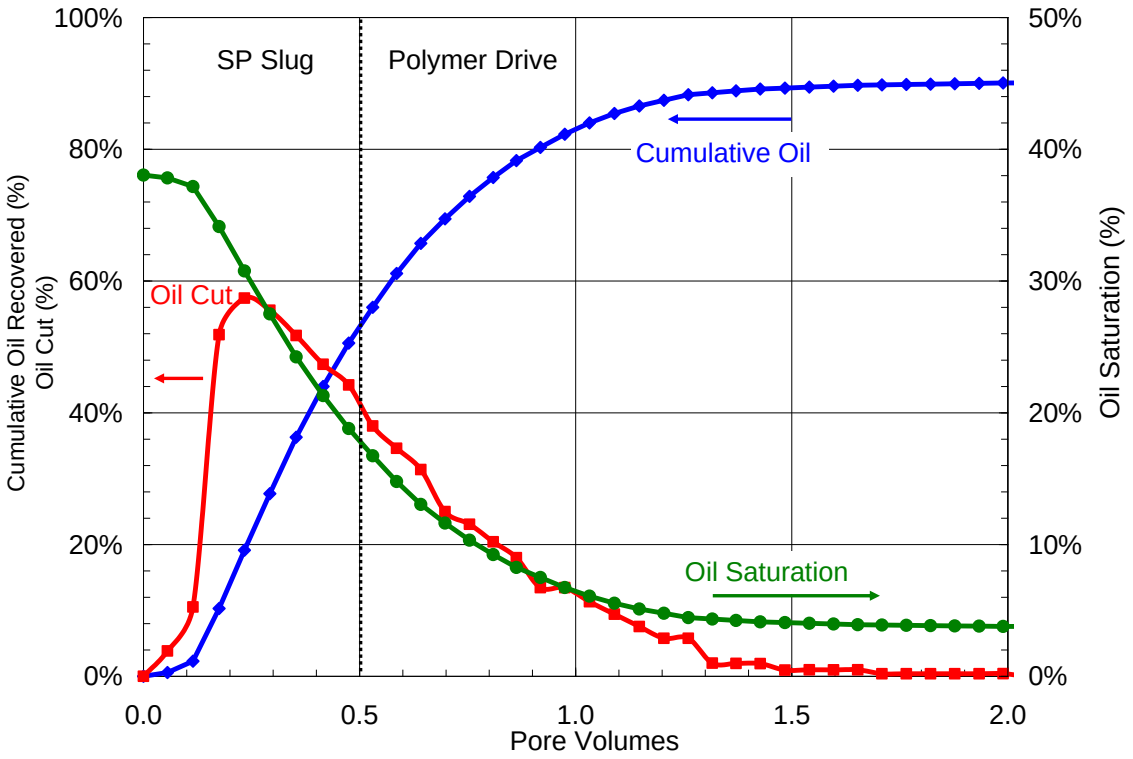

Figure 5-4: Oil recovery from coreflood in Silurian dolomite at 78 °C.

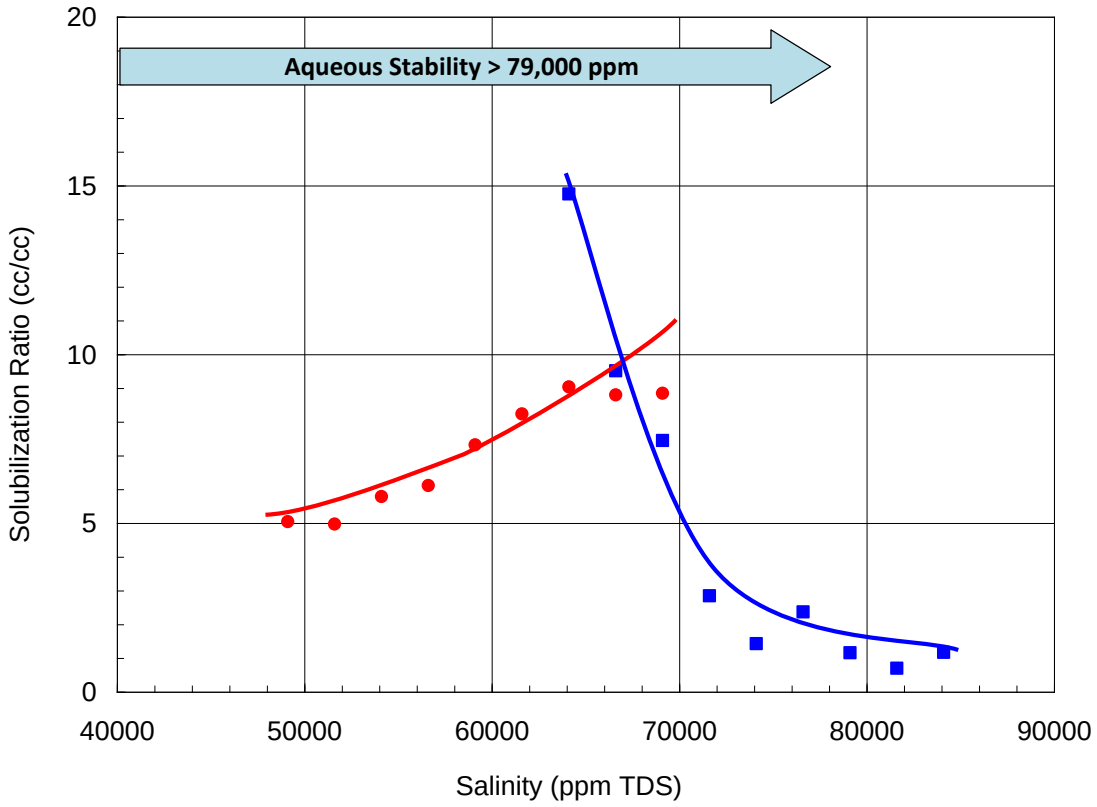

Figure 5-5: Phase behavior of 0.65 wt% C_{28}-25PO-45EO-carboxylate, 0.2 wt% C_{15-18}-IOS, 0.45 wt% C_{19-28}-IOS, 0.2 wt% Tallow amine-12EO for oil #2 at 78 °C with 30 vol% oil concentration after 12 days.

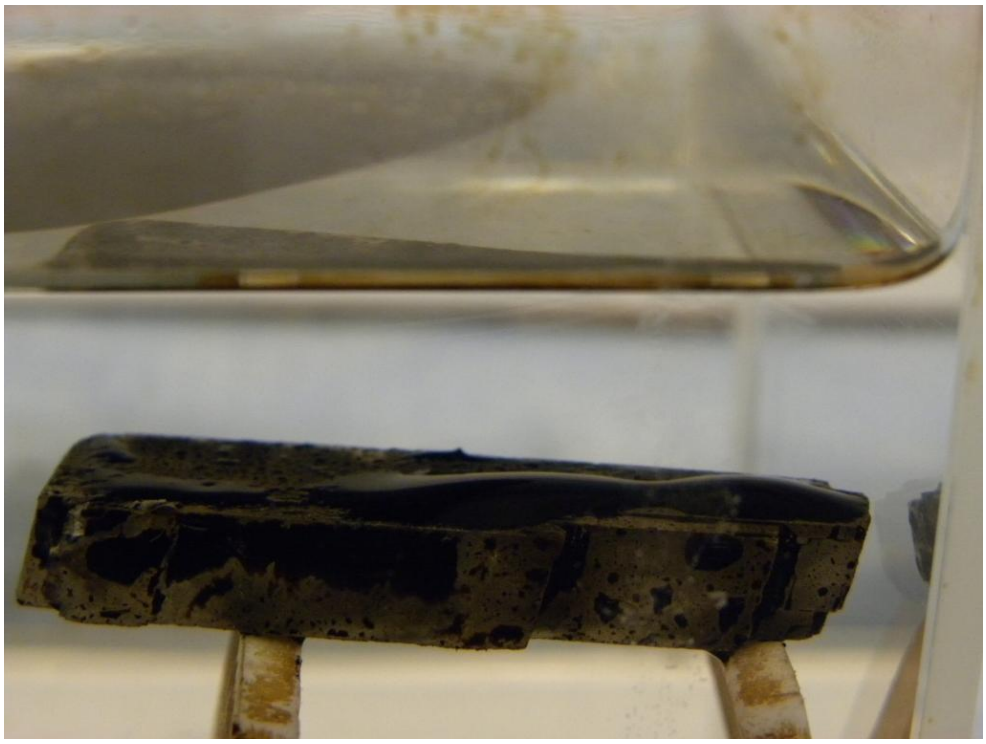

Figure 5-6: Photograph of calcite plate in formation brine after aging.

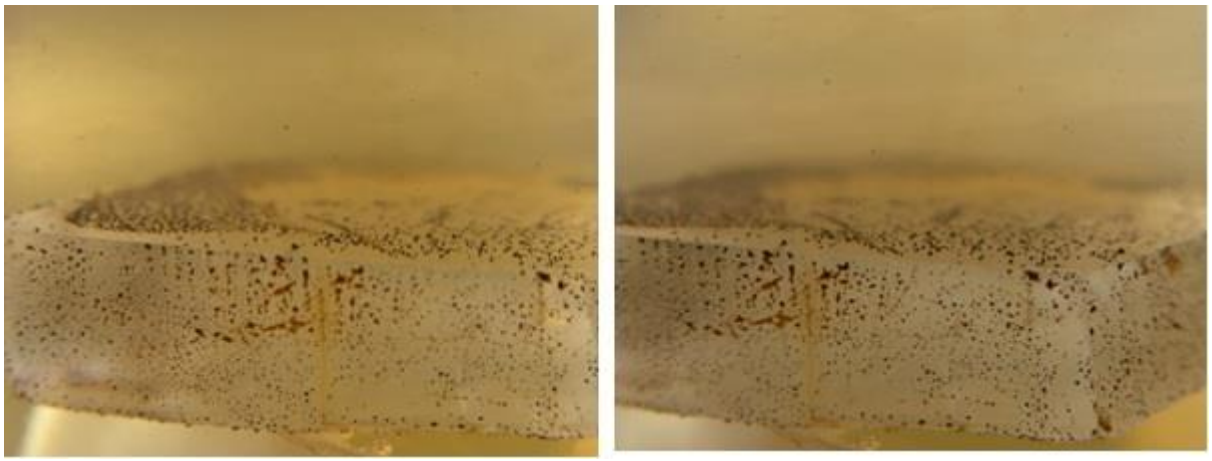

Figure 5-7: Photograph of calcite plate in surfactant solution at optimum salinity.

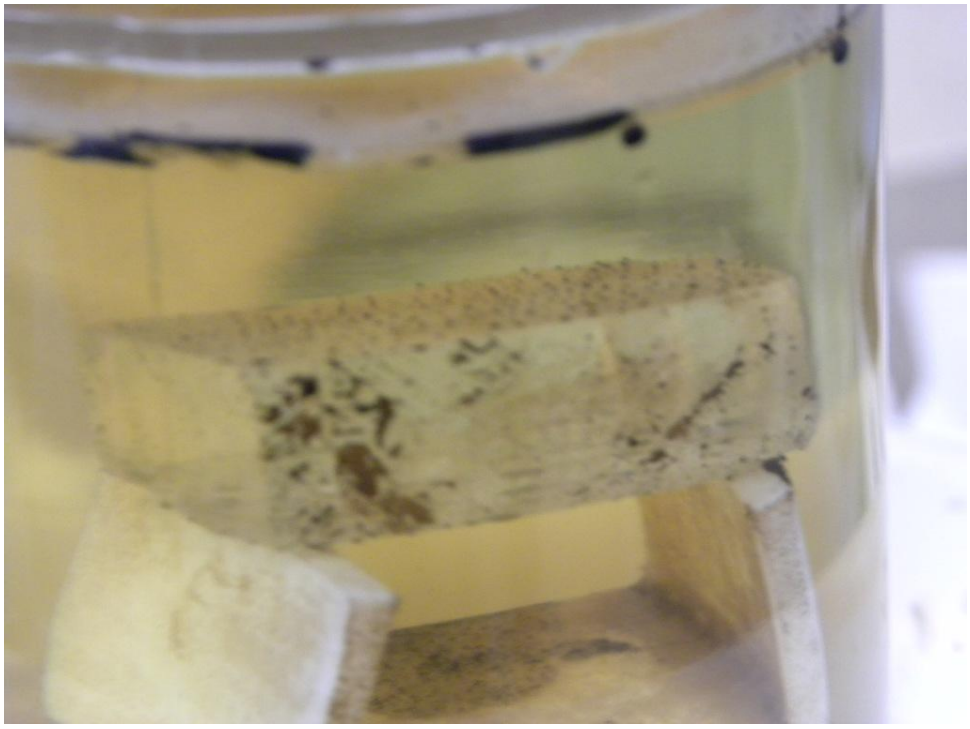

Figure 5-8: Photograph of calcite plate in surfactant solution at under optimum salinity.

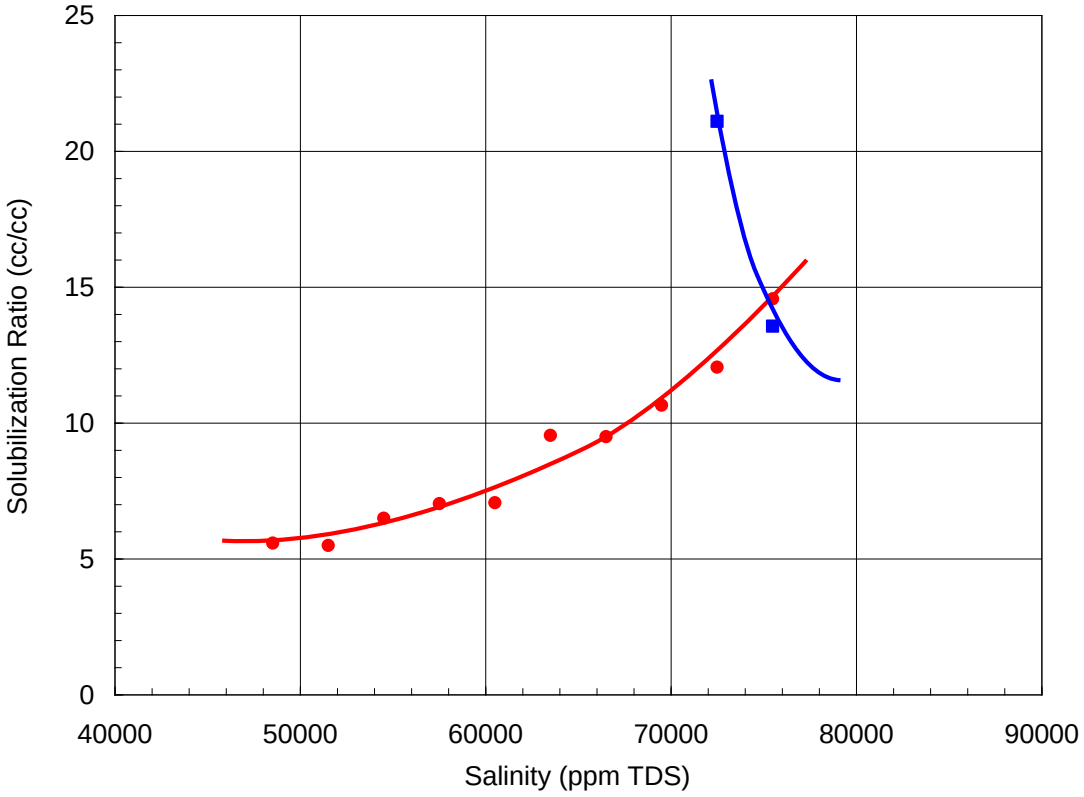

Figure 5-9: Phase behavior of 0.35 wt% C_{24}-25PO-18EO-carboxylate, 0.35 wt% C_{19-28}-IOS, 0.3 wt% Ethomeen T25, 1.0 wt% TEGBE for oil #3 at 55 °C with 50 vol% oil concentration after 42 days.

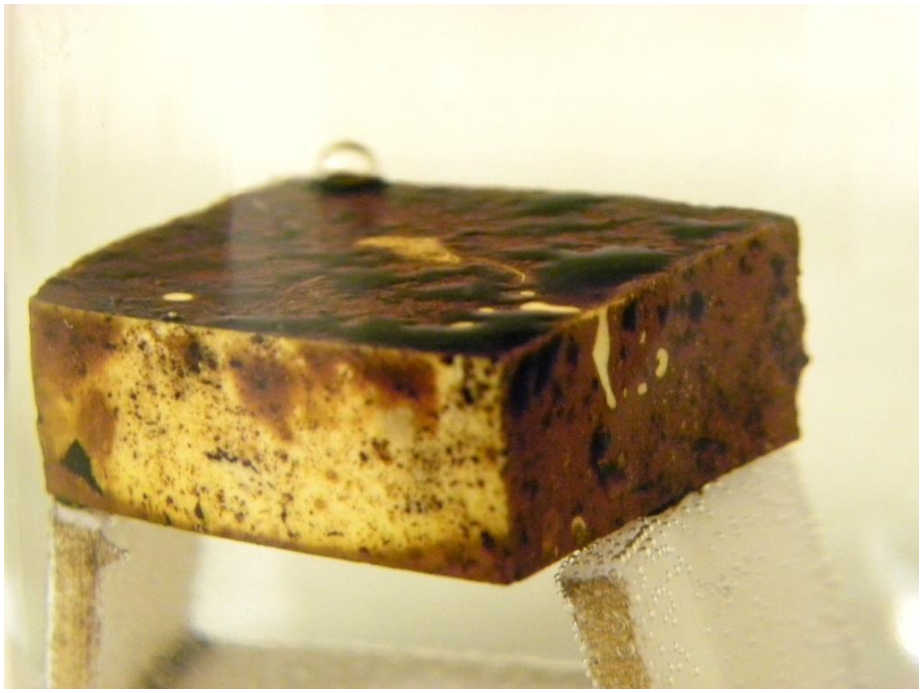

Figure 5-10: Photograph of cristobalite plate in formation brine after aging.

Figure 5-11: Photograph of cristobalite plate in surfactant solution at optimum salinity.

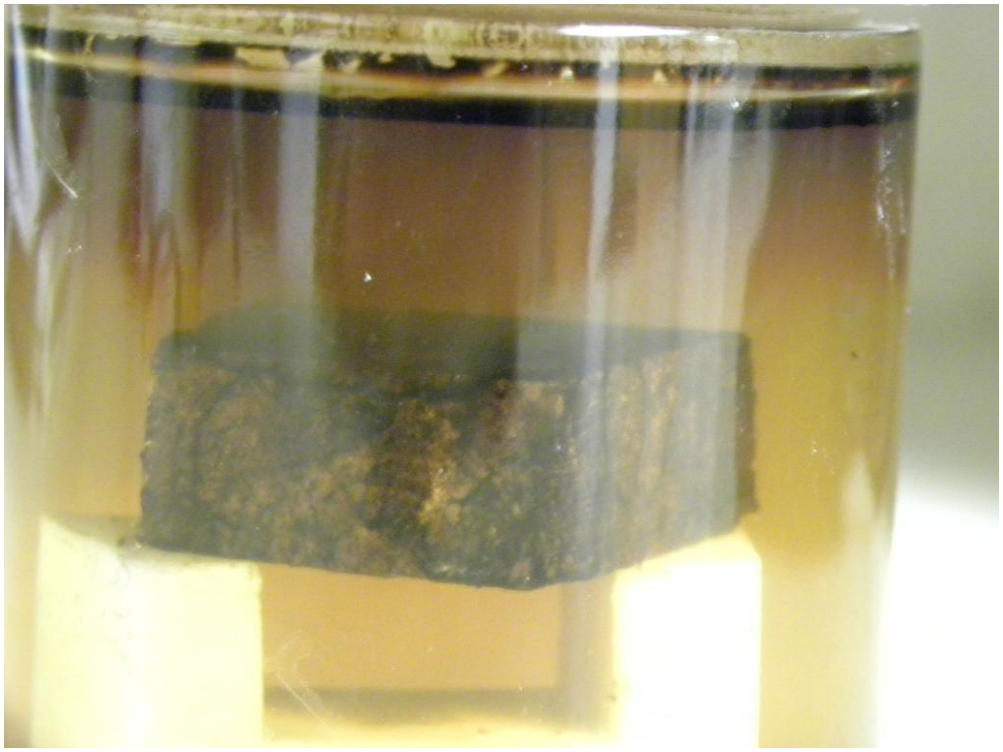

Figure 5-12: Photograph of cristobalite plate in surfactant solution at under optimum salinity.

Chapter VI: Summary, Conclusions and Recommendations

SUMMARY AND CONCLUSIONS

The first goal of this research was to develop and experimentally test new and improved chemical formulations for enhanced oil recovery using a new class of branched large-hydrophobe alkoxy carboxylate surfactants mixed with novel co-surfactants and co-solvents to both lower IFT and alter wettability at high temperatures and high salinities.

These novel alkoxy carboxylate surfactants with large branched hydrophobes were tested and found to show excellent performance in corefloods over a wide range of reservoir conditions up to at least 120°C. The number of PO and EO groups in these new surfactants were optimized for a wide variety of oils over a broad range of salinity, hardness and temperature and mixed with various co-surfactants and co-solvents to develop high-performance formulations based on the microemulsion phase behavior. Both ultra-low IFT and clear aqueous solutions at optimum salinity were obtained for both active and inactive oils and both light and medium gravity oils over a wide range of temperatures. Both sandstone and carbonate corefloods using these carboxylate surfactants showed excellent performance at high temperature, high hardness and high salinity as indicated by high oil recovery, low pressure gradients and low surfactant retention. The advent of such a new class of cost-effective surfactants significantly broadens the potential application of chemical enhanced oil recovery processes using surfactants under harsh reservoir conditions (Chapter 2).

Two surfactant formulations consisting of novel large-hydrophobe Guerbet alkoxy carboxylate surfactants and IOS co-surfactants were developed and evaluated for a fractured carbonate reservoir. Ultra-low interfacial tension (IFT) and good aqueous stability were achieved in a hard brine at a high reservoir temperature of 100 °C. The

surfactants both reduce the IFT to ultra-low values and alter the wettability of the rock toward more favorable water-wet conditions.

The first surfactant formulation was used in a fractured carbonate reservoir core at 0.25 ft/day frontal velocity. The cumulative oil recovery was 76.8 % after the water flood, and the oil saturation decreased from 0.336 to 0.078. The second surfactant formulation was tested in both static and dynamic imbibition experiments using a fractured carbonate reservoir core. 65.9% oil recovery was obtained in fractured coreflood compared to 33.3 % oil recovery in static imbibition test. The surfactant retention was low at 0.086 mg/g of rock. The results are excellent taking into account that (1) the core was extremely vuggy and fractured, (2) no mobility control was used, and (3) only a small surfactant slug was injected. The oil recovery from the dynamic coreflood was higher than that for a similar static imbibition experiment (Chapter 3). The transverse pressure gradient between the fractures and matrix was proposed as the driven force to transport surfactant into matrix altering wettability and reducing IFT for main oil recovery mechanisms.

Novel chemical formulations consisting of anionic and nonionic surfactant mixtures were identified for different oils at different reservoir conditions. All the formulations showed ultra-low IFT and good aqueous stability. The formulation for oil #2 was able to effectively displace residual oil after waterflood from a heterogeneous Silurian dolomite core. The anionic-nonionic surfactant formulations for oil #2 and #3 altered the oil-wet calcite or cristobalite plates to water-wet by the indication of almost no oil remained on the surface of plates after immersed in surfactant solutions of ultra-low and high IFTs. Further experiments are needed to evaluate the effects of such anionic-nonionic surfactant formulations on wettability alteration in the future (Chapter 5).

The second goal of this research was to evaluate the effect of buoyancy on oil recovery from cores using ultra-low IFT surfactant formulations under conditions where the use of polymer for mobility control is either difficult or unnecessary, determine the conditions that are favorable for a gravity-stable surfactant flood, and further improve the performance of gravity-stable surfactant floods by optimizing the microemulsion properties, especially its viscosity. The microemulsion viscosity can be varied by adjusting the structure of the surfactants and co-solvents and their concentrations.

Predictions made using classical stability theory applied to surfactant flooding experiments were determined to be inaccurate because such theory does not take into account the microemulsion phase that forms in-situ when surfactant mixes with the oil. The modification of the classical theory to account for the effect of the microemulsion on the critical velocity for a stable displacement is one of the major contributions of this research. New experiments were done to test the modified theory and it was found to be in good agreement with these experiments. Furthermore, a new method to increase the stable velocity by optimizing the microemulsion viscosity was proposed and validated by a series of coreflood experiments designed and conducted for that specific purpose.

Three series of experiments were performed including phase behavior tests, microemulsion viscosity measurements, and surfactant floods in both sandpacks and Bentheimer sandstone cores. Surfactant formulations were developed for each flood with ultra-low IFT and good aqueous stability. The modified stability theory was found to be in good agreement with the experimental results. The critical velocity of surfactant flood #1 in a 5500 md sandpack with formulation #1 was experimentally found to be 0.20 ft/D at a microemulsion viscosity of ~24 cp at 38 °C. By replacing IBA with TEGBE as co-solvent in formulation #2, the microemulsion viscosity was reduced to ~10 cp and allowed to increase the critical velocity to 0.35 ft/D in a 5000 md sandpack (flood #4) at

38 °C. The performance of a stable flood with the same formulation was observed in a Bentheimer sandstone core of 2500 md (flood #5) at 0.20 ft/D and 38 °C.

A less viscous oil (oil #3) and a higher temperature of 58 °C were selected to further lower the microemulsion viscosity. Formulation #3 was developed to obtain a microemulsion viscosity of ~4 cp. The critical velocity was then increased to 1.0 ft/D in a sandpack of 4200 md (flood #6). To perform the stable surfactant flood in a 2300 md Bentheimer sandstone core (flood #7), formulation #4 with less co-solvent than formulation #3 was used with a microemulsion viscosity of ~8 cp. In flood #7, a stable surfactant flood was performed at 0.40 ft/D. Surfactant flood #6 was repeated in another sandpack of 4300 md, but with an injection of 0.5 PV surfactant slug followed by a brine drive at a stable velocity of 1.0 ft/D.

All these experiments provided new insight into how a gravity stable surfactant displacement behaves and in particular the importance of the microemulsion phase and its properties, especially its viscosity. This insight opens up a new pathway for optimizing surfactant floods without mobility control. It is possible to design an efficient surfactant flood without any mobility control if the surfactant solution is injected at a stable velocity in horizontal wells at the bottom of the formation and the oil captured in horizontal wells at the top. Some of the world's largest oil reservoirs are deep, high-temperature, high-permeability, light-oil reservoirs and thus candidates for gravity stable surfactant floods under favorable reservoir conditions (Chapter 4).

RECOMMENDATIONS

Further evaluation of large-hydrophobe alkoxy carboxylate surfactants

Examples of synergism between large-hydrophobe alkoxy carboxylate surfactants and co-surfactants have been shown in Chapter II, but there are many additional co-

surfactants and co-solvents that could be tested to exploit this type of synergism. Other applications of these synergistic surfactant mixtures should be studied. For example, they could be used for foam flooding.

Ultra-low IFT surfactant imbibition

There is a need to develop better models for the imbibition of surfactants in fractured rocks. One such approach to developing such models for the special case of ultra-low IFT was proposed by Pope (2012). New experiments should be designed and conducted specifically to test new these new models. One of the most important reasons for such models is to determine how to reliably scale up the lab results to predict oil recovery from fractured oil reservoirs. It would also be useful to test new surfactant formulations to improve performance and in particular to speed up oil recovery at the reservoir scale.

Improve gravity stable surfactant flood modeling

The theory and model discussed in Chapter IV can be further refined or improved by taking into account more properties of the microemulsion phase or considering the microemulsion phase as a transition zone. For example, the changes of relative permeability, viscosity and density of the microemulsion also need to be taken into account.

Modification of fractional flow theory

Fractional flow theory is a very useful way to model first order effects of surfactant floods and in particular gravity stable surfactant floods can be modeled using fractional flow theory. The microemulsion viscosity is particularly important and should be taken into account in a modified fractional flow theory.

Further evaluation of anionic-nonionic and anionic-cationic surfactant formulations

Need to find a way to measure the contact angles. The spontaneous imbibition tests in outcrop and reservoir cores can be performed using anionic, nonionic/cationic, and anionic-nonionic/anionic-cationic surfactant solutions, respectively, to investigate the oil recovery mechanism of different formulations recovering from oil-wet cores.

The selected surfactant formulations based on contact angle measurements and spontaneous imbibition tests can be used in artificial sawed fractured cores. The anionic and nonionic surfactant mixture are expected to recovery not only mobilized oil but also immobilized oil trapped by capillary pressure. The relative permeability after waterflood and after surfactant flood can be measured to compare the wettability changes before and after surfactant flood. Surfactant flood in artificially fractured oil-wet carbonate cores could be conducted using in-situ CT imaging to investigate the imbibition efficiency.

Bibliography

Abbasi-Asl, Y., Pope, G.A., and Delshad, M., "Mechanistic Modeling of Chemical Transport in Naturally Fractured Oil Reservoirs," SPE 129661 presented at SPE IOR Symposium, Tulsa, OK, 24-28 April, 2010.

Abe, M., Schechter, R.S., Selliah, R.D., Sheikh, B. and Wade, W.H. 1987. Phase Behavior of Branched Tail Ethoxylated Carboxylate Surfactant/Electrolyte/Alkane Systems. Journal of Dispersion Science and Technology 8 (2): 157-172.

Adibhatla, B. and Mohanty, K.K., "Oil Recovery from Fractured Carbonates by Surfactant-Aided Grabity Drainage: Laboratory Experiments and Mechanistic Simulations," SPE 99773 presented at SPE IOR Symposium, Tulsa, OK, 22-26 April, 2006.

Adkins, S., Arachchilage, G. P., Solairaj, S., Lu, J., Weerasooriya, U., and Pope, G. A., "Development of Thermally and Chemically Stable Large-Hydrophobe Alkoxy Carboxylate Surfactants," SPE 154256 presented at SPE IOR Symposium, Tulsa, OK, 14-18 April, 2012.

Adkins, S., Liyanage, P.J., Arachchilage, G.W., Mudiyanselage, T., Weerasooriya, U., and Pope, G.A. "A New Process for Manufacturing and Stablizing High-Performance EOR Surfactants at Low Cost for High Temperature, High Salinity Oil Reservoirs," SPE 129923, presented at the SPE Improved Recovery Symposium, Tulsa, Oklahoma, 25-28 April, 2010.

Ahmadi, M.A., Shadizadeh, S.R., 2013. Implementation of high performance surfactant for enhanced oil recovery from carbonate reservoir. J. Petrol. Sci. Eng. 110, 66–73.

Akbar, M., Chakravorty S., Russell S.D., Al Deeb, M.A., Efnik, R.S., Thower, R., and Salman Mohamed S., "Unconventional approach to Resolving Primary and Secondary Porosity in Gulf Carbonates from Conventional Logs and Borehole Images," SPE 87297 presented at the 9th Abu Dhabi International Petroleum Exhibition and Conference, Abu Dhabi, U.A.E. 15-18 October, 2000.

Austad, T. and Milter, J., "Spontaneous Imbibition of Water into Low Permeable Chalk at Different Wettabilities Using Surfactants," SPE 37236 presented at the SPE International Symposium on Oilfield Chemistry, Houston, Texas, 18-21 February, 1997.

Austad, T., Matre, B., Milter, J., Saevareid, A., and Oyno, L., "Chemical Flooding of Oil Reservoirs 8. Spontaneous Oil Expulsion from Oil- and Water-Wet Low Permeable Chalk Material by Imbibition of Aqueous Surfactant Solutions," Colloids and Surfaces A: Physico. Eng. Aspects 137 (1-3): 117-129, 1998.

Barnes, J. R., Dirkzwager, H., Smit, J., Smit, J., On, A., Navarrete, R.C., Ellison, B., and Buijse, M.A., "Application of Internal Olefin Sulfonates and Other Surfactants to EOR. Part 1: Structure - Performance Relationships for Selection at Different Reservoir Conditions", SPE 129766 presented at SPE IOR Symposium, Tulsa, OK, 24-28 April, 2010.

Barnes, J. R., Groen, K., On, A., Dubey, S., Reznik, C., Buijse, M.A., and Shepherd, A.G., "Controlled Hydrophobe Branching to Match Surfactant to Crude Oil Composition for Chemical EOR", SPE 154084, presented at SPE IOR Symposium, Tulsa, OK, 14-18 April, 2012.

Barnes, J.R., Smit, J.P., Smit, J.R., Shpakoff, P.G., and Raney, K.H., Development of Surfactants for Chemical Flooding at Difficult Reservoir Conditions, Paper SPE 113313, presented at the SPE Improved Recovery Symposium, Tulsa, Oklahoma, 19-23 April, 2008.

Bataweel, M.A., and Nasr-El-Din, H.A., "ASP vs. SP Flooding in High Salinity/Hardness and Temperature in Sandstone Cores," SPE 155679, presented at SPE EOR Conference at Oil and Gas West Asia, Muscat, Oman, 16-18 April 2012.

Behler, A., Biermann, M., Hill, K., Raths, H.-C., Victor, M.-e.S. and Uphues, G. 2001. Industrial Surfactant Syntheses. In Reactions and Synthesis in Surfactant Systems, ed. J. Texter, Chap. 1, 1-44. New York, New York: Marcel Dekker Inc.

Bourrel, M. and Schechter, R. S. "Microemulsions and Related Systems", Marcel Dekker, Inc., New York, NY, 1988.

Buijse, M. A., Prelicz, R. M., Barnes, J. R., and Cosmo, C., "Application of Internal Olefin Sulfonates and Other Surfactants to EOR. Part 2: The Design and Execution of an ASP Field Test", SPE 129769, presented at SPE IOR Symposium, Tulsa, OK, 2010.

Cayias, J.L., Schechter, R.S., Wade, W.H., "Modeling Crude Oils for Low Interfacial Tension", SPE 5813, presented at SPE-AIME IOR Symposium, Tulsa, OK, 22-24 March, 1976.

Chen, P. and Mohanty, K.K., "Surfactant-Mediated Spontaneous Imbibition in Carbonate Rocks at Harsh Reservoir Conditions," SPE Journal, SPE 153960, 2013.

Chen, P., Enhanced Oil Recovery in Fractured Vuggy Carbonates, PhD Dissertation, The University of Texas at Austin, Austin, Texas, 2014.

Chen, S., Hou, Q., Jian, G., Zhu, Y., Luo, Y., Wang, Z. and Li, W. (2014) 'Synthesis and performance evaluation of novel alcohol ether carboxylate surfactants for alkali-surfactant-polymer flooding', Int. J. Oil, Gas and Coal Technology, Vol. 7, No. 1, pp.52–67.

Chilingar, G.V. and Yen, T.F., "Some Notes on Wettability and Relative Permeability of Carbonate Rocks," II . Energy and Sources, 7(1), 67-75, 1983.

Chuoke, R. L., van Meurs, P., and van der Poel, C., "The Instability of Slow, Immiscible, Viscous Liquid-Liquid Displacments in Permeable Media," Aime 216, 1959.

DanChem Technologies Inc. 2011. Neodox Alcohol Ethoxycarboxylate, www.danchemtechnology.com/neodox.html, (accessed 15 April 2011).

Dean, R.M., Selection and Evaluation of Surfactants for Field Pilots, MS Thesis, The University of Texas at Austin, Austin, Texas, 2011.

Delshad, M., Najafabadi, N.F., Anderson, G.A., Pope, G.A., and Sepehrnoori, K., "Modeling Wettability Alteration in Naturally Fractured Reservoirs," SPE Reservoir Evaluation & Engineering, 12(3): 361-370, 2009.

Dumore, J. M., "Stability Consideration in Downward Miscible Displacements," Soc. Pet. Eng. Jour. (Dec., 1964) 356.

Engelberts, W.F., and Klinkenberg, L.J. "Laboratory Experiments on the Displacement of Oil by Water from Packs of Granular Material," World Petroleum Congress, the Netherlands, 1951.

Falls, A. H., Thigpen, D. R., Nelson, R. C., Claston, J. W., Lawson, J. B., Good, P. A., Ueber, R. C., and Shahin, G. T., 1994,"Field Test of Cosurfactant-Enhanced Alkaline Flooding," SPERE, Aug. 217-223.

Fayers, F.J. and Sheldon, J.W. "The effect of capillary pressure and gravity on two-phase fluid flow in a porous medium," Petrol. Trans. AIME 216, 147, 1959.

Flaaten, A.K., Experimental Study of Microemulsion Characterization and Optimization in Enhanced Oil Recovery: A Design Approach for Reservoirs with High Salinity and Hardness, MS Thesis, The University of Texas at Austin, Austin, Texas, 2007.

Flaaten, A.K., Nguyen, Q.P., Zhang, J., Mohammadi, H., and Pope, G.A. "Alkaline/Surfactant/Polymer Chemical Flooding Without the Need for Soft Water," SPE J. 15(1): 184-196. SPE 116754, 2010.

Flatten, A.K., Nguyen, Q.P., Pope, G.A., and Zhang, J., A Systematic Laboratory Approach to Low-Cost, High-Performance Chemical Flooding, Paper SPE 113469, presented at the Symposium on Improved Oil Recovery, Tulsa, Oklahoma, 19-23 April, 2008.

Gao, B., and Sharma, M.M., "A New Family of Anionic Surfactants for Enhanced-Oil-Recovery Applications," SPE J. 18(5): 829-840. SPE 159700, 2013.

Gao, S., and Gao, Q., "Recent progress and evaluation of ASP flooding for EOR in Daqing oil field," SPE 127714 presented at SPE EOR Conference at Oil & Gas West Asia, 11-13 April 2010, Muscat, Oman.

Glass, R.J., and Yarrington, L. “Simulation of gravity fingering in porous media using a modified invasion percolation model,” Geoderma 70, 231, 1996.

Glinsmann, G.R., “Surfactant Flooding with Microemulsions Formed In-situ – Effect of Oil Characteristics”, SPE 8326, presented at SPE-AIME ATCE Symposium, Dallas, TX, 1979.

Glover, C.J., Puerto, M.C., Maerker, J.M., and Sandvik, E.L., "Surfactant Phase Behavior and Retention in Porous Media", SPEJ, June, 183-193, 1979.

Goudarzi,A., Delshad,M., Mohanty,K.K, Sepehrnoori,K., “Impact of Matrix Block Size on Oil Recovery Response Using Surfactants in Fractured Carbonates,” SPE 160219 presented at SPE ATCE, San Antonio, TX, 8-10 October, 2012.

Green, D. W. and Willhite, G. P. “Enhanced Oil Recovery”, SPE Textbook Series, Henry L. Doherty Memorial Fund of AIME, Society of Petroleum Engineers, Richardson, Texas, Volume 6, 1998.

Hand, D. B. 1939, “Dineric Distribution: I. The Distribution of a Consolute Liquid Between Two Immiscible Liquids,” Journal of Physics and Chem 34: 1961-2000.

Hickernell, F.J. and Yortsos, Y.C. “Linear stability of miscible displacement processes in porous media in the absence of dispersion,” Stud. Appl. Math. 74, 93, 1986.

Hill, S., “Channeling in packed columns,” Chemical Engineering Science, 1(6), 247-253, 1952.

Hirasaki, G. and Zhang, D.L., “Surface Chemistry of Oil Recovery from Fractured, Oil-Wet, Carbonate Formations,” SPEJ, 9(2): 151-162, 2004.

Hirasaki, G.J., van Domselaar, H.R., and Nelson, R.C., "Evaluation of the Salinity Gradient Concept in Surfactant Flooding," SPEJ, June, 486-500, 1983.

Homsy, G.M. “Viscous fingering in porous media,” Annu. Rev. Fluid Mech. 19, 271, 1987.

Huh, C., “Interfacial Tensions and Solubilizing Ability of a Microemulsion Phase that Coexists with Oil and Brine,” Journal of Colloid and Interface Science (September 1979), 408.

Jackson, A.C. “Experimental Study of the Benefits of Sodium Carbonate on Surfactants for Enhanced Oil Recovery” M.S. Thesis, University of Texas at Austin, Austin Texas, December 2006.

Jang, S. H., Liyanage, P. J., Lu, J., Kim, D. H., Arachchilage, G. W. P. P., Britton, C., Weerasooriya, U., and Pope, G. A., “Microemulsion Phase Behavior Measurements Using Live Oils at High Temperature and Pressure,” SPE 169169 presented at SPE IOR Symposium, Tulsa, OK, 12-16 April, 2014.

Kumar, K., Dao, E. K., and Mohanty, K. K.,"Atomic Force Microscopy Study of Wettability Alteration of Surfactants," SPE 93009 presented at SPE International Symposium of Oilfield Chemistry, Houston, Feb, 2005.

Lake, L.W. "Enhanced Oil Recovery", Prentice-Hall, Upper Saddle River, NJ, 1989.

Levitt, D.B., Dufour, S., Pope, G. A., Morel, D., and Gauer, P., "Design of an ASP Flood in a High-Temperature, High-Salinity, Low-Permeability Carbonate", IPTC 14915 presented at IPTC, Bangkok, Thailand, 7-9 February, 2012.

Levitt, D.B., Experimental Evaluation of High Performance EOR Surfactants for a Dolomite Oil Reservoir, MS Thesis, The University of Texas at Austin, Austin, Texas, 2006.

Levitt, D.B., Jackson, A.C., Heinson, C., Britton, L.N., Malik, T., Dwarakanath, V., and Pope, G.A. "Identification and Evaluation of High-Performance EOR Surfactants," SPE Res. Eval. Eng. 12(2): 243-253. SPE 100089, 2009.

Li, G.-Z., Mu, J.-H., Li, Y., Xiao, H.-D. and Gu, Q. 2000. What Is the Criterion for Selecting Alkaline/Surfactant/Polymer Flooding Formulation: Phase Behavior or Interfacial Tension. Journal of Dispersion Science and Technology 21 (3): 305-314.

Li, G.Z., Xu, J., Mu, J.H., Zhai, L.M., Shui, L.L. and Chen, W.J. 2005. Design and Application of an Alkaline-Surfactant-Polymer Flooding System in Field Pilot Test. Journal of Dispersion Science and Technology 26: 709-717.

Li, Y., Zhang, W., Kong, B., Puerto, M., Bao, X., Sha, O., Shen, Z., Yang, Y., Liu, Y., Gu, S., Miller, C., and Hirasaki, G.J., "Mixtures of Anionic-Cationic Surfactants: A New Approach for Enhanced Oil Recovery in Low-Salinity, High-Temperature Sandstone Reservoir", SPE 169051 presented at SPE IOR Symposium, Tulsa, OK, 12-16 April, 2014.

Liu, Q., Dong, M., Ma, S. and Tu, Y. 2007. Surfactant Enhanced Alkaline Flooding for Western Canadian Heavy Oil Recovery. Colloids and Surfaces, A: Physicochemical and Engineering Aspects 293 (1-3): 63-71.

Liyanage, P.J., Solairaj, S., Arachchilage, G.W., Linnemeyer, H.C., Kim, D., Weerasooriya, U., and Pope, G.A., Alkaline Surfactant Polymer Flooding using a Novel Class of Large Hydrophobe Surfactants, Paper SPE 154274, presented at the SPE Improved Recovery Symposium, Tulsa, Oklahoma, 14-18 April, 2012.

Lu, J., Goudarzi, A., Chen, P., Kim, D.H., Britton, C., Delshad, M., Mohanty, K.K., Weerasooriya, U., and Pope, G. A., "Surfactant Enhanced Oil Recovery from Naturally Fractured Reservoirs," Paper SPE 159979, presented at the Annual Technical Conference and Exhibition, San Antonio, Texas, 8-10 October, 2012.

Lu, J., Liyanage, P.J., Solairaj, S., Adkins, S., Arachchilage, G.P., Kim, D.H., Britton, C., Weerasooriya, U., and Pope, G.A., "New Surfactant Developments for Chemical

Enhanced Oil Recovery," Journal of Petroleum Science and Engineering, 2014a (in press).

Lu, J., Britton, C., Solairaj, S., Liyanage, P.J., Kim, D.H., Adkins, S., Arachchilage, G.P., Weerasooriya, U., and Pope, G.A., "Novel Large-Hydrophobe Alkoxy Carboxylate Surfactants for Enhanced Oil Recovery," SPE J., SPE 154256, 2014b (in press).

Lu, J., Weerasooriya, U., and Pope, G.A., "Investigation of gravity-stable surfactant floods", Fuel, 124: 76-84, 2014c.

Luo, P., Wu, Y., and Huang, S.-S.S., "Optimized Surfactant-Polymer Flooding for Western Canadian Heavy Oils", SPE 165396 presented at SPE Heavy Oil Conference-Canada, 11-13 June, Calgary, Alberta, Canada, 2013.

Manickam, O., and Homsy, G.M. "Fingering instability in vertical miscible displacement flows in porous media," J. Fluid Mech. 288, 75, 1995.

Meheust, Y., Lovoll, G., Maloy, K.J., and Schmittbuhl, J. "Interface scaling in a two dimensional porous medium under combined viscous, gravity and capillary effects," Phys. Rev. E 66, 051603, 2002.

Morrow, N.R. and Mason, G., "Recovery of Oil by Spontaneous Imbibition," Current Opinion in Colloid and Interfacial Science, 6(4): 321-337, 2001.

Nayfeh, A.H., "Stability of liquid interfaces in porous medium," Phys. Fluids 15, 1751, 1972.

O'Lenick, A.J. 2001. Guerbet Chemistry. Journal of Surfactants and Detergents 4 (3): 311-315.

Ould-Amer, Y., and Chikh, S. "Transient behavior of water-oil interface in an upward flow in porous media," J. Porous Media 6, 99, 2003.

Perrine, R. L., "A Unified Theory for Stable and Unstable Miscible Displacement," Soc. Pet. Eng. Jour. (Sep,, 1963) 205.

Perrine, R. L., "The Development of Stability Theory for Miscible Liquid-Liquid Displacement," Soc. Pet. Eng. Jour. (March, 1961) 17.

Peters, E.J., and Flock, D.L. "The onset of instability during two-phase immiscible displacements in porous media," SPE J. 21, 249, 1981.

Pope, G.A., Wang, B. and Tsaur, K. "A Sensitivity Study of Micellar/Polymer Flooding," SPEJ, December, 357-368, 1979.

Pope, G.A., Wu, W., Narayanaswamy, G., Delshad, M., Sharma, M.M., and Wang, P. 2000. Modeling Relative Permeability Effects in Gas-Condensate Reservoirs with a New Trapping Model. SPE J. 3 (2): 171-178.

Puerto, M, Hirasaki, G. J., Miller, C. A., and Barnes, J. R., "Surfactant Systems for EOR in High-Temperature, High-Salinity Environments", SPE J. 17(1): 11-19. SPE 129675, 2012.

Puerto, M.C., and Reed, R.L. "A Three Parameter Representation of Surfactant/Oil/Brine Interactions", SPE Journal 23(4), 669-682, 1983.

Puerto, M.C., Hirasaki, G.J., Miller, C.A., Reznik, C., Dubey, S., Barnes, J.R., and vanKuijk, S., "Effects of Hardness and Cosurfactant on Phase Behavior of Alcohol-free Alkyl Propoxylated Sulfate Systems", SPE 169096 presented at SPE IOR Symposium, Tulsa, OK, 12-16 April, 2014.

Raghavan, S. and Marsden, S.S. "The stability of immiscible liquid layers in a porous medium," J. Fluid Mech. 48, 143, 1971.

Riaz A. and Tchelepi H.A. "Linear Stability Analysis of Immiscible Two-phase Flow in Porous Media with Capillary Dispersion and Density Variation," Physics of Fluids, Volume 16, Issue 12, 2004.

Roehl, P.O. and Choquette, P.W., "Carbonate Petroleum Reservoirs," Springer-Verlag, New York, 1985.

Rosen, M.J. 2004. Surfactants and Interfacial Phenomena. Hoboken, NJ, USA: Wiley.

Roshanfekr, M. "Effect of Pressure and Methane on Microemulsion Phase Behavior and its Impact on Surfactant-Polymer Flood Oil Recovery", PhD Dissertation, The University of Texas at Austin, December, 2010.

Roshanfekr, M., Johns, R. T., Pope, G.A., Britton, L., Linnemeyer, H., Britton, C., Vyssotski, A. "Simulation of the Effect of Pressure and Solution Gas on Oil Recovery From Surfactant/Polymer Floods", SPE J. 17(3): 705-716. SPE 125095, 2012.

Sahni, V., Dean, R.M., Britton, C., Kim, D.H., Weerasooriya, U. and Pope, G.A. "Low-Cost, High-Performance Chemicals for Enhanced Oil Recovery," SPE 130007, Proceedings of the 2010 SPE Improved Oil Recovery Symposium held in Tulsa, OK, April 24-28

Sahni, V., Experimental Evaluation of Co-solvents in Development of High Performance Alkali/Surfactant/Polymer Formulations for Enhanced Oil Recovery, M.S. Thesis, The University of Texas at Austin, Austin, Texas, 2009.

Salager, J.L., Bourrel, M.U., Schechter, R.S., and Wade, W.H. "Mixing Rules for Optimum Phase-Behavior Formulations of Surfactant/Oil/Water Systems", SPEJ 19(5), 271-278, 1979.

Sasol, 2011. Marlowet Ether Carboxylic Acids, www.innovadex.eu/Lubricants/Detail/3857/110895/Marlowet--Ether-Carboxylic-Acids (accessed 15 April 2011).

Seethepalli, A., Adibhatla, B., and Mohanty, K.K., "Physicochemical Interactions During Surfactant Flooding of Carbonate Reservoirs," SPEJ 9(4): 411-418, 2004.

Sharma, A., Azizi-Yarand, A., Clayton, B., Baker, G., McKinney, P., Britton, C., Delshad, M., and Pope, G. A., "The Design and Execution of an Alkaline-Surfactant-Polymer Pilot Test," SPE 154318 presented at SPE IOR Symposium, Tulsa, OK, 14-18 April, 2012.

Sharma, G., and Mohanty, K.K., "Wettability Alteration in High Temperature and High Salinity Carbonate Reservoirs", SPE 147306 presented at the SPE ATCE, Denver, October 31-November 2, 2011.

Shaw, J.E. 1984. Carboxylate Surfactant Systems Exhibiting Phase Behavior Suitable for Enhanced Oil Recovery. Journal of the American Oil Chemists' Society 61 (8): 1395-1399.

Sheldon, J.W., Zondek, B., and Cardwell, W.T. "One-dimensional, incompressible, noncapillary, two-phase fluid flow in a porous medium," Petrol. Trans. AIME 216, 290, 1959.

Sheng, J. J. "Modern Chemical Enhanced Oil Recovery: Theory and Practice", Elsevier, Burlington, MA, 2011.

Shiau, B. J. B., Hsu, T.-P., Lohateeraparp , P., Rojas, M. R., Budhathoki, M., Raj, A., Wan, W., Bang, S., Harwell, J.H., "Recovery of Oil from High Salinity Reservoir Using Chemical Flooding: From Laboratory to Field Tests", SPE 165251 presented at SPE Enhanced Oil Recovery Conference, 2-4 July, Kuala Lumpur, Malaysia, 2013.

Solairaj, S. "New Method of Predicting Optimum Surfactant Structure for EOR" M.S. Thesis, University of Texas at Austin, Austin Texas, December, 2011.

Solairaj, S., Britton, C., Lu, J., Kim, D.H., Weerasooriya, U., and Pope, G. A., "New Correlation to Predict the Optimum Surfactant Structure for EOR," SPE 154262 presented at SPE IOR Symposium, Tulsa, OK, 14-18 April, 2012.

Standnes D C, Nogaret L A D, Chen H-L, et al. 2002. An Evaluation of Spontaneous Imbibition of Water into Oil-wet Carbonate Reservoir Cores using a Nonionic and a Cationic Surfactant. Energy & Fuels. 16 (6): 1557-1564.

Standnes, D. C., and Austad, T.,"Wettability Alteration in Chalk 2: Mechanism for Wettabiity Alteration from Oil-Wet to Water-Wet using Surfactants," Journal of Petroleum Science and Engineering, 28(2000): 123-143.

Stephen, K.D., Pickup, G.E., and Sorbie, K.S. "The local analysis of changing force balances in immiscible incompressible two-phase flow," Transp. Porous Media 45, 63, 2001.

Stoll, W. M., Shureqi, H., Finol, J., Al-Harthy, S. A. A., Oyemade, S., de Kruijf, A., van Wunnik, J., Arkesteijn, F., Bouwmeester, R., and Faber, M. J., 2011,

"Alkaline/Surfactant/Polymer Flood: From the Laboratory to the Field," SPERE, Dec. 702-712.

Tabary, R., Bazin, B., Douarche, F., Moreau, P., and Oukhemanou-Destremaut, F. "Surfactant Flooding in Challenging Conditions: Towards Hard Brines and High Temperatures," Paper SPE 164359, presented at the SPE Middle East Oil and Gas Show and Conference, Manama, Bahrain, 10-13 March, 2013.

Talley, L.D. 1988. Hydrolytic Stability of Alkyethoxy Sulfates. SPE Reservoir Engineering 3 (1): 235-242.

Tan, C.T., and Homsy, G.M. "Simulation of nonlinear viscous fingering in miscible displacement." Phys. Fluids 31, 1330, 1988.

Tan, C.T., and Homsy, G.M. "Stability of miscible displacements in porous media: radial source flow," Phys. Fluids 30, 1239, 1987.

Tavassoli, S., Lu, J., Pope, G.A., Sepehrnoori, K. "Investigation of the Critical Velocity Required for a Gravity Stable Surfactant Flood," SPE 163624 will present at SPE Reservoir Simulation Symposium, Woodlands, TX, 18-20 February, 2013.

Terwilliger, P.L., Wilsey, L.E., Hall, N.H., Bridges, P.M., and R.A. Morse. "An experimental and theoretical investigation of gravity drainage performance," Petrol. Trans. AIME 192, 285, 1951.

Tong, Z.X., Morrow, N.R., and Xie, X., "Spontaneous Imbibition for Mixed-Wettability State in Sand Stones Induced by Adsorption from Crude Oil," 7th International Symposium on Reservoir Wettability, Tasmania, Australia, 12-14 March, 2002.

Vijapurapu C.S. and Rao D.N. 2004. Compositional Effects of Fluids on Spreading, Adhesion and Wettability in Porous Media. Colloids and Surfaces A: Physicochemical and Engineering Aspects 241 (1-3): 335-342.

Walker, D.L. Experimental Investigation of the Effect of Increasing the Temperature of ASP Flooding, M.S. Thesis, The University of Texas at Austin, Austin, Texas, 2011.

Wang, D., Liu, C., Wu, W., and Wang, G., "Novel Surfactants that Attain Ultra-Low Interfacial Tension between Oil and High Salinity Formation Water without adding Alkali, Salts, Co-surfactants, Alcohols and Solvents", SPE 127452 presented at SPE EOR Conference at Oil & Gas West Asia, 11-13 April, Muscat, Oman, 2010.

Xie, X., Weiss, W.W., Tong, Z., and Morrow, N.R., "Improved Oil Recovery from Carbonate Reservoirs by Chemical Stimulation," SPEJ 10(103): 276-285, 2005.

Yang, H., Britton, C., Liyanage, P.J., Solairaj, S., Kim, D., Nguyen, Q., Weerasooriya, U., and Pope, G.A., Low-cost, High-performance Chemicals for Enhanced Oil Recovery, Paper SPE 129978, presented at the SPE Improved Recovery Symposium, Tulsa, Oklahoma, 24-28 April, 2010.

Yin, D., Zhang, X., 2013. Evaluation and research on performance of a blend surfactant system of alkyl polyglycoside in carbonate reservoir. J. Petrol. Sci. Eng. 111, 153–158.

Zhang, D.L., Liu, S., Puerto, M., Miller, C.A., and Hirasaki, G.J., "Wettability Alteration and Instantaneous Imbibition in Oil-Wet Carbonate Formation," 8th International Symposium on Reservoir Wettability, Houston, 16-18 May, 2004.

Zhang, J., Nguyen, Q.P., Flaaten, A.K., and Pope, G.A., "Mechanisms of Enhanced Natural Imbibition with Novel Chemicals," SPE 113453 presented at SPE IOR Symposium, Tulsa, OK, 19-23 April, 2008.

Zhao, P., Howes, A. J., Dwarakanath, V., Thach, S., Malik, T., Jackson, A., Karazincir, O., Campbell, C., and Waite, J., "Evaluation and Manufacturing Quality Control of Chemicals for Surfactant Flooding," SPE 129892, presented at the Symposium on Improved Oil Recovery, Tulsa, Oklahoma, 24-28 April, 2010.

Zhao, P., Jackson, A.C., Britton, C., Kim, D.H., Britton, L.N., Levitt, D.B., and Pope, G.A., "Development of High-Performance Surfactants for Difficult Oils," SPE 113432, presented at SPE/DOE IOR Symposium, Tulsa, OK, April, 2008.

Zhou, X., Morrow, N.R., and Ma, S., "Interrelationship of Wettability, Initial Water Saturation, Aging Time and Oil Recovery by Spontaneous Imbibition and Waterflooding," SPEJ 5(2): 199-207, 2000.